

Monte Carlo sampling with integrator snippets

Christophe Andrieu, Mauro Camara Escudero and Chang Zhang

February 17, 2025

School of Mathematics, University of Bristol

Abstract

Assume interest is in sampling from a probability distribution μ defined on $(\mathbf{Z}, \mathcal{Z})$. We develop a framework for sampling algorithms which takes full advantage of ODE numerical integrators, say $\psi: \mathbf{Z} \rightarrow \mathbf{Z}$ for one integration step, to explore μ efficiently and robustly. The popular Hybrid Monte Carlo (HMC) algorithm [29, 48] and its derivatives are examples of such a use of numerical integrators. A key idea developed here is that of sampling integrator snippets, that is fragments of the orbit of an ODE numerical integrator ψ , and the definition of an associated probability distribution $\bar{\mu}$ such that expectations with respect to μ can be estimated from integrator snippets distributed according to $\bar{\mu}$. The integrator snippet target distribution $\bar{\mu}$ takes the form of a mixture of pushforward distributions which suggests numerous generalisations beyond mappings arising from numerical integrators, e.g. normalising flows. Very importantly this structure also suggests new principled and robust strategies to tune the parameters of integrators, such as the discretisation stepsize, effective integration time, or number of integration steps, in a Leapfrog integrator.

We focus here primarily on Sequential Monte Carlo (SMC) algorithms, but the approach can be used in the context of Markov chain Monte Carlo algorithms. We illustrate performance and, in particular, robustness through numerical experiments and provide preliminary theoretical results supporting observed performance.

Contents

1 Overview and motivation: SMC sampler with HMC	4
2 An introductory example	6
2.1 An SMC-like algorithm	6
2.2 Justification	9
2.3 Integrator snippets and variance reduction	14
2.4 Direct extensions	15
2.5 Rational and computational considerations	16
2.6 Links to the literature	17
3 Adaptation with Integrator Snippet SMC	19
3.1 Need for adaptation and review of classical criteria	19
3.2 Adapting γ only	20
3.3 Adapting γ and ϵ for fixed T	21
3.3.1 Methodology	21
3.3.2 Simulations	26
3.4 Full adaptation	29
3.4.1 Methodology	32
3.4.2 Simulations	34
4 Discussion	34
A Notation and definitions	39
B Background on Radon-Nikodym derivative	40
C Proofs for Section 2	43
D Sampling Markov snippets	45
D.1 Markov snippet SMC sampler or waste free SMC with a difference	45
D.2 Theoretical justification	48
D.3 Revisiting sampling with integrator snippets	52
D.4 More complex integrator snippets	54
E Early experimental results: HMC-IS	55
E.1 Numerical illustration: logistic regression	55
E.2 Numerical illustration: orthant probabilities	57
F Early experimental results: filamentary distributions	60
F.1 Numerical illustration: simulating from filamentary distributions	60
F.2 Going round the bend: bananas and pears	65
G Adaptation: implementational details	68
G.1 About the structure of the mother distribution	68
G.2 Kullback-Leibler minimisation	69
G.3 Calculations in the inverse Gaussian scenario	70

H	Additional theoretical properties	71
H.1	Variance using folded mixture samples	71
H.2	Variance using unfolded mixture samples	72
H.2.1	Relative efficiency for unfolded estimators	72
H.2.2	Optimal weights	75
H.3	More on variance reduction and optimal flow	75
H.3.1	Hamiltonian contour decomposition	76
H.3.2	Advantage of averaging and control variate interpretation	79
H.3.3	Towards an optimal flow?	81
I	MCMC with integrator snippets	82
I.1	Windows of states	82
I.2	Multinomial HMC	83

1 Overview and motivation: SMC sampler with HMC

Assume interest is in sampling from a probability distribution μ on a probability space (Z, \mathcal{Z}) . The main ideas of sequential Monte Carlo (SMC) samplers to simulate from μ are (a) to define a sequence of probability distributions $\{\mu_n, n \in \llbracket 0, P \rrbracket\}$ on (Z, \mathcal{Z}) where $\mu_P = \mu$, μ_0 is chosen by the user, simple to sample from and the sequence $\{\mu_n, n \in \llbracket P-1 \rrbracket\}$ “interpolates” μ_0 and μ_P , (b) and to propagate a cloud of samples $\{z_n^{(i)} \in Z, i \in \llbracket N \rrbracket\}$ for $n \in \llbracket 0, P \rrbracket$ to represent $\{\mu_n, n \in \llbracket 0, P \rrbracket\}$ using an importance sampling/resampling mechanism [28].

After initialisation, for $n \in \llbracket P \rrbracket$, samples $\{z_{n-1}^{(i)}, i \in \llbracket N \rrbracket\}$, representing μ_{n-1} , are propagated thanks to a user-defined mutation Markov kernel $M_n: Z \times \mathcal{Z} \rightarrow [0, 1]$, as follows. For $i \in \llbracket N \rrbracket$ sample $\tilde{z}_n^{(i)} \sim M_n(z_{n-1}^{(i)}, \cdot)$ and compute the importance weights, assumed to exist for the moment,

$$\omega_n^{(i)} = \frac{d\mu_n \widehat{\otimes} L_{n-1}}{d\mu_{n-1} \otimes M_n}(z_{n-1}^{(i)}, \tilde{z}_n^{(i)}), \quad (1)$$

where $L_{n-1}: Z \times \mathcal{Z} \rightarrow [0, 1]$ is a user-defined “backward” Markov kernel required to define importance sampling on $Z \times Z$ and swap the rôles of $z_{n-1}^{(i)}$ and $\tilde{z}_n^{(i)}$, in the sense that for $f: Z \rightarrow \mathbb{R}$ μ_n -integrable,

$$\int f(z') \frac{d\mu_n \widehat{\otimes} L_{n-1}}{d\mu_{n-1} \otimes M_n}(z, z') \mu_{n-1}(dz) M_n(z, dz') = \mu_n(f).$$

More details are provided in Appendices A-B concerning the existence and definition of these weights, but can be omitted on a first reading.

The mutation step is followed by a selection step where for $i \in \llbracket N \rrbracket$, $z_n^{(i)} = \tilde{z}_n^{(a_i)}$ for a_i the random variable taking values in $\llbracket N \rrbracket$ with $\mathbb{P}(a_i = k) \propto \omega_n^{(k)}$. The procedure is summarized in Alg. 1.

Given $\{M_n, n \in \llbracket P \rrbracket\}$, theoretically optimal choice of $\{L_{n-1}, n \in \llbracket P \rrbracket\}$ is well understood but tractability is typically obtained by assuming that M_n is μ_{n-1} -invariant, or considering approximations of $\{L_{n-1}, n \in \llbracket P \rrbracket\}$ and that M_n is μ_n -invariant. This makes Markov chain Monte Carlo (MCMC) kernels very attractive choices for M_n .

```

1 for  $i \in \llbracket N \rrbracket$  do
2   | Sample  $z_0^{(i)} \sim \mu_0(\cdot)$ ;
3   | Set  $\omega_0^{(i)} = 1$ 
4 end
5 for  $n \in \llbracket P \rrbracket$  do
6   | for  $i \in \llbracket N \rrbracket$  do
7     | Sample  $\tilde{z}_n^{(i)} \sim M_n(z_{n-1}^{(i)}, \cdot)$ ;
8     | Compute  $w_n^{(i)}$  as in (1).
9   | end
10  | for  $i \in \llbracket N \rrbracket$  do
11    | Sample  $a_i \sim \text{Cat}(\omega_n^{(1)}, \dots, \omega_n^{(N)})$ 
12    | Set  $z_n^{(i)} = \tilde{z}_n^{(a_i)}$ 
13  | end
14 end
```

Algorithm 1: Generic SMC sampler

A possible choice of MCMC kernel is the Hybrid Monte Carlo (HMC) method, a Metropolis-Hastings (MH) update using a discretisation of Hamilton’s equations [29, 48] to update the state, a particular instance of the use

of numerical integrators of ODEs in this context. More specifically, assume that interest is in sampling π defined on $(\mathbf{X}, \mathcal{X})$. First the problem is embedded into that of sampling from the joint distribution $\mu(dz) := \pi \otimes \varpi(dz) = \pi(dx)\varpi(dv)$ defined on $(\mathbf{Z}, \mathcal{Z}) = (\mathbf{X} \times \mathbf{V}, \mathcal{X} \otimes \mathcal{V})$, where v is an auxiliary variable facilitating sampling. Following the SMC framework we set $\mu_n(dz) := \pi_n \otimes \varpi_n(dz)$ for $n \in \llbracket 0, P \rrbracket$, a sequence of distributions on $(\mathbf{Z}, \mathcal{Z})$ with $\pi_P = \pi$, $\{\pi_n, n \in \llbracket 0, P-1 \rrbracket\}$ probabilities on $(\mathbf{X}, \mathcal{X})$ and $\{\varpi_n, n \in \llbracket 0, P \rrbracket\}$ on $(\mathbf{V}, \mathcal{V})$. With $\psi: \mathbf{Z} \rightarrow \mathbf{Z}$ an integrator of an ODE of interest, one can use $\psi^k(z)$ for some $k \in \mathbb{N}$ as a proposal in a MH update mechanism; v is a source of randomness allowing “exploration”, resampled every now and then. Again, hereafter we let $z =: (x, v) \in \mathbf{X} \times \mathbf{V}$ be the corresponding components of z .

Example 1 (Leapfrog integrator of Hamilton’s equations). Assume that $\mathbf{X} = \mathbf{V} = \mathbb{R}^d$, that $\{\pi_n, \varpi_n, n \in \llbracket 0, P \rrbracket\}$ have densities, denoted $\pi_n(x)$ and $\varpi_n(v)$, with respect to the Lebesgue measure and let $x \mapsto U_n(x) := -\log \pi_n(x)$. For $n \in \llbracket 0, P \rrbracket$ and U_n differentiable, Hamilton’s equations for the potential $H_n(x, v) := U_n(x) + \frac{1}{2}|v|^2$ are

$$\dot{x}_t = v_t, \dot{v}_t = -\nabla U_n(x_t), \quad (2)$$

and possess the important property that $H_n(x_t, v_t) = H_n(x_0, v_0)$ for $t \geq 0$. The corresponding leapfrog integrator is given, for some $\epsilon > 0$, by

$$\begin{aligned} \psi_n(x, v) &= {}_{\text{B}}\psi \circ {}_{\text{A}}\psi_n \circ {}_{\text{B}}\psi(x, v) \\ {}_{\text{B}}\psi(x, v) &:= (x, v - \frac{1}{2}\epsilon \nabla U_n(x)), \quad {}_{\text{A}}\psi_n(x, v) = (x + \epsilon v, v). \end{aligned} \quad (3)$$

We point out that, with the exception of the first step, only one evaluation of $\nabla U(x)$ is required per integration step since the rightmost ${}_{\text{B}}\psi$ in (3) recycles the last computation from the last iteration. Let $\sigma: \mathbf{Z} \rightarrow \mathbf{Z}$ be such that for any $f: \mathbf{Z} \rightarrow \mathbf{Z}$, $f \circ \sigma(x, v) = f(x, -v)$, then in its most basic form the HMC update leaving μ_n invariant proceeds as follows, for $(z, A) \in \mathbf{Z} \times \mathcal{Z}$

$$M_{n+1}(z, A) = \int \varpi_n(dv') [\alpha_n(x, v'; T) \mathbf{1}\{\psi_n^T(x, v') \in A\} + \bar{\alpha}_n(x, v'; T) \mathbf{1}\{\sigma(x, v) \in A\}], \quad (4)$$

with, for some user defined $T \in \mathbb{N}$,

$$\alpha_n(z; T) := 1 \wedge \frac{\mu_n \circ \psi_n^T(z)}{\mu_n(z)}, \quad (5)$$

and $\bar{\alpha}_n(z; T) = 1 - \alpha_n(z; T)$.

Other ODEs, capturing other properties of the target density, or other types of integrators are possible. However a common feature of integrator based updates is the need to compute recursively an integrator snippet $\mathbf{z} := (z, \psi(z), \psi^2(z), \dots, \psi^T(z))$, for a given mapping $\psi: \mathbf{Z} \rightarrow \mathbf{Z}$, of which only the endpoint $\psi^T(z)$ is used. This raises the question of recycling intermediate states, all the more so that computation of the snippet often involves quantities shared with the evaluation of U_n . In Example 1, for instance, expressions for $\nabla U_n(x)$ and $U_n(x)$ often involve the same computationally costly quantities and evaluation of the density $\mu_n(x)$ where $\nabla U_n(x)$ has already been evaluated is therefore often virtually free; consider for example $U(x) = x^\top \Sigma^{-1} x$ for a covariance matrix Σ , then $\nabla U(x) = 2\Sigma^{-1}x$.

In turn these quantities offer the promise of being able to exploit points used to generate the snippet while preserving accuracy of the estimators of interest, through importance sampling or reweighting. For example an algorithm exploiting the snippet fully could use the following mixture of μ_n -invariant Markov chain transition kernels [42, 48, 39],

$$\mathfrak{M}_{n+1}(z, A) = \frac{1}{T+1} \sum_{k=0}^T \int \varpi_n(dv') P_{n,k}(x, v'; A),$$

where for $(z, A) \in Z \times \mathcal{Z}$ and $k \in \llbracket P - 1 \rrbracket$

$$P_{n,k}(z, A) := \alpha_n(z; k) \mathbf{1}\{\psi_n^k(z) \in A\} + \bar{\alpha}_n(z; k) \mathbf{1}\{\sigma(z) \in A\}. \quad (6)$$

As we shall see our work shares the same objective but we adopt a strategy more closely related to [47] (see Appendix I for a more detailed discussion) which however leads to a comparison between states along a snippet. Further, an advantage of SMC samplers is that they provide population wide information about tuning parameters, in particular of numerical integrators, therefore suggesting robust self-tuning procedures.

The manuscript is organised as follows. In Section 2 we first provide a high level description of particular instances of the class of algorithms considered and provide a justification through reinterpretation as standard SMC algorithms in Subsection 2.2. In Subsection 2.4 we discuss direct extensions of our algorithms, some of which we explore in the present manuscript. This work has links to related recent attempts in the literature [55, 26, 61]; these links are discussed and contrasted with our work in Subsection 2.5 where some of the motivations behind these algorithms are also discussed. Early exploratory simulations demonstrating the interest of our approach are provided in Appendices E-F. Our main focus is however on the development of adaptive algorithms in Section 3 where, focussing on the Leapfrog integrator, we develop novel criteria and updating strategies to adapt the discretisation stepsize and integration time by taking advantage of the population-wide information available; in simulation the resulting algorithms display remarkable robustness on the examples we have considered We draw some conclusions in Section 4.

The manuscript contains a number of appendices, containing supporting material and additional developments. Notation, definitions and basic mathematical background can be found in Appendices A-B. Proofs for Section 2 are provided in Appendix C. In Appendix D we introduce the more general framework of Markov snippets Monte Carlo and associated formal justifications; the algorithms used in Appendix E.2 rely on some of these extensions. Appendix D.3 details the link with the scenario considered in Section 2. In Appendix D.4 we provide general results facilitating the practical calculation of some of the Radon-Nikodym involved, highlighting why some of the usual constraints on mutation and backward kernels in SMC can be lifted here. Appendix G contains ancillary supporting details for Section 3. In Appendix H we provide elements of a theoretical analysis explaining expected properties of the algorithms proposed in this manuscript, although a fully rigorous theoretical analysis is beyond the present methodological contribution. In Appendix I we explore the use of some of the ideas developed here in the context of MCMC algorithms and establish links with earlier suggestions, such as “windows of states” techniques proposed in the context of HMC [47, 48].

A Python implementation of the algorithms developed in this paper is available at <https://github.com/MauroCE/IntegratorSnippets>.

2 An introductory example

We still aim to sample from a probability distribution μ on (Z, \mathcal{Z}) as described above Example 1 using an SMC sampler relying on the leapfrog integrator of Hamilton’s equations. As in the previous section we introduce an interpolating sequence of distributions $\{\mu_n, n \in \llbracket 0, P \rrbracket\}$ on (Z, \mathcal{Z}) and assume for now the existence of densities for $\{\mu_n, n \in \llbracket 0, P \rrbracket\}$ with respect to a common measure ν , say the Lebesgue measure on \mathbb{R}^{2d} , denoted $\mu_n(z) := d\mu_n/d\nu(z)$ for $z \in Z$ and $n \in \llbracket 0, P \rrbracket$ and denote ψ_n the corresponding integrator, which again is measure preserving in this setup.

2.1 An SMC-like algorithm

Primary interest in this paper is in algorithms of the type given in Alg. 2 and variations thereof; throughout $T \in \mathbb{N} \setminus \{0\}$.

```

1 Sample  $z_0^{(i)} \stackrel{\text{iid}}{\sim} \mu_0$  for  $i \in \llbracket N \rrbracket$ .
2 for  $n \in \llbracket P \rrbracket$  do
3   for  $i \in \llbracket N \rrbracket$  do
4     for  $k \in \llbracket 0, T \rrbracket$  do
5       Compute  $z_{n-1,k}^{(i)} := \psi_n^k(z_{n-1}^{(i)})$  and
6
7         
$$\bar{w}_{n,k}(z_{n-1}^{(i)}) := \frac{\mu_n(z_{n-1,k}^{(i)})}{\mu_{n-1}(z_{n-1}^{(i)})} = \frac{\mu_n \circ \psi_n^k(z_{n-1}^{(i)})}{\mu_{n-1}(z_{n-1}^{(i)})},$$

8     end
9   end
10  for  $j \in \llbracket N \rrbracket$  do
11    Sample  $\llbracket N \rrbracket \times \llbracket 0, T \rrbracket \ni (b_j, a_j) \sim \text{Cat}(\{\bar{w}_{n,k}(z_{n-1}^{(i)})\}, (i, k) \in \llbracket N \rrbracket \times \llbracket 0, T \rrbracket)$ 
12    Set  $\bar{z}_n^{(j)} := (\bar{x}_{n-1}^{(j)}, \bar{v}_{n-1}^{(j)}) = z_{n-1,a_j}^{(b_j)}$ 
13    Rejuvenate the velocities  $z_n^{(j)} = (\bar{x}_{n-1}^{(j)}, v_n^{(j)})$  with  $v_n^{(j)} \sim \varpi_n$ .
14  end
end

```

Algorithm 2: Unfolded Hamiltonian Snippet SMC algorithm

The SMC sampler-like algorithm in Alg. 2 therefore involves propagating N “seed” particles $\{z_{n-1}^{(i)}, i \in \llbracket N \rrbracket\}$, with a mutation mechanism consisting of the generation of N integrator snippets $\mathbf{z} := (z, \psi_n(z), \psi_n^2(z), \dots, \psi_n^T(z))$ started at every seed particle $z \in \{z_{n-1}^{(i)}, i \in \llbracket N \rrbracket\}$, resulting in $N \times (T + 1)$ particles which are then whittled down to a set of N seed particles using a standard resampling scheme; after rejuvenation of velocities this yields the next generation of seed particles—this is illustrated in Fig. 1; a more realistic depiction of Alg. 2 in the context of Example 1 with π a two dimensional distribution is presented in Fig. 2. This algorithm should be contrasted with standard implementations of SMC samplers where, after resampling, a seed particle normally gives rise to a single particle in the mutation step, in Fig. 1 the last or first state on the snippet when using an MH as mutation kernel. Intuitively validity of the algorithm follows from the fact that if $\{(z_{n-1}^{(i)}, 1), i \in \llbracket N \rrbracket\}$ represent μ_{n-1} , then $\{(z_{n-1,k}^{(i)}, \bar{w}_{n,k}(z_{n-1}^{(i)})), (i, k) \in \llbracket N \rrbracket \times \llbracket 0, T \rrbracket\}$ represents μ_n in the sense that for $f: \mathbf{Z} \rightarrow \mathbb{R}$ summable, one can use the approximation

$$\mu_n(f) \approx \sum_{i=1}^N \sum_{k=0}^T f \circ \psi_n^k(z_{n-1}^{(i)}) \frac{\mu_n \circ \psi_n^k(z_{n-1}^{(i)}) / \mu_{n-1}(z_{n-1}^{(i)})}{\sum_{j=1}^N \sum_{l=0}^T \mu_n \circ \psi_n^l(z_{n-1}^{(j)}) / \mu_{n-1}(z_{n-1}^{(j)})}, \quad (7)$$

where the self-normalization of the weights is only required in situations where the ratio $\mu_n(z)/\mu_{n-1}(z)$ is only known up to a constant.

Simple numerical experiments demonstrating robustness and efficiency of our approach are provided in Appendices E-F. However our primary objective, beyond establishing correctness, is to show that our proposed framework naturally lends itself to novel adaptation strategies, for example of the stepsize ϵ and integration time T ; see Section 3. To that purpose we first provide justification for the correctness of Alg. 2 and the estimator (7) by recasting the procedure as a standard SMC sampler targetting a particular sequence of distributions in Section 2.2 and using properties of mixtures. Direct generalizations are provided in Section 2.4 and the adaptation strategies of Section 3 then follow.

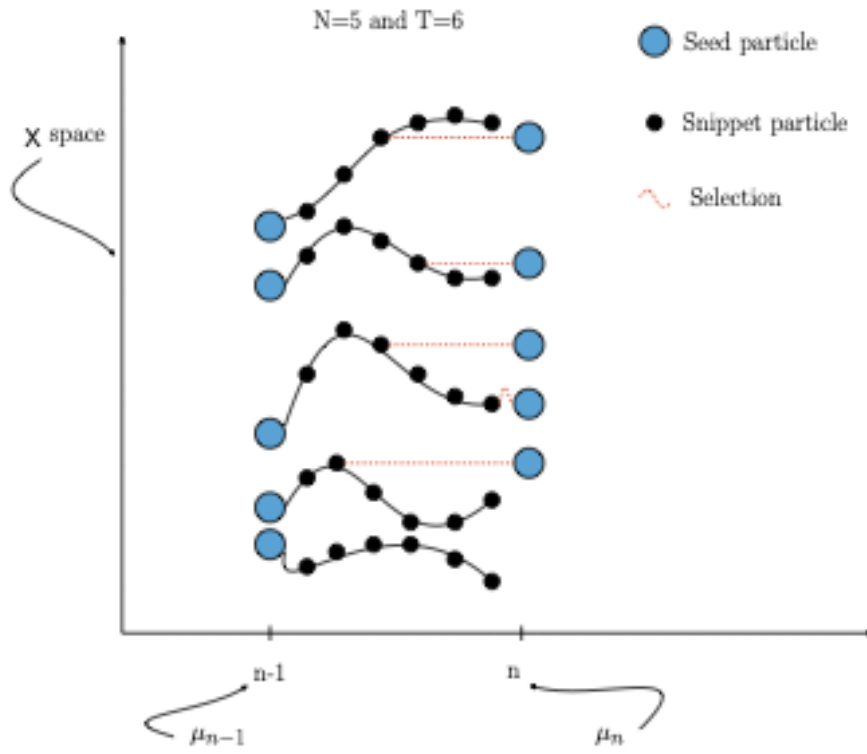


Figure 1: Illustration of the transition from μ_{n-1} to μ_n with integrator snippet SMC. A snippet grows (black dots) out of each seed particle (blue). The middle snippet gives rises through selection (dashed red) to two seed particles while the bottom snippet does not produce any seed particle.

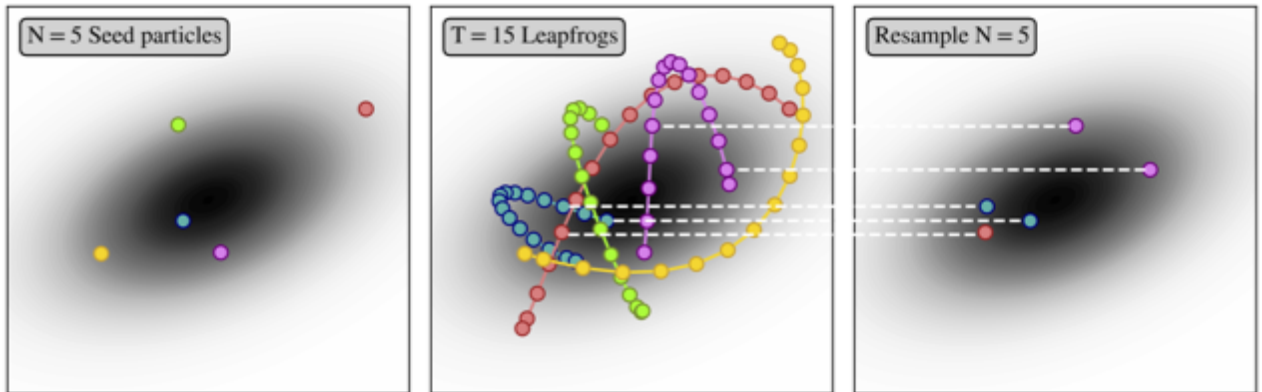


Figure 2: Evolution of the x components of 5 seed particles and their integrator snippets ($T = 15$) targeting a normal distribution π defined on \mathbb{R}^2 , using the leapfrog integrator of Example 1.

2.2 Justification

We now outline the main ideas underpinning the theoretical justification of Alg. 2. Key to this is establishing that Alg. 2 is a standard SMC sampler targeting a particular sequence of probability distributions $\{\bar{\mu}_n, n \in \llbracket 0, P \rrbracket\}$ from which samples can be processed to approximate expectations with respect to $\{\mu_n, n \in \llbracket 0, P \rrbracket\}$. This has the advantage that no fundamentally new theory is required and that standard methodological ideas can be re-used in the present scenario, while the particular structure of $\{\bar{\mu}_n, n \in \llbracket 0, P \rrbracket\}$ can be exploited for new developments. This section focuses on identifying $\{\bar{\mu}_n, n \in \llbracket 0, P \rrbracket\}$ and establishing some of their important properties. Similar ideas are briefly touched upon in [26], but we will provide full details and show how these ideas can be pushed further, in interesting directions.

First for $(n, k) \in \llbracket 0, P \rrbracket \times \llbracket 0, T \rrbracket$ let $\psi_{n,k}: \mathbb{Z} \rightarrow \mathbb{Z}$ be measurable and invertible mappings, define $\mu_{n,k}(\mathrm{d}z) := \mu_n^{\psi_{n,k}^{-1}}(\mathrm{d}z)$, i.e. the distribution of $\psi_{n,k}^{-1}(z)$ when $z \sim \mu_n$. It is worth pointing out that invertibility of these mappings is not required theoretically, but important practically and facilitates interpretation throughout. Earlier we have focused on the scenario where $\psi_{n,k} = \psi_n^k$ for an integrator $\psi_n: \mathbb{Z} \rightarrow \mathbb{Z}$, but this turns out not to be a requirement, although it is our main motivation. Useful applications of this general perspective can be found in Subsection 2.4. Introduce the probability distributions on $(\llbracket 0, T \rrbracket \times \mathbb{Z}, \mathcal{P}(\llbracket 0, T \rrbracket) \otimes \mathcal{Z})$

$$\bar{\mu}_n(k, \mathrm{d}z) = \frac{1}{T+1} \mu_{n,k}(\mathrm{d}z),$$

for $n \in \llbracket 0, P \rrbracket$. We will show that Alg. 2 can be interpreted as an SMC sampler targeting the sequence of marginal distributions on $(\mathbb{Z}, \mathcal{Z})$

$$\bar{\mu}_n(\mathrm{d}z) = \frac{1}{T+1} \sum_{k=0}^T \mu_{n,k}(\mathrm{d}z), \quad (8)$$

which we may refer to as a mixture. Note that the conditional distribution is

$$\bar{\mu}_n(k | z) = \frac{1}{T+1} \frac{d\mu_{n,k}}{d\bar{\mu}_n}(z), \quad (9)$$

which can be computed in most scenarios of interest.

Example 2. For $n \in \llbracket 0, P \rrbracket$ assume the existence of a density $\mu_n(z)$ w.r.t. the Lebesgue measure. Assuming that $\psi_{n,k}$ is “volume preserving”, then for $k \in \llbracket 0, T \rrbracket$,

$$\mu_{n,k}(z) := \frac{d\mu_{n,k}}{d\nu}(z) = \mu_n \circ \psi_{n,k}(z) \text{ and } \bar{\mu}_n(z) := \frac{d\bar{\mu}_n}{d\nu}(z) = \frac{1}{T+1} \sum_{k=0}^T \mu_n \circ \psi_{n,k}(z),$$

and therefore

$$w_{n,k}(z) := \frac{d\mu_{n,k}}{d(\sum_{l=0}^T \mu_{n,l})}(z) = \frac{\mu_n \circ \psi_{n,k}(z)}{\sum_{l=0}^T \mu_n \circ \psi_{n,l}(z)}.$$

When $\{\psi_{n,k}, k \in \llbracket P \rrbracket\}$ are not volume preserving, additional multiplicative Jacobian determinant-like terms may be required (see Lemma 10 and the additional requirement that $\{\psi_{n,k}, k \in \llbracket P \rrbracket\}$ be differentiable).

A central point throughout this paper is how samples from μ_n can be used to obtain samples from the marginal $\bar{\mu}_n$ and vice-versa, thanks to the mixture structure relating the two distributions. Naturally, given $z \sim \mu_n$, sampling $k \sim \mathcal{U}(\llbracket 0, T \rrbracket)$ and returning $\psi_{n,k}^{-1}(z)$ yields a sample from the marginal $\bar{\mu}_n$. More importantly, we have

Proposition 3 (Knitting-Tinking”). For $n \in \llbracket 0, P \rrbracket$,

1. Assume $z \sim \bar{\mu}_n$ and sample $k \sim \bar{\mu}_n(\cdot | z)$. Then $z | k \sim \mu_n^{\psi_{n,k}^{-1}}(dz)$ and $\psi_{n,k}(z) \sim \mu_n$.
2. For $f: Z \rightarrow \mathbb{R}$ μ_n -integrable and $k \in \llbracket 0, T \rrbracket$

$$\int f(z) \mu_n(dz) = \int \left\{ \sum_{k=0}^T f \circ \psi_{n,k}(z) \bar{\mu}_n(k | z) \right\} \bar{\mu}_n(dz), \quad (10)$$

Proof. For $f: Z \rightarrow \mathbb{R}$ μ_n -integrable and $k \in \llbracket 0, T \rrbracket$, a change of variable (see Theorem 9) yields

$$\int f \circ \psi_{n,k}(z) \mu_{n,k}(dz) = \int f \circ \psi_{n,k}(z) \mu_n^{\psi_{n,k}^{-1}}(dz) = \int f(z) \mu_n(dz),$$

Therefore

$$\begin{aligned} \int f(z) \mu_n(dz) &= \frac{1}{T+1} \sum_{k=0}^T \int f \circ \psi_{n,k}(z) \mu_{n,k}(dz) \\ &= \sum_{k=0}^T \int f \circ \psi_{n,k}(z) \bar{\mu}_n(k, dz) \\ &= \int \left\{ \sum_{k=0}^T f \circ \psi_{n,k}(z) \bar{\mu}_n(k | z) \right\} \bar{\mu}_n(dz), \end{aligned}$$

Using $f = \mathbf{1}_A$ for $A \in \mathcal{Z}$ formally establishes the earlier claim that if $(k, z) \sim \bar{\mu}_n$ then $\psi_{n,k}(z) \sim \mu_n$. \square

Note that, as suggested by Example 2, construction of the estimator corresponding to (10) will only require evaluations of the density μ_n and function f at $z, \psi_{n,1}(z), \psi_{n,2}(z), \dots, \psi_{n,T}(z)$. It should be clear that the results of Proposition 3 extend well beyond the leapfrog integrator setup, a fact we discuss and exploit in the remainder of the manuscript.

We now turn to the description of an SMC algorithm targeting $\{\bar{\mu}_n, n \in \llbracket 0, P \rrbracket\}$, Alg. 3, and then establish that it is probabilistically equivalent to Alg. 2, in a sense made precise below. With $z = (x, v)$ for $n \in \llbracket P \rrbracket$ we introduce the following mutation kernel

$$\bar{M}_n(z, dz') := \sum_{k=0}^T \bar{\mu}_{n-1}(k | z) R_n(\psi_{n-1,k}(z), dz'), \quad R_n(z, dz') := (\delta_x \otimes \varpi_{n-1})(dz'), \quad (11)$$

where we note that the refreshment kernel has the property that $\mu_{n-1}R_n = \mu_{n-1}$. With the assumption $\mu_{n-1} \gg \bar{\mu}_n$, from Lemma 13 one can identify the corresponding near optimal kernel $\bar{L}_{n-1}: Z \times \mathcal{Z} \rightarrow [0, 1]$, which leads to the SMC sampler importance weights, at step $n \in \llbracket P \rrbracket$,

$$\bar{w}_n(z, z') := \frac{d\bar{\mu}_n \otimes \bar{L}_{n-1}}{d\bar{\mu}_{n-1} \otimes \bar{M}_n}(z, z') = \frac{d\bar{\mu}_n}{d\mu_{n-1}}(z'). \quad (12)$$

that is for $f: Z \rightarrow \mathbb{R}$ such that $\bar{\mu}_n(|f|) < \infty$,

$$\int f(z') \frac{d\bar{\mu}_n}{d\mu_{n-1}}(z') \bar{\mu}_{n-1} \otimes \bar{M}_n(d(z, z')) = \bar{\mu}_n(f).$$

The corresponding standard SMC sampler is given in Alg. 3 where,

- the weighted particles $\{(z_n^{(i)}, 1), i \in \llbracket N \rrbracket\}$ represent $\bar{\mu}_n$ and $\{(z_{n,k}^{(i)}, w_{n,k}(z_n^{(i)})), (i, k) \in \llbracket N \rrbracket \times \llbracket 0, T \rrbracket\}$ represent μ_n from (10),
- steps 3-8 correspond to sampling from the mutation kernel \bar{M}_{n+1} in (11),
- $\{(z_n^{(i)}, 1), i \in \llbracket N \rrbracket\}$ represent μ_n ,
- $\{(z_n^{(i)}, \bar{w}_{n+1}(z_n^{(i)})), i \in \llbracket N \rrbracket\}$ represent $\bar{\mu}_{n+1}$, and so do $\{(z_{n+1}^{(i)}, 1), i \in \llbracket N \rrbracket\}$.

Notice that we assume here $\psi_0 = \text{Id}$, hence that $\bar{\mu}_0 = \mu_0$, and that the weights $w_{n,k}$ appear as being computed twice in step 4 and step 9 when evaluating the resampling weights at the previous iteration, for the only reason that it facilitates exposition. The identities (10) and (9) suggest, for any $n \in \llbracket P \rrbracket$, the estimator of $\mu_n(f)$ for $f: Z \rightarrow \mathbb{R}$ μ_n -integrable,

$$\begin{aligned} \check{\mu}_n(f) &= \frac{1}{N} \sum_{i=1}^N \sum_{k=0}^T \frac{1}{T+1} \frac{d\mu_{n,k}}{d\bar{\mu}_n}(z_n^{(i)}) f \circ \psi_{n,k}(z_n^{(i)}). \\ &= \frac{1}{N} \sum_{i=1}^N \sum_{k=0}^T \frac{\mu_n \circ \psi_{n,k}}{\sum_{l=0}^T \mu_n \circ \psi_{n,l}}(z_n^{(i)}) f \circ \psi_{n,k}(z_n^{(i)}), \end{aligned} \quad (13)$$

where the second line is correct under the assumptions of Example 2. Further, when $\mu_{n-1} \gg \mu_{n,k}$ for $k \in \llbracket 0, T \rrbracket$ one can also write (10) for $f: Z \rightarrow \mathbb{R}$ summable as

$$\mu_n(f) = \int \left\{ \frac{1}{T+1} \sum_{k=0}^T f \circ \psi_{n,k}(z) \frac{d\mu_{n,k}}{d\mu_{n-1}}(z) \right\} \mu_{n-1}(dz),$$

```

1 sample  $\check{z}_0^{(i)} \stackrel{\text{iid}}{\sim} \bar{\mu}_0 = \mu_0$  for  $i \in \llbracket N \rrbracket$ .
2 for  $n = 0, \dots, P-1$  do
3   for  $i \in \llbracket N \rrbracket$  do
4     for  $k \in \llbracket 0, T \rrbracket$  do
5       compute  $\check{z}_{n,k}^{(i)} = (\check{x}_{n,k}^{(i)}, \check{v}_{n,k}^{(i)}) := \psi_{n,k}(\check{z}_n^{(i)}), w_{n,k}(\check{z}_n^{(i)})$ 
6     end
7     sample  $a_i \sim \text{Cat}(w_{n,0}(\check{z}_n^{(i)}), w_{n,1}(\check{z}_n^{(i)}), w_{n,2}(\check{z}_n^{(i)}), \dots, w_{n,T}(\check{z}_n^{(i)}))$ 
8     set  $z_n^{(i)} = (\check{x}_{n,a_i}^{(i)}, v_n^{(i)})$  with  $v_n^{(i)} \sim \varpi_n$ 
9
10    
$$\bar{w}_{n+1}(z_n^{(i)}) = \frac{d\bar{\mu}_{n+1}}{d\mu_n}(z_n^{(i)}),$$

11  end
12  for  $j \in \llbracket N \rrbracket$  do
13    sample  $b_j \sim \text{Cat}(\bar{w}_{n+1}(z_n^{(1)}), \dots, \bar{w}_{n+1}(z_n^{(N)}))$ 
14    set  $\check{z}_{n+1}^{(j)} = z_n^{(b_j)}$ 
15  end

```

Algorithm 3: Folded Hamiltonian Snippet SMC algorithm

which can be estimated, using self-renormalization when required, with

$$\hat{\mu}_n(f) = \sum_{i=1}^N \sum_{k=0}^T \frac{\frac{d\mu_{n,k}}{d\mu_{n-1}}(z_{n-1}^{(i)})}{\sum_{j=1}^N \sum_{l=0}^T \frac{d\mu_{n,l}}{d\mu_{n-1}}(z_{n-1}^{(j)})} f \circ \psi_{n,k}(z_{n-1}^{(i)}), \quad (14)$$

therefore justifying the estimator suggested in (7) in the particular case where the conditions of Example 2 are satisfied, once we establish the equivalence of Alg. 3 and Alg. 2 in Proposition 4. In fact it can be shown (Proposition 4) that, with \mathbb{E}_i referring to the expectation of the probability distribution underpinning Alg. i ,

$$\mathbb{E}_3(\check{\mu}_n(f) \mid z_{n-1}^{(j)}, j \in \llbracket N \rrbracket) = \hat{\mu}_n(f),$$

a form of Rao-Blackwellization implying lower variance for $\hat{\mu}_n(f)$ while the two estimators share the same bias. Interestingly a result we establish later in the paper, Proposition 5, suggests that the variance $\check{\mu}_n(f)$ is smaller than that of the standard Monte Carlo estimator that assumes N samples $z_n^{(i)} \stackrel{\text{iid}}{\sim} \mu_n$, due to the control variate nature of integrator snippets estimators. Another point is that computation of the weight $\mu_n \circ \psi_{n,k} / \bar{\mu}_n$ only requires knowledge of μ_n up to a normalizing constant, that is the estimator is unbiased if $z_n^{(i)} \sim \bar{\mu}_n$ for $i \in \llbracket N \rrbracket$ even if μ_n is not completely known, while the estimator (7) will most often require self-normalisation, hence inducing a bias.

We now provide the probabilistic argument justifying Alg. 2 and the shared notation $\{z_n^{(i)}, i \in \llbracket N \rrbracket\}$ in Alg. 2 and Alg. 3. The result is illustrated in Fig. 3.

Proposition 4. *Alg. 2 and Alg. 3 are probabilistically equivalent. More precisely, letting \mathbb{P}_i refer to the probability of Algorithm i for $i \in \{2, 3\}$,*

1. for $n \in \llbracket P-1 \rrbracket$ the distributions of $\{z_n^{(i)}, i \in \llbracket N \rrbracket\}$ conditional upon $\{z_{n-1}^{(i)}, i \in \llbracket N \rrbracket\}$ in Alg. 3 and Alg. 2 are the same,

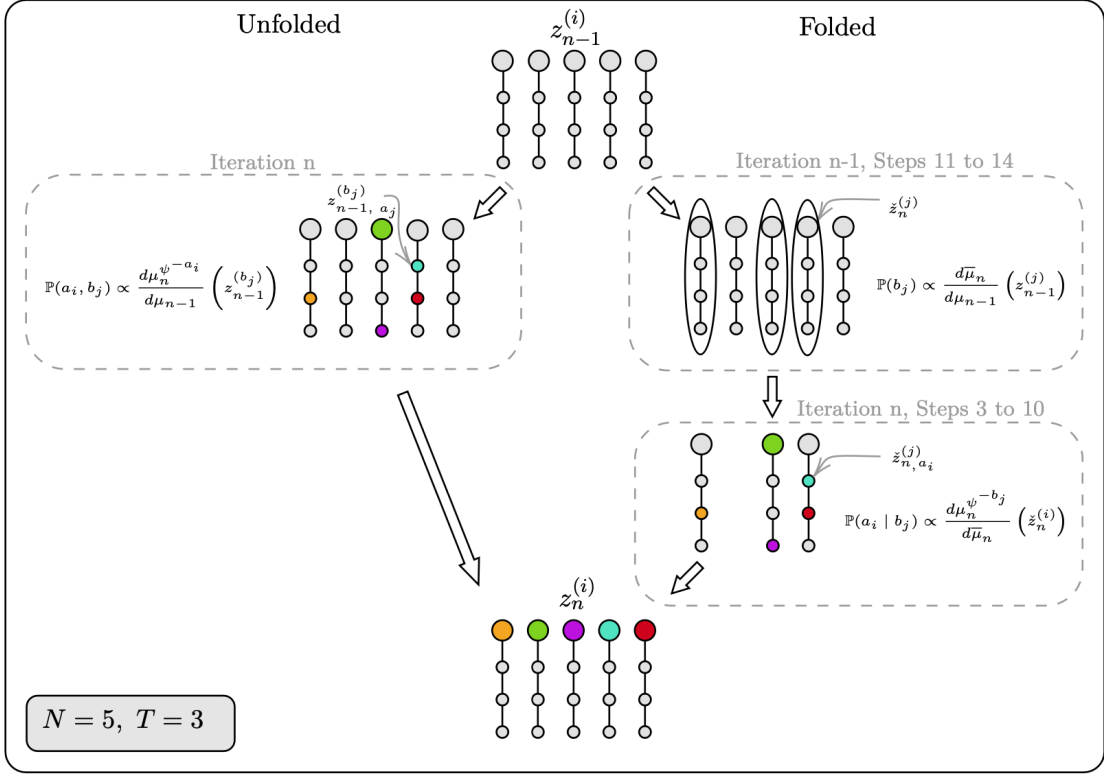


Figure 3: Alg. 2 and Alg. 3 are equivalent.

2. the joint distributions of $\{z_n^{(i)}, i \in \llbracket N \rrbracket, n \in \llbracket 0, P-1 \rrbracket\}$ are the same under \mathbb{P}_2 and \mathbb{P}_3 ,
3. for $n \in \llbracket P \rrbracket$, any $f: \mathbb{Z} \rightarrow \mathbb{R}$ μ_n -integrable with $\check{\mu}_n(f)$ and $\hat{\mu}_n(f)$ as in (13) and (14),

$$\mathbb{E}_3(\check{\mu}_n(f) | z_{n-1}^{(j)}, j \in \llbracket N \rrbracket) = \hat{\mu}_n(f).$$

Since the justification of the latter interpretation of the algorithm is straightforward, as a standard SMC sampler targeting instrumental distributions $\{\bar{\mu}_n, n \in \llbracket 0, P \rrbracket\}$, and allows for further easy generalisations we will adopt this perspective in the remainder of the manuscript for simplicity.

This reinterpretation also allows the use of known facts about SMC sampler algorithms. For example it is well known that the output of SMC samplers can be used to estimate unbiasedly unknown normalising constants by virtue of the fact that, in the present scenario,

$$\prod_{n=0}^{P-1} \left[\frac{1}{N} \sum_{i=1}^N \frac{d\bar{\mu}_{n+1}}{d\mu_n}(z_n^{(i)}) \right]$$

has expectation 1 under \mathbb{P}_3 . Now assume that the densities of $\{\mu_n, n \in \llbracket 0, P \rrbracket\}$ are known up to a constant only,

say $d\mu_n/d\nu(z) = \tilde{\mu}_n(z)/Z_n$ and $\nu \gg \nu^{\psi_n^{-k}}$ for $k \in \llbracket 0, T \rrbracket$, then

$$Z_n = Z_n \int \mu_n^{\psi_n^{-1}}(dz) = \int \tilde{\mu}_n \circ \psi_n^k(z) \frac{d\nu^{\psi_n^{-1}}(z)}{d\nu}(z) \nu(dz),$$

and the measure $Z_n \bar{\mu}_n(dz)$ shares the same normalising constant as $\tilde{\mu}_n(z)\nu(dz)$,

$$Z_n = \int Z_n \bar{\mu}_n(dz) = \sum_{k=1}^T \frac{1}{T} \int \tilde{\mu}_n \circ \psi_n^k(z) \frac{d\nu^{\psi_n^{-1}}(z)}{d\nu}(z) \nu(dz).$$

Consequently

$$\prod_{n=0}^{P-1} \left[\frac{1}{N(T+1)} \sum_{i=1}^N \sum_{k=0}^N \frac{\tilde{\mu}_{n+1} \circ \psi_{n+1,k}(z_n^{(i)})}{\tilde{\mu}_n} \frac{d\nu^{\psi_{n+1,k}^{-1}}(z_n^{(i)})}{d\nu} \right],$$

is an unbiased estimator of Z_P/Z_0 .

2.3 Integrator snippets and variance reduction

The aim in this section is to establish that integrator snippets naturally come with variance reduction properties. Variance reduction is only one of the benefits of our methodology but the result below provides us with a crucial principled criterion to determine the parameters of the integrator used in our algorithms. We use the following simplified notation throughout. For $\{\psi_k : Z \rightarrow \mathbb{R}, k \in \llbracket 0, T \rrbracket\}$, invertible mappings, define

$$\bar{\mu}(k, dz) := \frac{1}{T+1} \mu_k(dz),$$

with $\mu_k := \mu^{\psi_k^{-1}}$.

Proposition 5. *For any $f : Z \rightarrow \mathbb{R}$ μ -integrable, with $\bar{f}(k, z) := f \circ \psi_k(z)$, we have*

1. *unbiasedness*

$$\mathbb{E}_{\bar{\mu}}(\mathbb{E}_{\bar{\mu}}(\bar{f}(T, \check{Z}) \mid \check{Z})) = \mathbb{E}_{\bar{\mu}}(\bar{f}(T, \check{Z})) = \mathbb{E}_{\mu}(f(Z)),$$

2. *variance reduction*

$$\text{var}_{\bar{\mu}}(\mathbb{E}_{\bar{\mu}}(\bar{f}(T, \check{Z}) \mid \check{Z})) = \text{var}_{\mu}(f(Z)) - \mathbb{E}_{\bar{\mu}}(\text{var}_{\bar{\mu}}(\bar{f}(T, \check{Z}) \mid \check{Z})).$$

Proof. The first statement follows directly from (4) by adaptation of the notation. The variance decomposition identity yields

$$\text{var}_{\bar{\mu}}(\bar{f}(T, \check{Z})) = \text{var}_{\bar{\mu}}(\mathbb{E}_{\bar{\mu}}(\bar{f}(T, \check{Z}) \mid \check{Z})) + \mathbb{E}_{\bar{\mu}}(\text{var}_{\bar{\mu}}(\bar{f}(T, \check{Z}) \mid \check{Z})),$$

but from the first statement,

$$\begin{aligned} \text{var}_{\bar{\mu}}(\bar{f}(T, \check{Z})) &= \mathbb{E}_{\bar{\mu}}(\bar{f}(T, \check{Z})^2) - \mathbb{E}_{\bar{\mu}}(\bar{f}(T, \check{Z}))^2 \\ &= \mathbb{E}_{\mu}(f(Z)^2) - \mathbb{E}_{\mu}(f(Z))^2 \\ &= \text{var}_{\mu}(f(Z)). \end{aligned}$$

□

The result is clearly relevant when using the ‘‘Rao-Blackwellized estimator,’’

$$\check{\mu}(f) = N^{-1} \sum_{i=1}^N \mathbb{E}_{\bar{\mu}}(\bar{f}(T, \check{Z}^{(i)}) \mid \check{Z}^{(i)}),$$

which corresponds to the estimator suggested by (10). For $\check{Z}^{(1)}, \dots, \check{Z}^{(N)} \stackrel{\text{iid}}{\sim} \bar{\mu}$ the variance of $\check{\mu}(f)$ is naturally given by $\text{var}_{\bar{\mu}}(\mathbb{E}_{\bar{\mu}}(\bar{f}(T, \check{Z}) \mid \check{Z})) / N$ and the second statement of Proposition 5 tells us that using $T > 1$ is in general better than setting $T = 1$. The term $\mathbb{E}_{\bar{\mu}}(\bar{f}(T, \check{Z}) \mid \check{Z}) - f(K, \check{Z})$ for $K \sim \bar{\mu}(k \mid \check{Z})$ can be thought of as a control variate for an estimator relying on copies of $f(K, \check{Z})$.

The distributional assumption on $\check{Z}^{(1)}, \dots, \check{Z}^{(N)}$ is naturally not satisfied in the context of algorithm Alg. 3. However the variance terms considered above are precisely the terms appearing in the analysis of SMC samplers [27, Chapter 9]. Indeed the variance of estimators obtained from an SMC can be decomposed as the sum of local variances at each iterations, which involve precisely the terms above, as $N \rightarrow \infty$.

An important implication of the variance identity is that for given μ and f an (ODE, integrator) pair, or more generally transformations, should be chosen or tuned to maximize $\mathbb{E}_{\bar{\mu}}(\text{var}_{\bar{\mu}}(\bar{f}(T, \check{Z}) \mid \check{Z}))$, that is deterministic integration should be performed along the roughest possible directions $k \mapsto f \circ \psi_k(\check{Z})$ in order to absorb as much Monte Carlo variability as possible.

It is worth noting that these ideas are not specific to the SMC context and could be used, for example, in the context of PISA (Pushforward Importance SAMpling) discussed in Appendix H.2.

2.4 Direct extensions

It should be clear that the algorithm we have described lends itself to numerous generalizations, which we briefly discuss below. This can be skipped on a first reading.

There is no reason to limit the number of snippets arising from a seed particle to one, which could be of interest on parallel machines. For example the velocity of a given seed particle can be refreshed multiple times, resulting in partial copies of the seed particle from which integrator snippets can be grown.

The main scenario motivating this work, corresponds to the choice, for $n \in \llbracket 0, P \rrbracket$, of $\{\psi_{n,k} = \psi_n^k, k \in \llbracket 0, T \rrbracket\}$ for a given $\psi_n: \mathbb{Z} \rightarrow \mathbb{Z}$. As should be apparent from the theoretical justification this can be replaced by a general family of invertible mappings $\{\psi_{n,k}: \mathbb{Z} \rightarrow \mathbb{Z}, k \in \llbracket 0, T \rrbracket\}$ where the $\psi_{n,k}$ ’s are now not necessarily required to be measure preserving in general, in which case the expression for $w_{n,k}(z)$ may involve additional terms of the ‘‘Jacobian’’ type. These mappings may correspond to integrators other than those of Hamilton’s equations but may be more general deterministic mappings; T may not have any temporal meaning anymore and only represent the number of deterministic transformations used in the algorithm. More specifically, assuming that $v \gg \mu_n$ and $v \gg v^{\psi_{n,k}^{-1}}$ for some σ -finite dominating measure v and letting $\mu_n(z) := d\mu_n/dv(z)$ the required weights are now of the form (see Lemmas 10-12)

$$\bar{w}_{n,k}(z) := \frac{1}{T+1} \frac{\mu_n \circ \psi_{n,k}(z)}{\mu_{n-1}(z)} \frac{dv^{\psi_{n,k}^{-1}}}{dv}(z).$$

Again when v is the Lebesgue measure and $\psi_{n,k}$ a diffeomorphism, then $dv^{\psi_{n,k}^{-1}}/dv$ is the absolute value of the determinant of the Jacobian of $\psi_{n,k}$. Non uniform weights may be ascribed to each of these transformations in the definition of $\bar{\mu}$ (36). A more useful application of this generality is in the situation where it is believed that using multiple integrators, specialised in capturing different geometric features of the target density, could be beneficial. Hereafter we simplify notation by setting $\nu \leftarrow \mu_n$ and $\mu \leftarrow \mu_{n+1}$. For the purpose of illustration consider two distinct integrators $\psi_i, i \in \llbracket 2 \rrbracket$ (again n disappears from the notation) we wish to use, each for $T_i \in \mathbb{N}$ time steps

with proportions $\gamma_i \geq 0$ such that $\gamma_1 + \gamma_2 = 1$. Again with $\mu = \pi \otimes \varpi$ define the mixture

$$\bar{\mu}(i, k, dz) := \frac{\gamma_i}{T_i + 1} \mu^{\psi_{i,k}^{-1}}(dz) \mathbf{1}\{k \in \llbracket 0, T_i \rrbracket\},$$

which still possesses the fundamental property that if $z \sim \bar{\mu}$ (resp. $(i, z) \sim \bar{\mu}$), then with $(i, k) \sim \bar{\mu}(k, i | z)$ (resp. $k \sim \bar{\mu}(k | i, z)$) we have $\psi_{i,k}(z) \sim \mu$. It is possible to aim to sample from $\bar{\mu}(dz)$, in which case the pair (i, k) plays the rôle played by k in the earlier sections. However, in order to introduce the sought persistency, that is use either ψ_1 or ψ_2 when constructing a snippet, we focus on the scenario where the pair (i, z) plays the rôle played by z earlier. In other words the target distribution is now $\bar{\mu}(i, dz)$, which is to $\mu(i, dz) := \gamma_i \cdot \mu(dz)$ what $\bar{\mu}_n(dz)$ in (36) was to $\mu_n(dz)$. The mutation kernel corresponding to (36) is given by

$$\bar{M}_{\nu, \mu}(i, z; j, dz') := \sum_{k=0}^{T_i} \bar{\nu}(k | i, z) R(i, \psi_{i,k}(z); j, dz'),$$

with now the requirement that $\bar{\nu}R(i, dz) = \nu(i, dz) = \gamma_i \cdot \nu(dz)$. A straightforward choice is $R(i, z; j, dz') = \gamma_j \cdot R_0(z, dz')$ with $\nu R_0(dz') = \nu(dz')$. With these choices and using the near-optimal backward kernel simple substitutions $(i, z) \leftarrow z$ and $(j, z') \leftarrow z'$ yields

$$\frac{d\bar{\mu} \otimes \bar{L}_{\nu, \mu}}{d\bar{\nu} \otimes \bar{M}_{\nu, \mu}}(i, z; j, z') = \frac{d\bar{\mu}}{d\nu}(j, z'),$$

and justifies our abstract presentation. This idea will be exploited later on in order to design adaptive algorithms.

Another direct extension consists of generalizing the definition of $\bar{\mu}_n$ by assigning non-uniform and possibly state-dependent weights to the integrator snippet particles as follows

$$\bar{\mu}_n(k, dz) = \omega_{n,k} \circ \psi_{n,k}(z) \mu_{n,k}(dz),$$

with $\omega_{n,k} : Z \rightarrow \mathbb{R}_+$ for $k \in \llbracket 0, T \rrbracket$ and such that $\sum_{k=0}^T \omega_{n,k}(z) = 1$ for any $z \in Z$; this should be contrasted with (8). In Appendix H.2.2 we show how such weighting can be optimised to reduce variance of expectation estimators, with potentially negative weights.

We leave exploration of some of these generalisations for future work.

2.5 Rational and computational considerations

Our initial motivation for this work was that computation of $\{z_{n,k}, k \in \llbracket T \rrbracket\}$ and $\{w_{n,k}, k \in \llbracket T \rrbracket\}$ most often involve common quantities, leading to negligible computational overhead, and reweighting offers the possibility to use all the states of a snippet in a simulation algorithm rather than the endpoint only. There are other reasons for which this approach may be beneficial.

The benefit of using all states along integrator snippets in sampling algorithms has been noted in the literature. For example, in the context of Hamiltonian integrators, with $H_n(z) := -\log \mu_n(z)$ and $\psi_{n,k} = \psi_n^k$, it is known that for $z \in Z$ the mapping $k \mapsto H_n \circ \psi_n^k(z)$ is typically oscillatory, motivating for example the x-tra chance algorithm of [16]. The “windows of state” strategy of [47, 48] effectively makes use of the mixture $\bar{\mu}$ as an instrumental distribution and improved performance is noted, with performance seemingly improving with dimension on particular problems; see Appendix I for a more detailed discussion; see also [9]. Further averaging is well known to address scenarios where components of x_t evolve on different scales and no choice of a unique integration time $\tau := T \times \epsilon$ can accommodate all scales [48, 39, section 3.2]; averaging addresses this issue effectively, see Example 35. We also note that, keeping $T \times \epsilon$ constant, in the limit as $\epsilon \rightarrow 0$ the average in (12) corresponds to the numerical integration,

Riemann like, along the contour of $H_n(z)$, effectively leading to some form of Rao-Blackwellization of this contour; this is discussed in detail in Appendix H.

Another benefit we have observed with the SMC context is the following. Use of a WF-SMC strategy involves comparing particles within each Markov snippet arising from a single seed particle, while our strategy involves comparing all particles across snippets, which proves highly beneficial in practice. This seems to bring particular robustness to the choice of the integrator parameters ϵ and T and can be combined with highly robust adaptation schemes taking advantage of the population of samples, in the spirit of [37, 39]; see Subsections E.1 and F.1.

At a computational level we note that, in contrast with standard SMC or WF-SMC implementations relying on an MH mechanism, the construction of integrator snippets does not involve an accept reject mechanism, therefore removing control flow operations and enabling lockstep computations on GPUs – actual implementation of our algorithms on such architectures is, however, left to future work.

Finally, when using integrators of Hamilton’s equations we naturally expect similar benefits to those enjoyed by HMC. Let $d \in \mathbb{N}$ and let $\mathbf{X} = \mathbb{R}^d$. We know that in certain scenarios [7, 15], the distributions $\{\mu_{n,d}, d \in \mathbb{N}, n \in \llbracket T(d) \rrbracket\}$ are such that for $n \in \mathbb{N}$, $\log(\mu_{n,d} \circ \psi_{n,d}^k / \mu_{n-1,d}(z)) \rightarrow_{d \rightarrow \infty} \mathcal{N}(\mu_n, \sigma_n^2)$, that is the weights do not degenerate to zero or one: in the context of SMC this means that the part of the importance weight (12) arising from the mutation mechanism does not degenerate. Further, with an appropriate choice of schedule, i.e. sequence $\{\mu_{n,d}, n \in \llbracket T(d) \rrbracket\}$ for $d \in \mathbb{N}$, ensures that the contribution $\mu_{n,d}(z) / \mu_{n-1,d}(z)$ to the importance weights (12) is also stable as $d \rightarrow \infty$. As shown in [7, 4, 15], while direct important sampling may require an exponential number of samples as d grows, the use of such a schedule may reduce complexity to a polynomial order.

2.6 Links to the literature

Alg. 2, and its reinterpretation Alg. 3, are reminiscent of various earlier contributions and we discuss here parallels and differences. This work was initiated in [66] and pursued and extended in [30].

Readers familiar with the “waste-free SMC” algorithm (WF-SMC) of [26] may have noticed a connection. Similarly to Alg. 2, seed particles are extended with an MCMC kernel leaving μ_{n-1} invariant at iteration n , yielding $N \times (T + 1)$ particles subsequently whittled down to N new seed particles. A first difference is that while generation of an integrator snippet can be interpreted as applying a sequence of deterministic Markov kernels (see Appendix D.3 for a detailed discussion) what we show is that the mutation kernels involved do not have to leave μ_{n-1} invariant; in fact we show in Appendix D that this indeed is not a requirement, therefore offering more freedom. Further, it is instructive to compare our procedure with the following two implementations of WF-SMC using an HMC kernel (4) for the mutation. A first possibility for the mutation stage is to run T steps of an HMC update in sequence, where each update uses one integrator step. Assuming no velocity refreshment along the trajectory this would lead to the exploration of a random number of states of our integrator snippet due to the accept/reject mechanism involved; incorporating refreshment or partial refreshment would similarly lead to a random number of useful samples. Alternatively one could consider a mutation mechanism consisting of an HMC build around T integration steps and where the endpoint of the trajectory would be the mutated particle; this would obviously mean discarding $T - 1$ potentially useful candidates. To avoid possible reader confusion, we note apparent typos in [26, Proposition 1], provided without proof, where the intermediate target distribution of the SMC algorithms, $\bar{\mu}_n$ in our notation (see (30)), seems improperly stated. The statement is however not used further in the paper.

Our work shares, at first sight, similarities with [55, 61], but differs in several respects. In the discrete time setup considered in [61] a mixture of distributions similar to ours is also introduced. Specifically for a sequence $\{\omega_k \geq 0, k \in \mathbb{Z}\}$ such that $\#\{\omega_k \neq 0, k \in \mathbb{Z}\} < \infty$ and $\sum_{l \in \mathbb{Z}} \omega_k = 1$, the following mixture is considered (in the notation of [61] their transformation is $T = \psi^{-1}$ and we stick to our notation for the sake of comparison and avoid

confusion with our T),

$$\bar{\mu}(\mathrm{d}z) = \sum_{k \in \mathbb{Z}} \omega_k \mu_k(\mathrm{d}z).$$

The intention is to use the distribution $\bar{\mu}$ as an importance sampling proposal to estimate expectations with respect to μ ,

$$\begin{aligned} \int f(z) \frac{\mathrm{d}\mu}{\mathrm{d}\bar{\mu}}(z) \bar{\mu}(\mathrm{d}z) &= \sum_{k \in \mathbb{Z}} \omega_k \int f(z) \frac{\mathrm{d}\mu}{\mathrm{d}\bar{\mu}}(z) \mu^{\psi^{-k}}(\mathrm{d}z) \\ &= \sum_{k \in \mathbb{Z}} \omega_k \int f \circ \psi^{-k}(z) \frac{\mathrm{d}\mu}{\mathrm{d}\bar{\mu}} \circ \psi^{-k}(z) \mu(\mathrm{d}z) \\ &= \sum_{k \in \mathbb{Z}} f \circ \psi^{-k}(z) \omega_k \frac{\mu \circ \psi^{-k}(z)}{\sum_{l \in \mathbb{Z}} \omega_l \mu \circ \psi^{l-k}(z)} \mu(\mathrm{d}z), \end{aligned}$$

where the last line holds when $v \gg \mu$, $v^\psi = v$ and $\mu(z) = \mathrm{d}\mu/\mathrm{d}v(z)$. The rearrangement on the second and third line simply capture the fact noted earlier in the present paper that with $z \sim \mu$ and $k \sim \text{Cat}(\{\omega_l : l \in \mathbb{Z}\})$ then $\psi^{-k}(z) \sim \bar{\mu}$. As such NEO relies on generating samples from μ first, typically exact samples, which then undergo a transformation and are then properly reweighted. In contrast we aim to sample from a mixture of the type $\bar{\mu}$ directly, typically using an iterative method, and then exploit the mixture structure to estimate expectations with respect to μ . Note also that some of the $\psi^{l-k}(z)$ terms involved in the renormalization may require additional computations beyond terms for which $\omega_{l-k} \neq 0$. Our approach relies on a different important sampling identity

$$\int f \circ \psi^k(z) \frac{\mathrm{d}\mu^{\psi^{-k}}}{\mathrm{d}\bar{\mu}}(z) \bar{\mu}(\mathrm{d}z) = \mu(f).$$

We note however that the conformal Hamiltonian integrator used in [55, 61] could be used in our framework, which we leave for future investigations. Their NEO-MCMC targets a ‘‘posterior distribution’’ $\mu'(\mathrm{d}z) = Z^{-1} \mu(\mathrm{d}z) L(z)$ and inspired by the identity

$$\int f(z) L(z) \frac{\mathrm{d}\mu}{\mathrm{d}\bar{\mu}}(z) \bar{\mu}(\mathrm{d}z) = \sum_{k \in \mathbb{Z}} \omega_k \int f \circ \psi^{-k}(z) L \circ \psi_k^{-1}(z) \frac{\mathrm{d}\mu}{\mathrm{d}\bar{\mu}} \circ \psi^{-k}(z) \mu(\mathrm{d}z),$$

which is an expectation of $\bar{f}(k, z) = f \circ \psi^{-k}(z)$ with respect to

$$\bar{\mu}'(k, \mathrm{d}z) \propto \mu(\mathrm{d}z) \cdot \omega_k \frac{\mathrm{d}\mu}{\mathrm{d}\bar{\mu}} \circ \psi^{-k}(z) \cdot L \circ \psi^{-k}(z)$$

and they consider algorithms targetting $\bar{\mu}'(\mathrm{d}z)$ which relying on exact samples from μ to construct proposals, resulting in a strategy which shares the weaknesses of an independent MH algorithm.

Much closer in spirit to our work is the ‘‘window of states’’ idea proposed in [47, 48], developed in [9], in the context of HMC algorithms. Although the MCMC algorithms of [47, 48] ultimately target μ and are not reversible, they involve a reversible MH update with respect to $\bar{\mu}$ and additional transitions permitting transitions from μ to $\bar{\mu}$ and $\bar{\mu}$ to μ ; see Section I for full details. Note that using these MCMC updates as mutation kernels in an SMC would not lead to integrator snippet SMC as they target μ , not $\bar{\mu}$.

A link we have not explored in the present manuscript is that to normalizing flows [59, 45] and related literature. In particular the ability to tune the parameter of the leapfrog integrator suggests that our methodology lends itself to learning normalising flows. We finally note an analogy of such approaches with umbrella sampling [60, 62], although the targetted mixture is not of the same form, and the ‘‘Warp Bridge Sampling’’ idea of [46].

3 Adaptation with Integrator Snippet SMC

3.1 Need for adaptation and review of classical criteria

Monte Carlo algorithms relying on discretization of Hamilton’s equation for the exploration of the support of a distribution of interest offer the promise of very efficient algorithms, as supported by practical [48, 17] and theoretical evidence [7, 15] in the MCMC scenario. However such procedures are known for their brittleness e.g. [41] in the particular case of the Langevin algorithm, and require precise calibration of their parameters in order to achieve their potential. In their simplest implementation these procedures rely on three, related, parameters: the discretisation stepsize $\epsilon > 0$, $T \in \mathbb{N}$ the number of integration steps and $\tau = \epsilon T \in \mathbb{R}_+$ the effective integration time, that is the time horizon we would have liked to use if Hamilton’s equations were tractable. Qualitatively the effect of a poor choice of these parameters is as follows.

For fixed $\tau > 0$, too large a stepsize ϵ will result in departure of the integrator from the Hamiltonian flow, therefore defeating the purpose of the method and empirically affecting performance, while too small an $\epsilon > 0$ requires T to be large, therefore increasing computational complexity to reach a vicinity of the Hamilton flow at time τ . This issue has motivated a substantial body of work e.g. [7, 15], which essentially provide guidelines on the choice of ϵ based on statistical properties of the Markov chain at stationarity; in particular monitoring the expected acceptance ratio is shown to be a suitable criterion. In practice the algorithm is run for a value of ϵ , the empirical expected acceptance probability estimated in preliminary runs or online, and ϵ adjusted to reach a nominal value suggested by theory. More specifically with the acceptance ratio $r(z; \epsilon, T) = \mu \circ \psi^T(z) / \mu(z)$ and acceptance ratio $\alpha(z; \epsilon, T) = 1 \wedge r(z; \epsilon, T)$ theory suggests finding ϵ such that

$$\chi(\epsilon, T) := \mathbb{E}_\mu(\alpha(z; \epsilon, T)) \approx 0.67, \text{ subject to } \tau = T\epsilon.$$

Poor choice of the effective integration time τ is also important. Too large a τ may result in the end point of the integrator snippet being close to the initial state, which should be clear in the two-dimensional setting, therefore wasting computations. Too small a τ may not take full advantage of such updates. However choosing τ optimally in general is a largely open problem with, to the best of our knowledge, very few theoretical results available. An exception is [20, Theorem 1.3] where, assuming the log-concavity of the target probability density and tractability of Hamilton’s equations, an optimal value for τ in terms of a coupling argument, which does not seem to have been exploited in practice; we discuss this further in the context of IS2MC later on. A popular and pragmatic approach was suggested in [38] to determine a good value of τ . The aim set in [38] is to identify the time τ_u (or k_u the corresponding number of steps for a given ϵ) where $t \mapsto \|\psi_{t,x}(z) - x\|^2$, with again $\psi_{t,x}$ indicates the first component of ψ_t , reaches its first maximum. While not a foolproof criterion, the no-U-turn criterion has been shown to be useful in practice [17].

SMC algorithms require additional calibration. Indeed, in the context of SMC we are further required to choose the interpolating sequence $\{\pi_n, n \in \llbracket 0, P \rrbracket\}$ which we hereafter assume to arise as the discretization of a family of probability distributions $\{\pi(\cdot; \gamma), \gamma \in [0, 1]\}$ on $(\mathbf{X}, \mathcal{X})$, or “probability path”, such that $\pi(\cdot; 1) = \pi(\cdot)$. For example in a Bayesian context one may consider

$$\pi(dx; \gamma) \propto L^\gamma(x)\eta(dx), \tag{15}$$

where η is a probability distribution, the prior, and $L(\cdot)$ is the likelihood function, which is combined with the prior in a gradual way. Defining $\mu(dz; \gamma) := \pi(dx; \gamma)\varpi(dv)$ we therefore need to choose $\Gamma := (P, \{\gamma_i \in [0, 1], i \in \llbracket 0, P \rrbracket\}) \in \cup_{k=1}^\infty \{k\} \times \mathbb{R}_+^{k+1}$ to determine $\{\mu_n, n \in \llbracket 0, P \rrbracket\}$, and subsequently $\{\bar{\mu}_n, n \in \llbracket 0, P \rrbracket\}$ in the integrator snippet framework. For an SMC running along a probability path $\{\mu(\cdot; \gamma), \gamma \in [0, 1]\}$ and using an optimal backward kernel, Γ is usually constructed in a sequential manner as follows. For $n \geq 0$ define

$$\chi_{\gamma, n+1}(\gamma) := \mathbb{E}_{\mu_n} \left\{ \left(\frac{d\mu(\cdot; \gamma)}{d\mu_n}(z) \right)^2 \right\}, \tag{16}$$

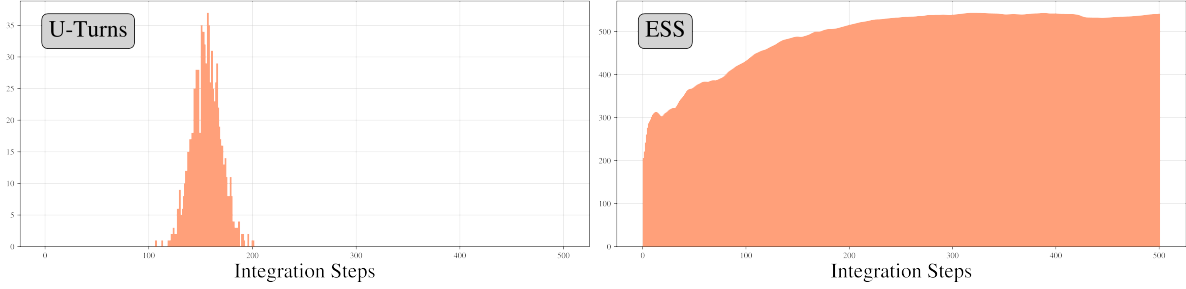


Figure 4: Illustration of information available about a the Leapfrog integrator in the particle population. For an SMC iteration, Left: histogram of the U-turn positions (k_u) across snippets, Right: average ESS along snippets for varying $k \in \llbracket T \rrbracket$.

then we have $\chi_{\gamma, n+1}(\gamma_n) = 1$, $\chi_n(\gamma) \geq 1$ from Jensen’s inequality and in typical scenarios one expects $\gamma \mapsto \chi_{\gamma, n+1}(\gamma)$ to be increasing for $\gamma \geq \gamma_n$. Note that the indexed γ should not be thought of as a value of the corresponding parameter, but as its name only; we use $\chi_\epsilon, \chi_\theta, \dots$ for other parameters and criteria below. This leads to the recursive definition

$$\gamma_{n+1} = \sup\{\gamma: \gamma_n \leq \gamma \leq 1, \chi_{\gamma, n+1}(\gamma) \leq \bar{\chi}_{\gamma, n+1}\} \wedge 1, \quad (17)$$

for some user defined $\bar{\chi}_{\gamma, n+1} > 1$, a user defined tolerance, hence defining $\{\mu_n, n \in \llbracket 0, P \rrbracket\}$, and subsequently $\{\bar{\mu}_n, n \in \llbracket 0, P \rrbracket\}$. This criterion is justified by results on self-normalized importance sampling bounds similar to those developed in Theorem (26). In practice this criterion is approximated with samples from μ_n obtained at the previous iteration of the SMC algorithm, defining the function estimate $\gamma \mapsto \hat{\chi}_{n+1, \gamma}(\gamma)$. Traditionally the above is formulated in terms of the so-called effective sample size (ESS) $N/\hat{\chi}_{n+1, \gamma}(\gamma)$ and the user defines a tolerance on the ESS scale.

In what follows we re-use and adapt some of these ideas in the context of IS²MC in order to define (γ_n, T_n) and the parameter of a distribution distribution on ϵ_n .

Integrator snippet SMC naturally provide extensive population level experimental information on the statistical properties arising from the use of an integrator in an SMC step, as illustrated in Fig. 4. This seems very promising to calibrate tuning parameters robustly. However, crucially, we show below that the mixture structure of the distributions targetted by integrator snippets, $\{\bar{\mu}_n, n \in \llbracket 0, P \rrbracket\}$, presents another opportunity to develop novel robust and computationally efficient adaptive SMC strategies to tune (τ, ϵ, T) .

3.2 Adapting γ only

Logistic regression for the Sonar dataset We consider sampling from the posterior distribution of a logistic regression model with a focus on estimating the normalizing constant, or evidence. Following [26] we consider the Sonar dataset, previously used as testbed in [23], which with covariates $\{\xi_i \in \mathbb{R}^{61}, i \in \llbracket 208 \rrbracket\}$ (containing intercept terms) and responses $\{y_i \in \{-1, 1\}, i \in \llbracket 208 \rrbracket\}$ has likelihood function

$$\mathbb{R}^{61} \ni x \mapsto L(x) = \prod_{i=1}^{208} (1 + \exp(-y_i \cdot \xi_i^\top x))^{-1}. \quad (18)$$

The prior distribution $\eta(x)$ is chosen to be a product of independent normal distributions with mean zero and standard deviation equal to 20 for the intercept and 5 for the other parameters. The probability path $\gamma \mapsto \pi(\cdot; \gamma)$ is then defined as in (15) and Γ determined sequentially using the standard approach described earlier.

We compare an Integrator Snippet and the implementation of Waste-Free SMC of [26], which uses a random walk Metropolis-Hastings kernel with covariance adaptively computed as $2.38^2 \hat{\Sigma}/d$, where $\hat{\Sigma}$ is the empirical covariance matrix obtained from the particles in the previous SMC step. For the Integrator Snippet we choose ψ_n to be the one-step Leapfrog integrator and $\varpi_n = \mathcal{N}(0, \text{Id})$.

HS selects the next tempering parameter using a commonly used ESS-based update [21], closely related to (16)-(17), and for both algorithms we target an ESS of $0.8N$ at each iteration. HS uses a stepsize of $\epsilon = 0.1$, selected using graduate descent to give good results. We will show in Section 3.3 that this value is automatically recovered by our adaptation strategy.

Fixed Budget Comparison We investigate the ability of the two algorithms to estimate the log-normalizing constant for a fixed total budget $N(T+1) = 10,000$, where for HS (resp. WF) N the number of seed particles (resp. number of Markov chain snippets) and T is the number of Leapfrog steps (resp. length of the Markov chain snippets). An important point is that both algorithms have comparable computational costs. Indeed the gradient $\nabla_x \log L(x)$ required by the Leapfrog integrator and $\log L(x)$ required for the evaluation of the weights $\bar{w}_{n,k}$ share the same costly terms as

$$\nabla_x \log L(x) = - \sum_{i=1}^{208} \frac{\exp(-y_i \cdot \xi_i^\top x)}{1 + \exp(-y_i \cdot \xi_i^\top x)} y_i \xi_i, \quad (19)$$

while the Metropolis-Hastings ratio of WF-SMC also requires the evaluation of $\log L(x)$.

Fig. 5 displays box-plots illustrating the variability and bias of the log-normalizing constant estimates across 100 independent runs of the two algorithms. We observe that for this fixed computational budget, what we interpret to be bias seems to increase together with variability for WF as the Markov snippets get shorter, whereas HS produces broadly consistent estimates for all (N, T) pairs considered. A similar bias in the WF estimates was observed with three independent code implementations: two separate implementations by the authors MCE and CZ and the original implementation available in the Particles package [22].

3.3 Adapting γ and ϵ for fixed T

We now focus on the scenario where T , i.e. the computational budget per iteration is fixed. Full adaptation of (ϵ, γ, T) is addressed in Section 3.4 and uses the update of this section.

3.3.1 Methodology

A mixture of competing integrator snippets In order to define and adaptive SMC able to select suitable stepsizes we first introduce the following instrumental “mother” probability distribution on which the target sequence $\{\bar{\mu}_n = \bar{\mu}(\cdot; \gamma_n, \theta_n), n \geq 0\}$ builds on. For a user defined family of probability distributions for ϵ , $\{\nu_\theta, \theta \in \Theta\}$ defined on $(\mathbb{R}_+, \mathcal{B}(\mathbb{R}_+))$, we consider $\bar{\mu}$ on $(\mathbb{Z} \times \mathbb{R}_+, \mathcal{Z} \otimes \mathcal{B}(\mathbb{R}_+))$ such that for $(\theta, \gamma) \in \Theta \times [0, 1]$

$$\bar{\mu}(k, d(\epsilon, z); \gamma, \theta) := \frac{1}{T+1} \mu(dz; \epsilon, \gamma, k) \nu_\theta(d\epsilon), \quad (20)$$

where $\mu(dz; \epsilon, \gamma, k) := \mu^{\psi_\epsilon^{-k}}(dz; \gamma)$, with $\mu(\cdot; \gamma)$ as defined below (17), and ψ_ϵ is the integrator using $\epsilon > 0$ as stepsize. As we shall see the idea is to let a population of stepsizes ϵ of distribution ν_θ compete, for a fitness criterion to be determined, and adjust this distribution, i.e. $\theta \in \Theta$, to focus on the most efficient values. As we shall see the

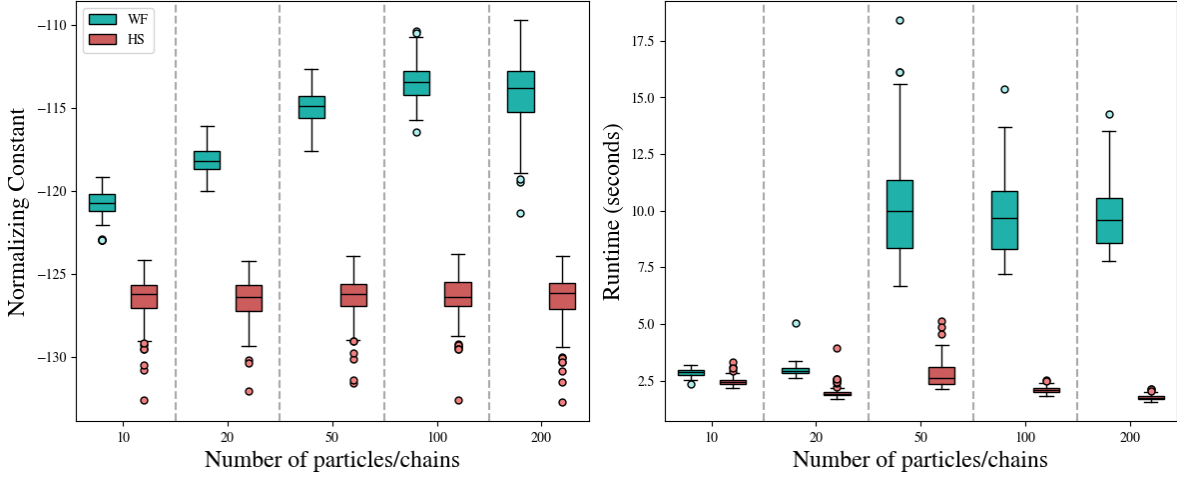


Figure 5: Left: Variability of the estimates of the log-normalizing constant for Waste-Free SMC (WF) and Hamiltonian Snippet (HS) for a fixed budget $N(T + 1) = 10000$. Right: Variability of runtime in seconds for the two algorithms. The lower runtime for HS is due to two factors: the lack of if-else statements to perform the MH accept-reject step, and no covariance estimation.

conditional independence structure of $\bar{\mu}$ plays a central rôle at several stages in our algorithm; additional details are provided in Appendix G.1 if needed. First, note that since for any $(k, \epsilon, \gamma) \in \mathbb{N} \times \mathbb{R}_+ \times [0, 1]$

$$\int f \circ \psi_\epsilon^k(z) \mu^{\psi_\epsilon^{-k}}(dz; \gamma) = \mu(f; \gamma),$$

we still retain the property that $\mathbb{E}_{\bar{\mu}(\cdot; \gamma, \theta)}(f \circ \psi_\epsilon^K(Z)) = \mu(f; \gamma) = \mathbb{E}_{\bar{\mu}(\cdot; \gamma, \theta)}\{\mathbb{E}_{\bar{\mu}(\cdot; \gamma, \theta)}(f \circ \psi_\epsilon^K(Z) \mid \epsilon, Z)\}$, or more explicitly,

$$\int \left\{ \sum_{k=0}^T \int f \circ \psi_\epsilon^k(z) \cdot \frac{d\mu^{\psi_\epsilon^{-k}}}{d\bar{\mu}}(z; \gamma, \epsilon) \bar{\mu}(dz \mid \epsilon; \gamma) \right\} \nu_\theta(d\epsilon) = \mu(f; \gamma).$$

Given this property, our goal is therefore to construct the sequence of target distributions $\{\bar{\mu}_n = \bar{\mu}(\cdot; \gamma_n, \theta_n), n \geq 0\}$ for some sequence $\{(\gamma_n, \theta_n) \in [0, 1] \times \Theta, n \geq 0\}$ determined sequentially to satisfy specific local criteria.

To optimize γ we use the update in (17), which departs from usual practice since one would normally consider the ESS for weighted particles representing $\{\bar{\mu}_n = \bar{\mu}(\cdot; \gamma_n, \theta_n), n \geq 0\}$, not $\{\mu_n, n \geq 0\}$. This would however incur a substantial computational cost since full snippets would have to be estimated for each value of γ used in the iterative algorithm used to achieve (17).

Performance measure for ϵ To optimise θ we use the straightforward adaptation of Proposition 5 to the multivariate scenario and aim to maximise the expected conditional variance of a user defined function $f: Z \rightarrow \mathbb{R}^m$, for some $m \in \mathbb{N}$, along snippets, that is with $\mathbb{E}_{\theta, \gamma}(\cdot) := \mathbb{E}_{\bar{\mu}(\cdot; \gamma, \theta)}(\cdot)$ we aim to maximise

$$\theta \mapsto \chi_\theta(\theta; \gamma) := \text{Tr} \left\{ \mathbb{E}_{\gamma, \theta} \left(\text{var}_{\gamma, \theta}(\bar{f}(\epsilon, K, Z) \mid \epsilon, Z) \right) \right\},$$

with, now, $\bar{f}(k, \epsilon, z) := f \circ \psi_\epsilon^k(z)$ – hereafter we focus on $f(z) = x$ for its intuitive interpretation, but other choices may be more suitable in particular applications. This quantity can be thought of as the averaged variance absorbed

by Rao-Blackwellization, interpretable here as Riemannian-like integration along snippets. With this criterion in hand we can now describe a new approach to tracking the optimal values of θ . Let $v_\gamma(\epsilon, z) := \text{Tr}[\text{var}_\gamma(\bar{f} \mid \epsilon, z)]$, which is indeed independent of θ , leaving f and T implicit for notational simplicity. Using the structure of $\bar{\mu}$ in detailed in Appendix G.1 one obtains

$$\begin{aligned}\chi_\theta(\theta; \gamma) &= \int v_\gamma(\epsilon, z) \bar{\mu}(d(\epsilon, z); \gamma, \theta) \\ &= \int v_\gamma(\epsilon, z) \bar{\mu}(dz \mid \epsilon; \gamma) \nu_\theta(d\epsilon).\end{aligned}\tag{21}$$

We briefly illustrate the relevance of this measure, that is its ability to discriminate between good and badly performing stepsizes. To that purpose we consider the following simple experiment, where we run Hamiltonian Snippet on the Sonar logistic regression problem with $N = 2500$, $T = 30$ and ν_θ is the uniform distribution over 18 log-linearly spaced step sizes between 0.001 and 10; θ has no use here and is therefore not adapted, but kept for pure notational consistency. At each iteration of the SMC algorithm, we estimate $\epsilon \mapsto \bar{v}_\gamma(\epsilon) := \int v_\gamma(\epsilon, z) \bar{\mu}(dz \mid \epsilon; \gamma)$ using (43). These quantities are displayed in Fig. 6 for four different values of the tempering parameter γ , as the SMC sampler progresses. Clearly some values of ϵ lead to a significantly larger variance reduction than others and the set of effective values evolves with γ , that is as the likelihood function is incorporated in the sampling. Notice in addition the asymmetry of the criterion around the mode: too large a stepsize leads to a sudden drop in performance while for smaller stepsizes deterioration is smoother. In the former scenario the integrator diverges from the underlying dynamic while in the latter the integrator is more precise but does not explore much of the space around the seed particle. Fig. 7 displays the same criterion but now as a function of γ for all the values of ϵ considered. We see clearly here that large values of ϵ are initially preferred for small values of γ as the target distribution is close to the prior distribution, a normal density, leading to a highly faithful integrator even for large stepsize values. Performance then drops sharply as the likelihood is incorporated and more moderate values of ϵ perform better. Interestingly the criterion is also able to discriminate between smaller values of ϵ for which the integrator is faithful across all temperatures γ , but among which some are more able to explore the space than others.

We note that [32, 13] have suggested an adaptive SMC relying on HMC which also relies on a population of stepsizes. However, their procedures focus on tuning parameters of a standard HMC-MH mutation kernel, not integrator snippets, and depart from the standard SMC framework by adaptively updating a population of stepsizes whose distribution is unspecified; we are not aware of any result justifying this approach.

Optimising with Bayes' rule An outline of the proposed procedure to update ν_θ is provided in Alg. 4 where $\tilde{\mu}(\cdot; \gamma, \theta)$ is the instrumental skewed probability distribution given by

$$\tilde{\mu}(d(\epsilon, z); \gamma, \theta) \propto v_\gamma(\epsilon, z) \nu_\theta(d\epsilon) \bar{\mu}(dz \mid \epsilon; \gamma).\tag{22}$$

In words, at iteration $n \geq 1$ one projects $\tilde{\mu}(\cdot; \gamma_{n-1}, \theta_{n-1})$, a distribution designed to give more weights to the better performing stepsizes, back onto the mother distribution $\{\bar{\mu}(\cdot; \gamma_{n-1}, \theta), \theta \in \Theta\}$ by minimizing the KL divergence $\theta \mapsto \text{KL}(\tilde{\mu}(\cdot; \gamma_{n-1}, \theta_{n-1}), \bar{\mu}(\cdot; \gamma_{n-1}, \theta))$ to obtain θ_n ; again this formulation is possible thanks to the conditional independence structure of $\bar{\mu}$. The intuition behind this choice is as follows. Given our current best guess of a distribution $\nu_{\theta_{n-1}}$ leading to a high average performance function $\theta \mapsto \chi_\theta(\theta; \gamma_{n-1})$ one can consider (and compute in practice) $\bar{\mu}_{n-1}(\cdot) = \bar{\mu}(\cdot; \gamma_{n-1}, \theta_{n-1})$ and find a new value θ_n which, a posteriori, would have led to a better average performance measure. This is achieved by adjusting θ_n in order to allocate more mass to better performing values of ϵ . This corresponds to the gradient-free algorithm recently studied in [1] where convergence is established in the scenario where the fitness function is time invariant and the variance of ν_θ made to vanish to ensure convergence to a point mass. In the present scenario one can only hope to track a sequence of high performing values.

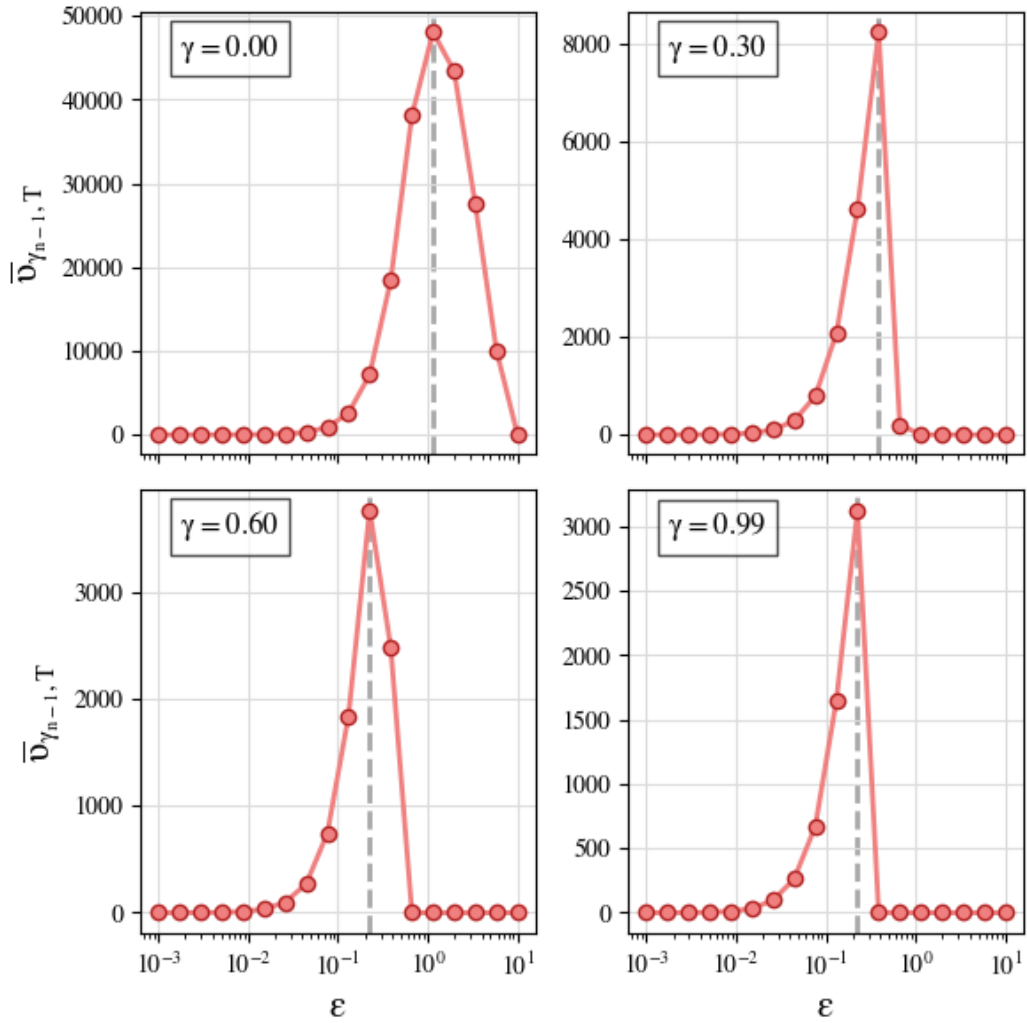


Figure 6: Estimates of $\epsilon \mapsto \bar{v}_{\gamma}(\epsilon) = \int v_{\gamma}(\epsilon, z) \bar{\mu}(dz | \epsilon; \gamma)$ for $\gamma = 0.0, 0.3, 0.6, 0.99$.

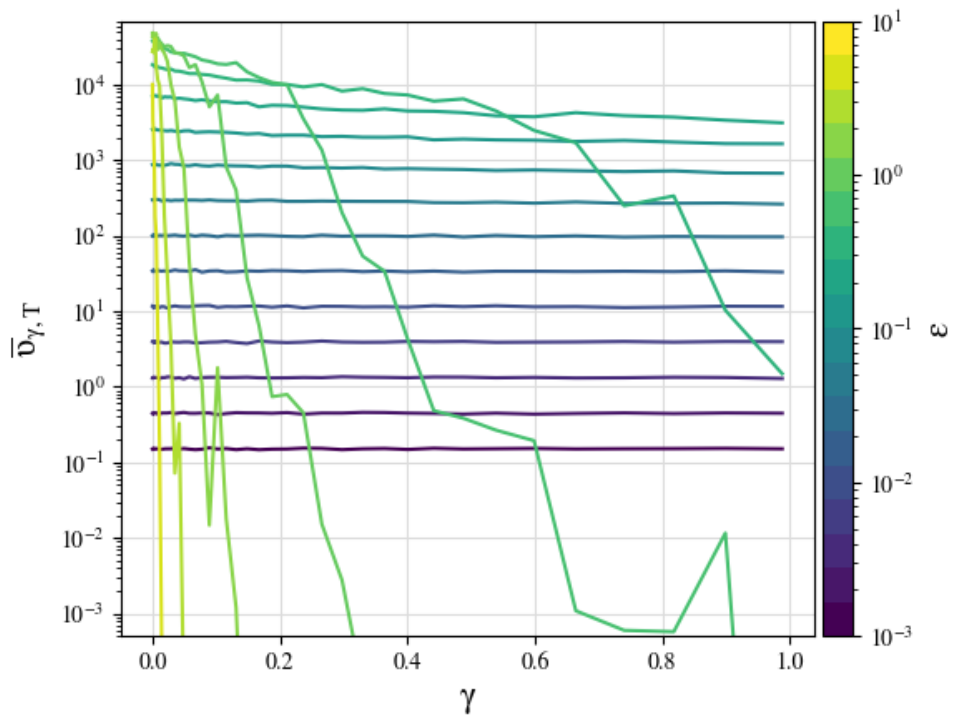


Figure 7: $\gamma \mapsto \bar{v}_{\gamma}(\epsilon)$ for a range of values of ϵ .

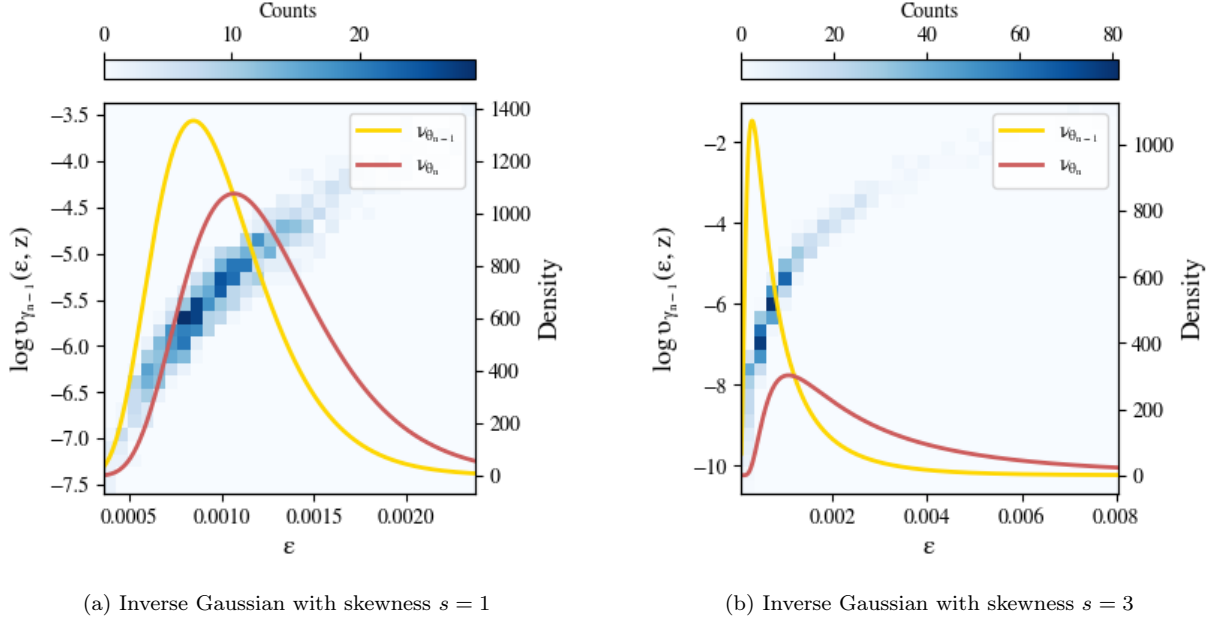


Figure 8: Illustration of the optimisation strategy.

We illustrate the optimisation strategy on Fig. 8a and 8b for ν_θ an inverse Gaussian distribution of skewness $s = 1$ and $s = 3$ respectively (see Appendix G.3 for details). The blue pixelated plot is a colour-coded histogram of the number of particles falling in cells of the $(\epsilon, \log(v_{\gamma_{n-1}}(\epsilon, z)))$ plane, superimposed with $\nu_{\theta_{n-1}}$ (yellow) and ν_{θ_n} (red), obtained by fitting ν_θ to $\nu_{\theta_{n-1}}$ skewed with $v_{\gamma_{n-1}}$ as in (22). The parameter s can be thought of as playing a rôle similar to that of the magnitude of a stepsize in a learning algorithm: a higher value can lead to faster exploration, but too high a value can also cause instability.

- 1 For $n \geq 0$, given the distribution $\bar{\mu}_n(\cdot) = \bar{\mu}(\cdot; \gamma_n, \theta_n)$ with $\bar{\mu}$ in (20).
- 2 Set $\gamma_{n+1} = \sup\{\gamma: \gamma_n \leq \gamma \leq 1, \chi_{\gamma, n+1}(\gamma) \leq \bar{\chi}_{\gamma, n}\} \wedge 1$, with $\chi_{\gamma, n+1}$ in (16).
- 3 Set

$$\theta_{n+1} = \arg \min_{\theta} \text{KL}(\tilde{\mu}(\cdot; \gamma_n, \theta_n), \bar{\mu}(\cdot; \gamma_n, \theta)).$$

- 4 Set $\bar{\mu}_{n+1}(\cdot) = \bar{\mu}(\cdot; \gamma_{n+1}, \theta_{n+1})$

Algorithm 4: Adapting ϵ and γ : sequential definition of $\{\bar{\mu}_n = \bar{\mu}(d(\epsilon, z); \gamma_n, \theta_n), n \geq 0\}$

Implementational details are provided in Appendix G.

3.3.2 Simulations

Logistic regression for the Sonar dataset We return to the Logistic Regression problem considered in Section 3.2. In order to test performance of our adaptive algorithm, we set up the following experiment. We fix $T = 30$, $N = 500$ and select 9 values of stepsizes log-linearly spaced between 0.001 and 10.0 used to determine the initial

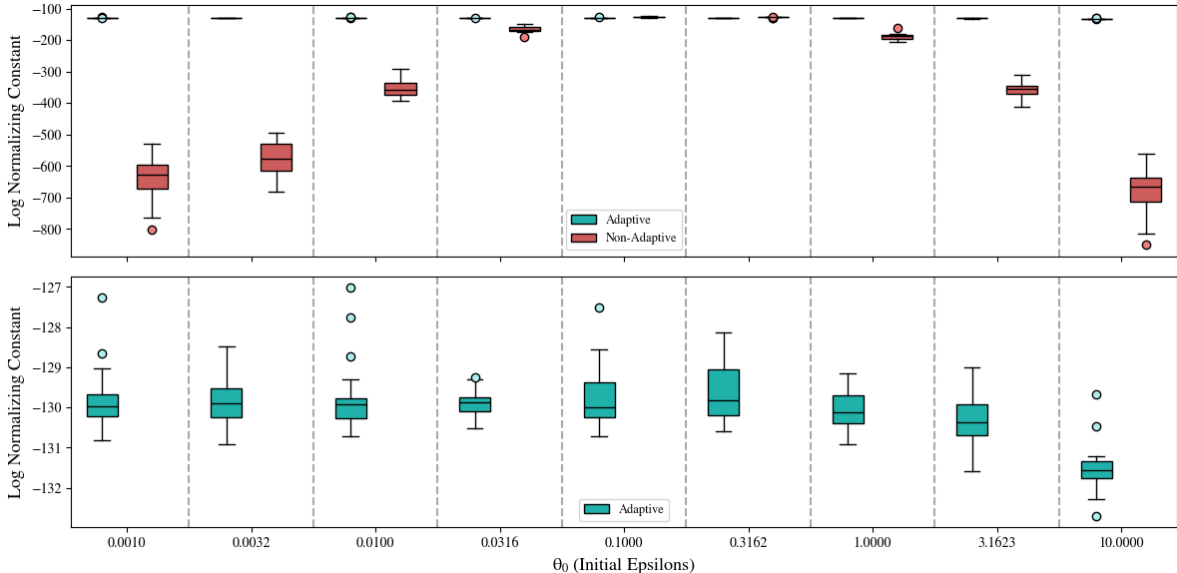


Figure 9: Boxplots of the estimates of the log normalizing constant as a function of different initial ϵ values provided by the user. Green boxplots show the results for an adaptive integrator snippet, red boxplots show estimates for the non-adaptive version.

stepsizes provided by the user to the algorithm. For each of these values, we run 20 independent runs of two versions of our integrator snippet. One version, non-adaptive, uses one of the 9 values as unique stepsize for all particles and keeps it fixed throughout the entire run. The second version, adaptive, uses the same value as the initial mean of ν_θ , again taken to be an inverse Gaussian with fixed skewness (see Appendix G.3) whose parameter is then adapted throughout the algorithm; for the inverse Gaussian this means that θ_0 is set to those predefined values.

The results of this experiment are shown in Fig. 9. In the top pane we compare the box plots of the estimates of the log-normalising constant for both algorithms, across all values of ϵ on the x-axis. Remarkably, our adaptive algorithm is able to maintain stable estimates over a range of initial values of ϵ that spans five orders of magnitude. In contrast, the non-adaptive algorithm presents precise estimates for $\epsilon = 0.1, 0.3$ but rapidly accumulates bias and variance. The bottom pane displays the boxplots for the adaptive algorithm only in order for the stability of the results to be better appreciated. We notice that compared to Fig. 5, we have accumulated a small bias but have gained remarkable robustness with respect to our initial guess of suitable stepsize magnitudes.

Fig. 10 displays boxplots of the final mean of ν_θ for the adaptive algorithm. Despite the wide range of initial stepsizes considered, the final means found by the algorithm are exceptionally stable and settle around 0.175. Fig. 22 displays boxplots representing ν_θ for different initializations of θ_0 , its mean parameter. We emphasize here that the y-axis uses a log scale and that our adaptive algorithm is able to recover the optimal step size value across 9 orders of magnitude. We note however, that for the most extreme initialisation values, the normalising constant estimates, whose computations relies on quantities computed at every SMC iteration, were observed to be heavily biased and variable due to bad performance in the early stages; these results are not reported here.

Log cox model for the Finnish Pines dataset In this paragraph we repeat the experiments above on a Log-Gaussian Cox model for the the Finnish Pines dataset considered in [33], [13] and [25]. In the Leapfrog integrator,

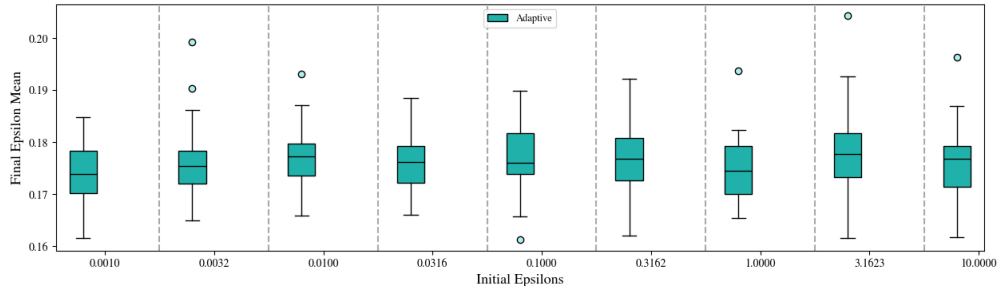


Figure 10: Boxplots of the mean of the distribution ν_θ on the final iteration of the adaptive integrator snippet.

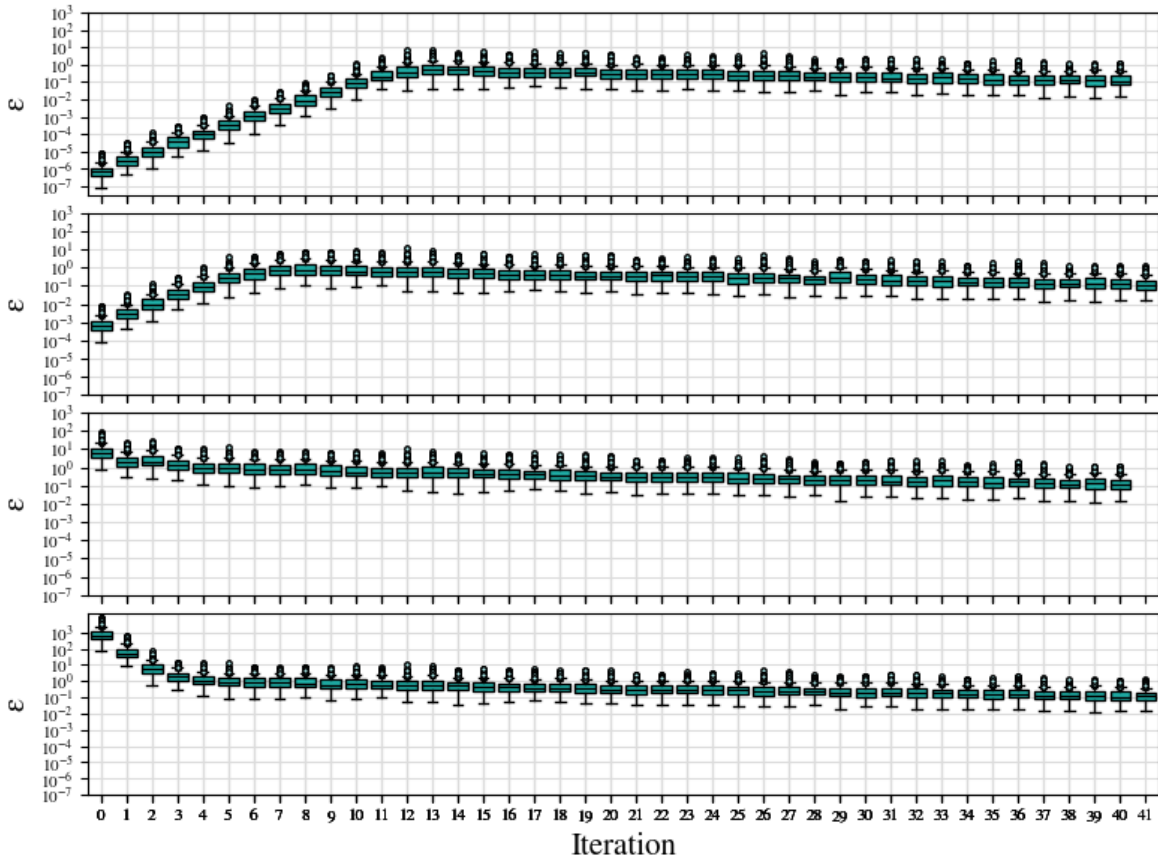


Figure 11: Evolution of ν_θ for different initializations of the initial epsilon mean $\theta_0 = 10^{-6}, 10^{-3}, 10, 10^3$

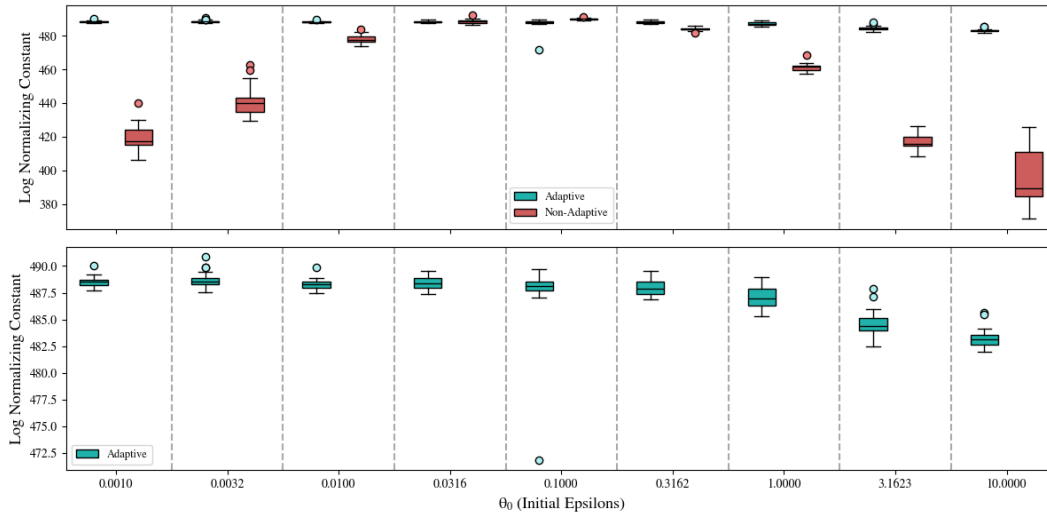


Figure 12: Boxplots of the estimates of the log normalizing constant for the Log-Gaussian Cox problem as a function of different initial epsilons provided by the user. Teal boxplots show the results for an adaptive Hamiltonian snippet (with ν_θ an Inverse Gaussian distribution with fixed skewness $s = 3$), red boxplots show estimates for the non-adaptive version.

we use the following metric tensor

$$M_\gamma = \gamma\Lambda + \Sigma^{-1}, \quad \Lambda_{ii} = (1/d_{\text{grid}}^2) \exp(\mu + \Sigma_{ii})$$

where μ is the (scalar) mean of the Gaussian process, Σ is the prior covariance matrix and d_{grid} is the dimensionality of our grid discretization. Fig. 12 shows the estimates of the log normalizing constants for our adaptive algorithm, using $N = 500$, $T = 30$ and a fixed skewness of $s = 3$ (so that the standard deviation of ν_θ is equal to its mean parameter). We can see that estimates for our adaptive algorithm are relatively stable for a wide range of initial mean parameters, with performance decreasing only for $\theta_0 = 3.1623, 10$. As for the Sonar problem, Fig. 13 shows that we consistently reach a value around 0.19 for the final mean parameter θ_P , which is very close to the value of 0.17 set manually in [36], see [40]. Furthermore, we briefly remark that we have found the ESS criterion (of $\bar{\mu}_n$) to be a highly unreliable metric for quantifying the performance of the algorithms, as shown in Fig. 14, as according to that metric $\theta_0 = 0.0032, 0.01, 0.0316$ would be the best step sizes for our non-adaptive Hamiltonian Snippet, but this is in stark contrast with Fig. 12 where we see that the corresponding log normalizing constant estimates are way off. Finally, Fig.15 displays the distribution ν_{θ_n} as a function $n \in \llbracket P \rrbracket$ for four values of θ_0 spanning 10 orders of magnitude. All four plots present a clear progression towards the optimal value and no oscillatory behavior, highlighting remarkable robustness of this adaptation approach.

3.4 Full adaptation

Adapting T offers the promise of reduced computations on an intrinsically sequential step of the procedure, and hence not parallelisable. Conceptually our focus is on determining an efficient effective integration time τ associated with Hamilton's flow since it is independent of (ϵ, T) , and can therefore be estimated using any such available pair.

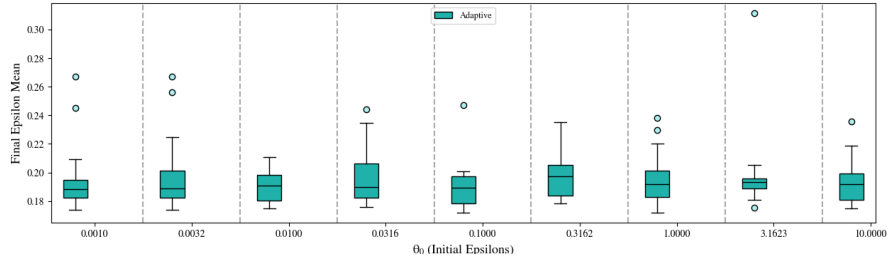


Figure 13: Boxplots of θ_P , the mean parameter of the distribution ν_θ on the final iteration of the adaptive integrator snippet, for the Log-Gaussian Cox problem.

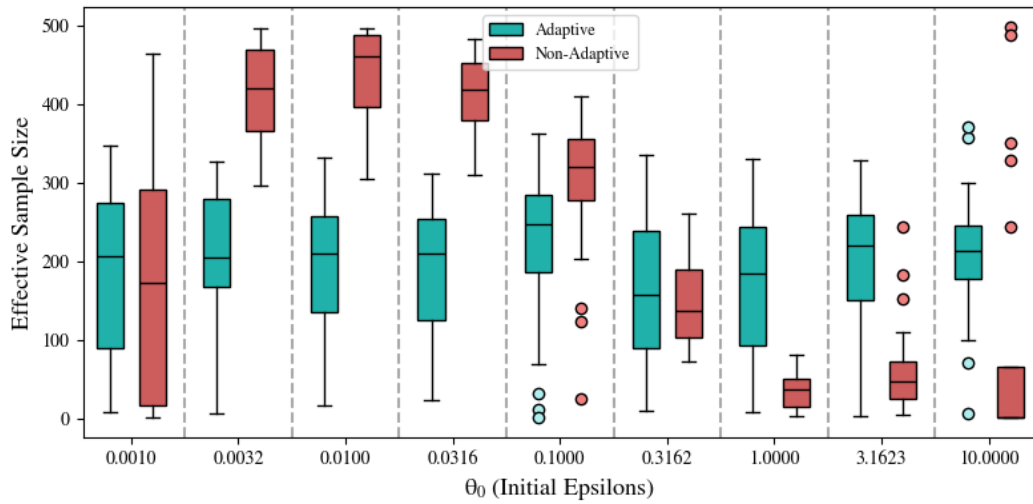


Figure 14: Boxplots of the final ESS for an adaptive and non-adaptive Hamiltonian Snippet.

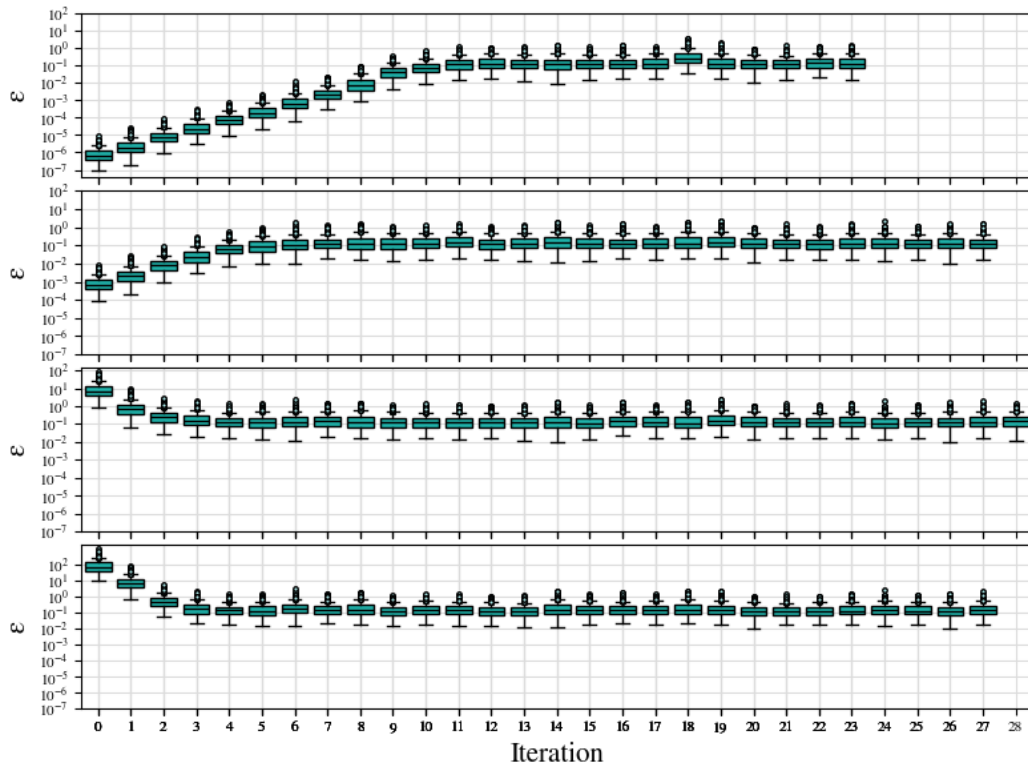


Figure 15: Boxplots of the estimates of the log normalizing constant for the Log-Gaussian Cox problem as a function of different initial epsilons provided by the user. Teal boxplots show the results for an adaptive Hamiltonian snippet (with ν_θ an Inverse Gaussian distribution with fixed skewness $s = 3$), red boxplots show estimates for the non-adaptive version.

3.4.1 Methodology

Our proposed tuning of ϵ for fixed T relies on a variance control argument. To choose τ we aim to optimise ergodicity of the mutation kernel \bar{M}_n in (11), that is its ability to forget initialisation. To that purpose our strategy relies on a coupling argument which can be motivated by the theoretical notion of Ricci curvature, which we review briefly.

Motivation Consider the Wasserstein distance between probability distributions ν_1 and ν_2 on X ,

$$W_1(\nu_1, \nu_2) = \min_{\nu \in \mathsf{C}(\nu_1, \nu_2)} \int \|y^{(1)} - y^{(2)}\| \nu(\mathrm{d}(y^{(1)}, y^{(2)})), \quad (23)$$

where $\mathsf{C}(\nu_1, \nu_2)$ is the set of couplings of (ν_1, ν_2) , that is the set of distributions ν of marginals ν_1 and ν_2 . Given a Markov kernel $Y \sim P(x, \cdot)$ its Ricci curvature is defined as $\mathrm{Ric}(P) = 1 - \kappa$ where

$$\kappa := \sup_{x^{(1)} \neq x^{(2)}} \frac{W_1(P(x^{(1)}, \cdot), P(x^{(2)}, \cdot))}{\|x^{(1)} - x^{(2)}\|},$$

see [49, 50] and also earlier ideas [57], related thanks to Kantorovich-Rubinstein duality. This can be thought of as a uniform measure of overlap between the distributions $P(x^{(1)}, \cdot)$ and $P(x^{(2)}, \cdot)$ or a measure of independence on $x^{(1)}$ and $x^{(2)}$ after one step of the Markov chain. It is particularly well suited to studying Markov chains defined via random mappings $Y^{(i)} = \varphi(x^{(i)}, U^{(i)})$ for random variables $U^{(i)}$, as suggested by the definition (23). These ideas have been used to study HMC-MCMC [20] using coupling techniques; see [6] for applications using an alternative formulation.

Coupling SMC particles Our criterion to estimate the effective integration time at SMC iteration $n \geq 1$ (see Alg. 3) from T_n , shared by all particles, and $\{(\epsilon_n^{(i)}, z_n^{(i)}), i \in \llbracket N \rrbracket\}$ is motivated by the mapping contractivity ideas above and takes advantage of the population of samples provided by SMC samplers. Full details of the procedure are given in Alg. 5 and we provide additional comments here. We describe a procedure based on $\{(\epsilon_n^{(i)}, z_n^{(i)}), i \in \llbracket N \rrbracket\}$ rather than $\{(\check{\epsilon}_n^{(i)}, \check{z}_n^{(i)}), i \in \llbracket N \rrbracket\}$ as the distribution of these points turns out to be of limited importance when interest is in a proxy for κ . We create $M \in \mathbb{N}$ pairs of distinct particles chosen at random and couple them by assigning each pair with either of their velocities and stepsizes, say $\{(v_j, \epsilon_j), j \in \llbracket M \rrbracket\}$, as their common corresponding quantities; more sophisticated couplings are possible but we have found this simple choice to work well for our purpose. We then compute the local contraction coefficients $\{\kappa_{j,m}, (j, m) \in \llbracket M \rrbracket \times \llbracket 0, T_n \rrbracket\}$ as in (24) in Alg. 5 and the corresponding effective integration times $\{\tau_{j,m} = m \times \epsilon_j, (j, m) \in \llbracket M \rrbracket \times \llbracket 0, T_n \rrbracket\}$. We note the following points. We here ignore the weights involved in the definition of \bar{M}_{n+1} , and implicitly replace them with uniform weights instead, for simplicity. This has nonetheless led to satisfactory results and we have not tested a weighted version of our work. In addition we conjecture that our choice has the additional advantage that it further decouples the choice of τ from the quality of the integrator, which is handled by the separate adaptation of ϵ . Naturally half of the snippets involved in the computation of $\{\kappa_{j,m}, (j, m) \in \llbracket M \rrbracket \times \llbracket 0, T_n \rrbracket\}$ can be recycled and used in the next SMC iteration by ignoring either of the coupled particles.

A direct approach to upperbounding κ could consist of using, for $k \in \llbracket 0, T_n \rrbracket$ and $\Psi_{\epsilon, x}(z, \cdot) := \delta_{\psi_{\epsilon, x}(z)}(\cdot)$, a Nadaraya-Watson estimator (or any nonlinear regression technique) of

$$(\epsilon, k, x^{(1)}, x^{(2)}) \mapsto \kappa(\epsilon, k, x^{(1)}, x^{(2)}) := \frac{\int \|\Psi_{\epsilon, x}^k(x^{(1)}, v; \cdot), \Psi_{\epsilon, x}^k(x^{(2)}, v; \cdot)\| \varpi(\mathrm{d}v)}{\|x^{(1)} - x^{(2)}\|},$$

and aim to minimise, $(\epsilon, k) \mapsto \sup_{x^{(1)}, x^{(2)}} \kappa(\epsilon, k, x^{(1)}, x^{(2)})$ on the set of available values of $k, \epsilon_n^{(i)}$ and $x_n^{(i_{j,1})}, x_n^{(i_{j,2})}$. This appears involved and potentially unreliable. Further, for a given π_n , there is no reason for the leapfrog

integrator to define a uniformly contracting mapping for any (k, ϵ) combination, although this is the case in the strongly convex, L -smooth scenario [20].

```

1 Given  $T_n$  and  $\{(\epsilon_n^{(i)}, z_n^{(i)}), i \in \llbracket N \rrbracket\}$  as in Alg. 3.
2 for  $j \in \llbracket M \rrbracket$  do
3   Draw  $(i_{j,1}, i_{j,2}) \sim \mathcal{U}(\llbracket N \rrbracket^2)$  subject to  $x_n^{(i_{j,1})} \neq x_n^{(i_{j,2})}$ .
4   Define the instrumental particle pairs, for  $v_j = v_n^{(i_{j,1})}$ ,  $\epsilon_j = \epsilon_n^{(i_{j,1})}$ 
      
$$\left( \mathfrak{z}_{1,j} = (\epsilon_j, x_n^{(i_{j,1})}, v_j), \mathfrak{z}_{2,j} = (\epsilon_j, x_n^{(i_{j,2})}, v_j) \right).$$

5   for  $m \in \llbracket 0, T_n \rrbracket$  do
6     Compute  $\tau_{j,m} = m \times \epsilon_j$  and the local contraction coefficients
      
$$\kappa_{j,m} = m^{-1} \sum_{k=0}^m \|\psi_{n+1,x}^k(\mathfrak{z}_{1,j}) - \psi_{n+1,x}^k(\mathfrak{z}_{2,j})\| / \|x_n^{(i_{j,1})} - x_n^{(i_{j,2})}\| \quad (24)$$

7   end
8 end
9 Define a grid of bin centres  $\check{\tau}_0 = -\check{\tau}_1, \check{\tau}_1 < \dots < \check{\tau}_b < \check{\tau}_{b+1} = \check{\tau}_b > \max\{\tau_{j,m}\}$ .
10 for  $i \in \llbracket b \rrbracket$  do
11   Compute
      
$$\bar{\kappa}_i := \frac{\sum_{(j,m) \in \llbracket M \rrbracket \times \llbracket 0, T_n \rrbracket} \kappa_{j,m} \mathbf{1}\{(\check{\tau}_{i-1} + \check{\tau}_i)/2 \leq \tau_{j,m} < (\check{\tau}_i + \check{\tau}_{i+1})/2\}}{\sum_{(j,m) \in \llbracket M \rrbracket \times \llbracket 0, T_n \rrbracket} \mathbf{1}\{(\check{\tau}_{i-1} + \check{\tau}_i)/2 \leq \tau_{j,m} < (\check{\tau}_i + \check{\tau}_{i+1})/2\}} \quad (25)$$

12 end
13 Set

```

$$\begin{aligned} \tau_n &= \min\{\check{\tau}_i : i \in \arg \min\{\bar{\kappa}_j : j \in \llbracket b \rrbracket\}\}, \\ T_{n+1} &= T_{\max} \wedge \lceil \tau_n / \text{median}(\{\epsilon_n^{(j)}, j \in \llbracket N \rrbracket\}) \rceil. \end{aligned} \quad (26)$$

Algorithm 5: Estimating τ_n and choosing T_{n+1}

Binned Average of the Integration Times Our approach is as follows. Given the pairs $\{(\tau_{j,m}, \kappa_{j,m}), (j, m) \in \llbracket M \rrbracket \times \llbracket 0, T_n \rrbracket\}$ we would like to solve the regression problem $\tau \mapsto \kappa(\tau)$ and set

$$\tau_n = \min\{\tau > 0 : \tau \in \arg \min\{\kappa(\tau') : \tau' > 0\}\}, \quad (27)$$

that is set τ_n to the smallest effective integration time minimising $\kappa(\tau)$. As illustrated in Fig. 16-20, where curves $m \mapsto (\tau_{j,m}, \kappa_{j,m})$ are displayed for an example and four SMC iterations, the data is unbalanced in that pairs with larger effective integration times $\tau_{j,m}$ are less frequent. There is a multitude of estimation techniques for this type of situations. Here we have focussed on a simple minded approach, which has proved sufficiently robust for our purpose. Define a grid of b bin centres $\check{\tau}_0 = -\check{\tau}_1, \check{\tau}_1 < \dots < \check{\tau}_b < \check{\tau}_{b+1} = \check{\tau}_b > \max\{\tau_{j,m}\}$, we then compute for $i \in \llbracket b \rrbracket$ the bin average contraction coefficients $\bar{\kappa}_i$ in (25). We then set τ_n to the empirical version of (27) in (26). Finally this now needs to be translated into the number of integration steps T_n . Here the strategy consists of

choosing T_{n+1} in such a way that the distance $|T_{n+1}\epsilon_n^{(i)} - \tau_n|$ is minimised in a statistical sense. A possible choice, presented here when $N \rightarrow \infty$, is

$$\arg \min_{T>0} \int |T\epsilon - \tau_n| \nu_{\theta_n}(\mathrm{d}\epsilon),$$

which is achieved for $\tau_n/T = \text{median}(\nu_{\theta_n})$, therefore leading to a $T_{n+1} = \lceil \tau_n / \text{median}(\nu_{\theta_n}) \rceil$ for iteration $n + 1$ of the SMC algorithm. The empirical version given in (26). In order to avoid incurring unnecessary high costs when the initial effective integration time provided by the user is much smaller than the optimal one, we clip this value T_{n+1} to the maximum value T_{\max} , corresponding to the user’s maximum budget.

3.4.2 Simulations

We ran experiments adapting both ϵ and T on the Sonar example of Section 3.2. Fig. 16 shows the contractivity curves as a function of the effective integration time, as well as the binned average and the resulting minimum τ_n for the third iteration of a Hamiltonian Snippet initialized with $N = 500$, $T = 100$, $\theta_0 = 0.001$ and skewness 3. The left pane demonstrates how the binned average is very effective at locating the minimum, even when this minimum is reached only by a handful of trajectories (see the histogram on the right hand side). Fig. 17 shows the same curves at the 30th iteration when much more data has been assimilated through tempering and thus the target is harder to navigate. Importantly, we see that even though some trajectories do not contract, and even blow up, our binned average approach remains stable and is still able to choose τ appropriately.

Due to estimation errors the procedure may mistakenly not choose the first encountered trough, as shown in Fig. 18 where the initial θ_0 was set to a large value. However, as shown in Fig. 19, at the next iteration the algorithm has already identified the second trough and by the third iteration in Fig. 20 has fully recovered.

Fig. 21 shows the final values of τ obtained from 20 runs of our adaptive algorithm starting from $T_0 = 80$. Fig. 22 shows the evolution of the optimal T_n as a function of the tempering parameter. Since the optimal stepsize is around 0.18 we can see that smaller stepsizes keep T_n to its maximum value for a longer time than larger stepsizes.

The strong regularity of the contractivity curves may seem surprising, if not suspicious. However one can establish that the likelihood function of a logistic regression model is m -strongly convex and L -smooth [3, Example 33], the scenario covered by [20]; this may be part of the explanation. We have observed similar regularity on other models and are currently investigating this point separately, included more localized adaptation of T_n .

4 Discussion

We have shown how mappings used in various Monte Carlo schemes relying on numerical integrators of ODE can be implemented to fully exploit all computations to design robust and efficient sampling algorithms. We have shown that the general framework we have identified, relying on a mixture of distributions obtained as pushforwards of the distribution of interest, facilitates the design of new algorithms, in particular adaptive algorithms. Numerous questions remain open, including the tradeoff between N and T . A precise analysis of this question is made particularly difficult by the fact that integration along snippets is straightforwardly parallelizable, while resampling does not lend itself to straightforward parallelisation.

Another point is concerned with the particular choice of mutation Markov kernel \bar{M}_n , or \bar{M} , in (11) or (35). Indeed such a kernel starts with a transition from samples approximating the snippet distribution $\bar{\mu}_{n-1}$ to μ_{n-1} , which is then followed by a reweighting of samples leading to a representation of $\bar{\mu}_n$. Instead, for illustration, one could suggest using an SMC sampler with (53) as mutation kernel.

In relation to the discussion in Remark 28, a natural question is how our scheme would compare with a ‘‘Rao-Blackwellized’’ SMC where weights of the type (49), derived from (6) are used.

We leave all these questions for future investigations.

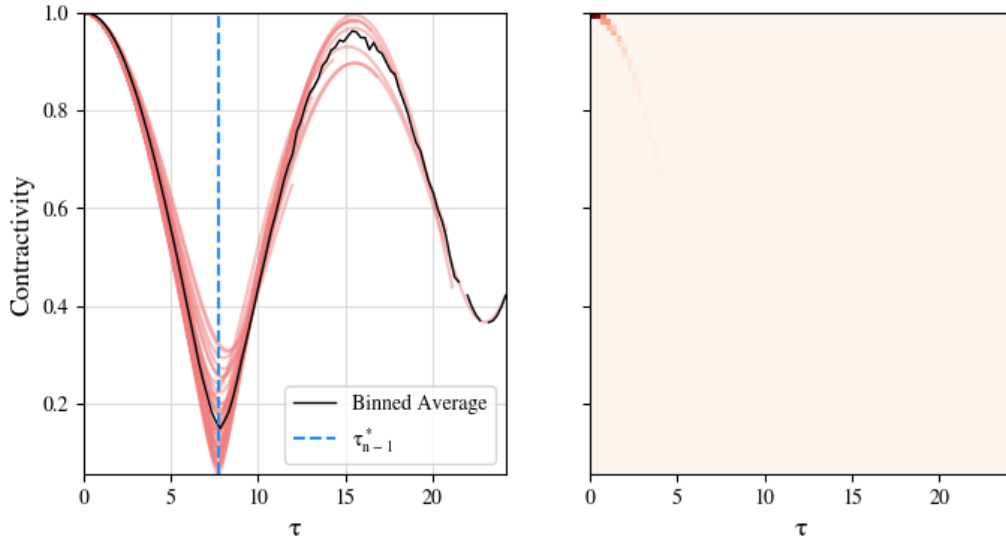


Figure 16: Left: Contractivity curves $m \mapsto \kappa_{j,m}$ for all $M = N/2$ pairs of coupled trajectories (red) binned averages $m \mapsto \bar{\kappa}_m$ (black) and the minimum, τ_n . Right: 2D histogram illustrating the number of snippets achieving a given contraction level at time τ . SMC iteration 3, $\theta_0 = 0.001$.

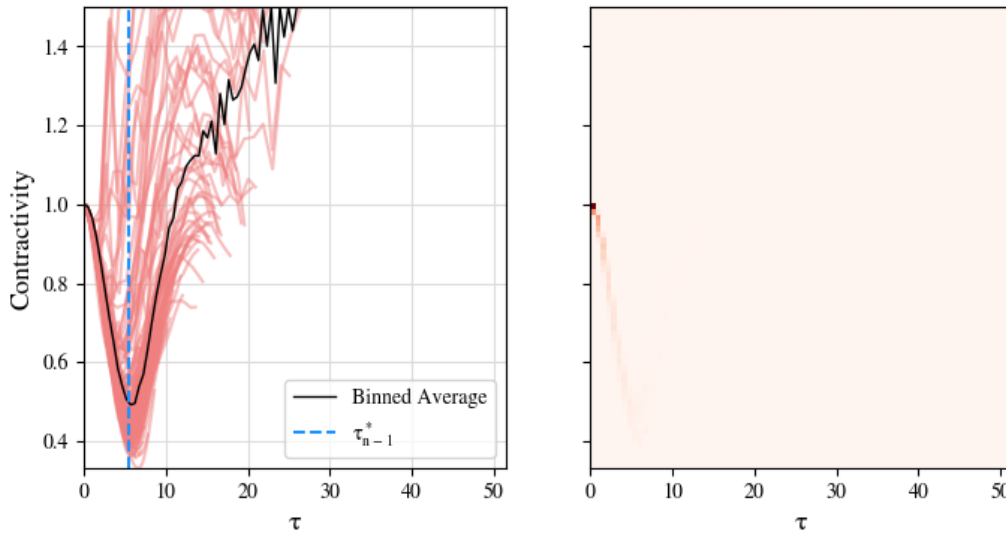


Figure 17: Left: Contractivity curves $m \mapsto \kappa_{j,m}$ for all $M = N/2$ pairs of coupled trajectories (red) binned averages $m \mapsto \bar{\kappa}_m$ (black) and the minimum, τ_n . Right: 2D histogram illustrating the number of snippets achieving a given contraction level at time τ . SMC iteration 30, $\theta_0 = 0.001$.

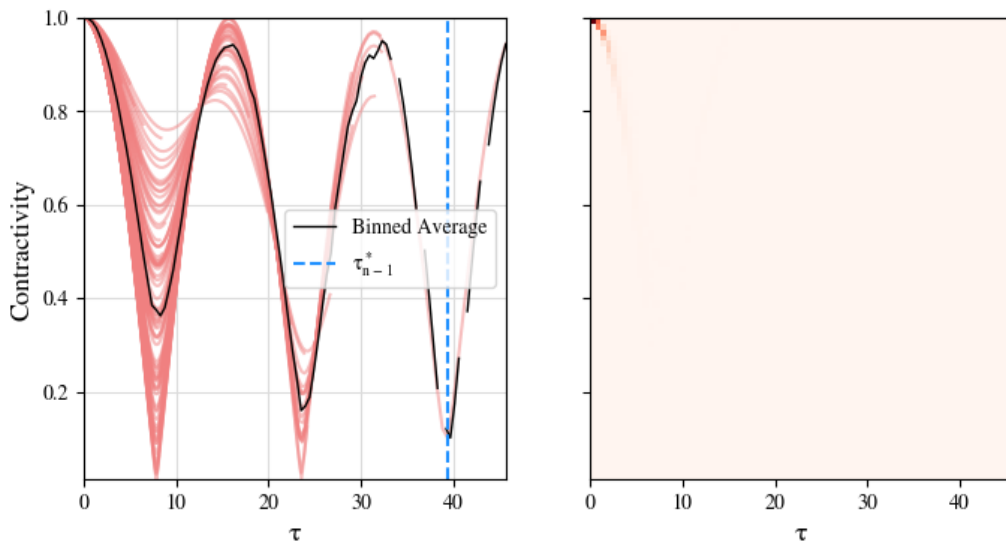


Figure 18: Left: Contractivity curves $m \mapsto \kappa_{j,m}$ for all $M = N/2$ pairs of coupled trajectories (red) binned averages $m \mapsto \bar{\kappa}_m$ (black) and the minimum, τ_n . Right: 2D histogram illustrating the number of snippets achieving a given contraction level at time τ . We can see that due to noise the binned average resulted lower on the third trough whereas visually we can notice that the first trough reaches a smaller contractivity. SMC iteration 1, $\theta_0 = 0.1$.

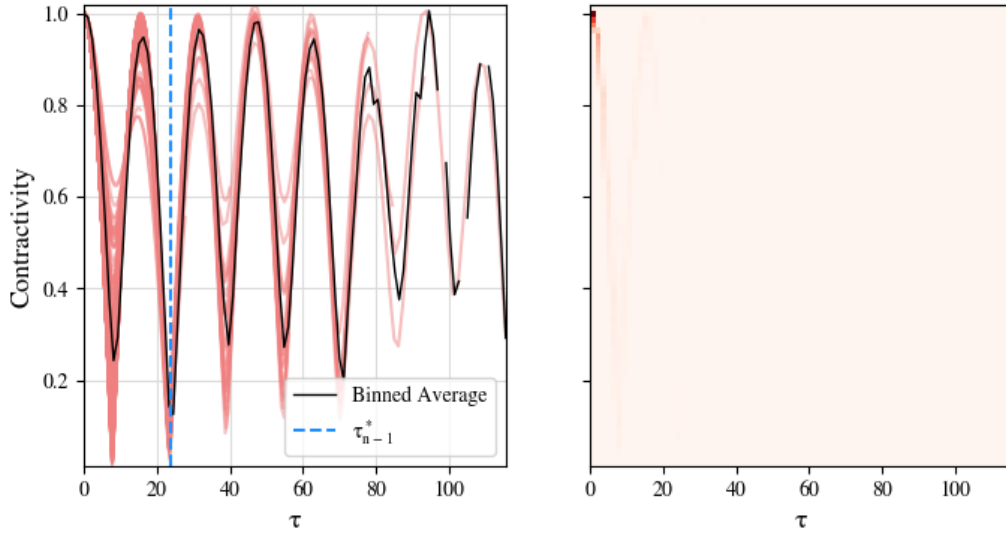


Figure 19: Left: Contractivity curves $m \mapsto \kappa_{j,m}$ for all $M = N/2$ pairs of coupled trajectories (red) binned averages $m \mapsto \bar{\kappa}_m$ (black) and the minimum, τ_n . Right: 2D histogram illustrating the number of snippets achieving a given contraction level at time τ . At the second iteration it has identified the second trough. SMC iteration 2, $\theta_0 = 0.1$.

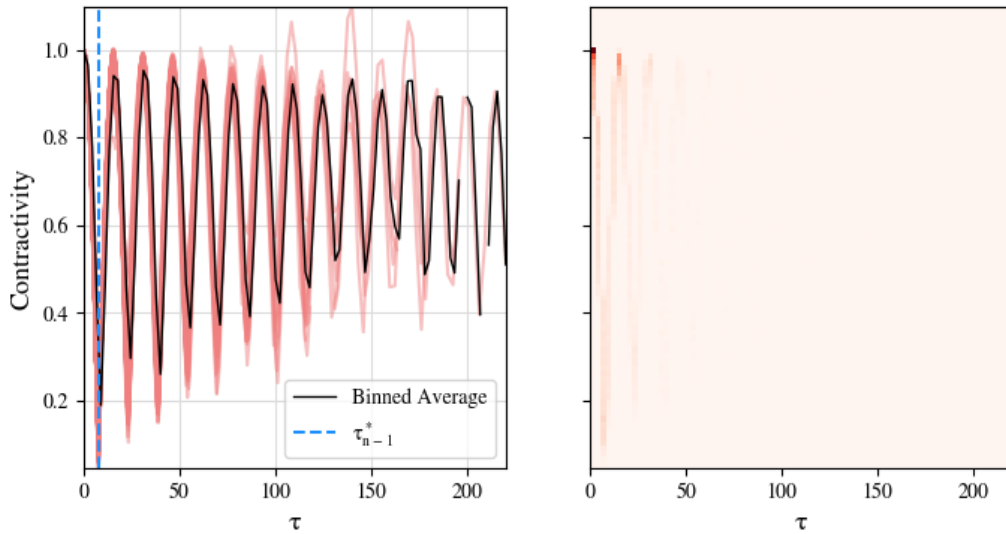


Figure 20: Left: Contractivity curves $m \mapsto \kappa_{j,m}$ for all $M = N/2$ pairs of coupled trajectories (red) binned averages $m \mapsto \bar{\kappa}_m$ (black) and the minimum, τ_n . Right: 2D histogram illustrating the number of snippets achieving a given contraction level at time τ . At the third iteration it has identified the first trough. SMC iteration 3, $\theta_0 = 0.1$.

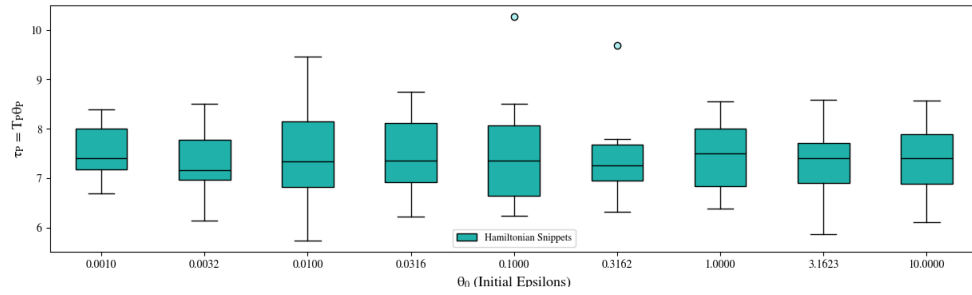


Figure 21: Boxplots of final integration time $\tau_P = T_P \times \theta_P$ over 20 runs of our adaptive Hamiltonian Snippet, for different initial values of θ_0 , the mean of ν_θ .

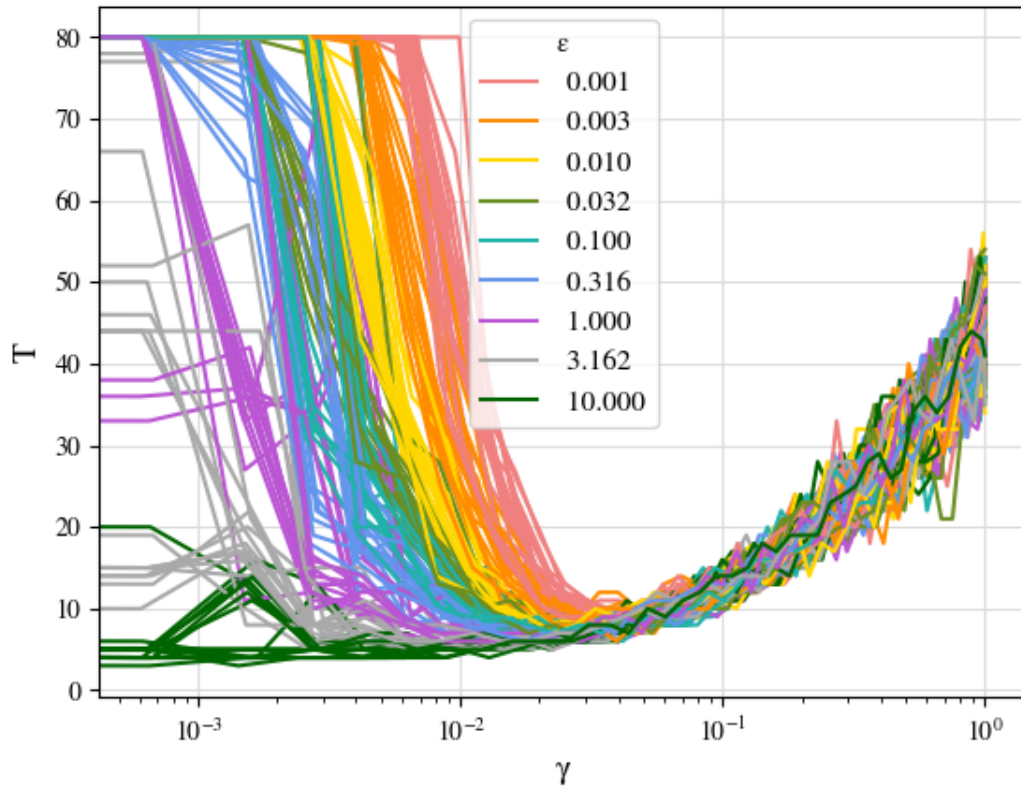


Figure 22: Evolution of the number of leapfrog steps as a function of iteration, for various different initial means of the epsilon distribution.

Acknowledgements

The authors would like to thank Carl Dettmann for very useful discussions on Boltzmann's conjecture. Research of CA and MCE supported by EPSRC grant 'CoSInES (COmputational Statistical INFerence for Engineering and Security)' (EP/R034710/1), and EPSRC grant Bayes4Health, 'New Approaches to Bayesian Data Science: Tackling Challenges from the Health Sciences' (EP/R018561/1). Research of CZ was supported by a CSC Scholarship.

A Notation and definitions

We will write $\mathbb{N} = \{0, 1, 2, \dots\}$ for the set of natural numbers and $\mathbb{R}_+ = (0, \infty)$ for positive real numbers. Throughout this section $(\mathbf{E}, \mathcal{E})$ is a generic measurable space.

- For $A \subset \mathbf{E}$ we let A^c be its complement.
- $\mathcal{M}(\mathbf{E}, \mathcal{E})$ (resp. $\mathcal{P}(\mathbf{E}, \mathcal{E})$) is the set of measures (resp. probability distributions) on $(\mathbf{E}, \mathcal{E})$
- For a set $A \in \mathcal{E}$, its complement in \mathbf{E} is denoted by A^c . We denote the corresponding indicator function by $\mathbf{1}_A : \mathbf{E} \rightarrow \{0, 1\}$ and may use the notation $\mathbf{1}\{z \in A\} := \mathbf{1}_A(z)$.
- For μ a probability measure on $(\mathbf{E}, \mathcal{E})$ and a measurable function $f : \mathbf{E} \rightarrow \mathbb{R}$ and , we let $\mu(f) := \int f(x)\mu(dx)$.
- For two probability measures μ and ν on $(\mathbf{E}, \mathcal{E})$ we let $\mu \otimes \nu$ be a measure on $(\mathbf{E} \times \mathbf{E}, \mathcal{E} \otimes \mathcal{E})$ such that $\mu \otimes \nu(A \times B) = \mu(A)\nu(B)$ for $A, B \in \mathcal{E}$.
- For a Markov kernel $P(x, dy)$ on $\mathbf{E} \times \mathcal{E}$, we write
 - $\mu \otimes P$ for the probability measure on $(\mathbf{E} \times \mathbf{E}, \mathcal{E} \otimes \mathcal{E})$ such that for $\bar{A} \in \mathcal{E} \otimes \mathcal{E}$, the minimal product σ -algebra, $\mu \otimes P(\bar{A}) = \int_{\bar{A}} \mu(dx)P(x, dy)$.
 - $\mu \hat{\otimes} P$ for the probability measure on $(\mathbf{E} \times \mathbf{E}, \mathcal{E} \otimes \mathcal{E})$ such that for $A, B \in \mathcal{E}$ $\mu \hat{\otimes} P(A \times B) = \mu \otimes P(B \times A)$.
- For μ, ν probability distributions on $(\mathbf{E}, \mathcal{E})$ and kernels $M, L : \mathbf{E} \times \mathcal{E} \rightarrow [0, 1]$ such that $\mu \otimes M \gg \nu \hat{\otimes} L$ then we denote

$$\frac{d\nu \hat{\otimes} L}{d\mu \otimes M}(z, z')$$

the corresponding Radon-Nikodym derivative such that for $f : \mathbf{E} \times \mathbf{E} \rightarrow \mathbb{R}$,

$$\int f(z, z') \frac{d\nu \hat{\otimes} L}{d\mu \otimes M}(z, z') \mu \otimes M(d(z, z')) = \int f(z, z') \nu \hat{\otimes} L(d(z', z)).$$

- A point mass distribution at x will be denoted by $\delta_x(dy)$; it is such that for $f : \mathbf{E} \rightarrow \mathbb{R}$

$$\int f(x) \delta_x(dy) = f(x)$$

- In order to alleviate notation, for $M \in \mathbb{N}$, $(z^{(i)}, w_i) \in \mathbf{E} \times [0, \infty)$, $i \in \llbracket M \rrbracket$, we refer to $\{(z^{(i)}, w_i), i \in \llbracket M \rrbracket\}$ as weighted samples to mean $\{(z^{(i)}, \tilde{w}_i), i \in \llbracket M \rrbracket\}$ where $\tilde{w}_i \propto w_i$ but $\sum_{i=1}^M \tilde{w}_i = 1$.

- We say that a set of weighted samples, or particles, $\{(z_i, w_i) \in \mathbb{Z} \times \mathbb{R}_+ : i \in \llbracket N \rrbracket\}$ for $N \geq 1$ represents a distribution μ whenever for f μ -integrable

$$\sum_{i=1}^N \frac{w_i}{\sum_{j=1}^N w_j} f(z_i) \approx \mu(f),$$

in either in the L^p sense for some $p \geq 1$.

- For $M \in \mathbb{N}$, $w_i \in [0, \infty)$, $i \in \llbracket M \rrbracket$, we let $K \sim \text{Cat}(w_1, w_2, \dots, w_M)$ mean that $\mathbb{P}(K = k) \propto w_k$.
- For $M, N \in \mathbb{N}$, $w_{ij} \in [0, \infty)$, $i \in \llbracket M \rrbracket \times \llbracket N \rrbracket$, we let $K \sim \text{Cat}(w_{ij}, i \in \llbracket M \rrbracket \times \llbracket N \rrbracket)$ mean that $\mathbb{P}(K = (k, l)) \propto w_{kl}$.
- for $f: \mathbb{R}^m \rightarrow \mathbb{R}^n$ we let
 - $\nabla \otimes f$ be the transpose of the Jacobian
 - for $n = 1$ we let $\nabla f = (\nabla \otimes f)^\top$ be the gradient,
 - $\nabla \cdot f$ be the divergence.

B Background on Radon-Nikodym derivative

The general formalism required and used throughout the paper relies on a unique measure theoretic tool, the Radon-Nikodym derivative. We gather here definitions and intermediate results used throughout, pointing out the simplicity of the tools involved and the benefits they bring.

Definition 6 (Pushforward). Let μ be a measure on $(\mathbb{Z}, \mathcal{Z})$ and $\psi: (\mathbb{Z}, \mathcal{Z}) \rightarrow (\mathbb{Z}', \mathcal{Z}')$ a measurable function. The pushforward of μ by ψ is defined by

$$\mu^\psi(A) := \mu(\psi^{-1}(A)), \quad A \in \mathcal{Z}',$$

where $\psi^{-1}(A) = \{z \in \mathbb{Z} : \psi(z) \in A\}$ is the preimage of A under ψ .

If μ is a probability distribution then μ^ψ is the probability measure associated with $\psi(Z)$ when $Z \sim \mu$.

Definition 7 (Dominating and equivalent measures). For two measures μ and ν on the same measurable space $(\mathbb{Z}, \mathcal{Z})$,

1. ν is said to dominate μ if for all measurable $A \in \mathcal{Z}$, $\mu(A) > 0 \Rightarrow \nu(A) > 0$ – this is denoted $\nu \gg \mu$.
2. μ and ν are equivalent, written $\mu \equiv \nu$, if $\mu \gg \nu$ and $\nu \gg \mu$.

We will need the notion of Radon-Nikodym derivative [11, Theorems 32.2 & 16.11]:

Theorem 8 (Radon-Nikodym). Let μ and ν be σ -finite measures on $(\mathbb{Z}, \mathcal{Z})$. Then $\nu \ll \mu$ if and only if there exists an essentially unique, measurable, non-negative function $f: \mathbb{Z} \rightarrow [0, \infty)$ such that

$$\int_A f(z) \mu(dz) = \nu(A), \quad A \in \mathcal{E}.$$

Therefore we can view $d\nu/d\mu := f$ as the density of ν w.r.t μ and in particular if g is integrable w.r.t. ν then

$$\int g(z) \frac{d\nu}{d\mu}(z) \mu(dz) = \int g(z) \nu(dz).$$

If μ is a measure and f a non-negative, measurable function then $\mu \cdot f$ is the measure $(\mu \cdot f)(A) = \int \mathbf{1}_A(z) f(z) \mu(dz)$, i.e. the measure $\nu = \mu \cdot f$ such that f is the Radon–Nikodym derivative $d\nu/d\mu = f$.

The following establishes the expression of an expectation with respect to the pushforward μ^ψ in terms of expectations with respect to μ [11, Theorem 16.13].

Theorem 9 (Change of variables). *A function $f : Z' \rightarrow \mathbb{R}$ is integrable w.r.t. μ^ψ if and only if $f \circ \psi$ is integrable w.r.t. μ , in which case*

$$\int_{Z'} f(z) \mu^\psi(dz) = \int_Z f \circ \psi(z) \mu(dz). \quad (28)$$

We now establish results useful throughout the manuscript. The central identity used throughout the manuscript is a direct application of Theorem 9 for $\psi : Z \rightarrow Z$ invertible

$$\int_{Z'} f \circ \psi(z) \mu^{\psi^{-1}}(dz) = \int_Z f(z) \mu(dz)$$

which seems tautological since it can be summarized as follows: for $Z \sim \mu$, then $\psi^{-1}(Z) \sim \mu^{\psi^{-1}}$ and $\psi \circ \psi^{-1}(Z) \sim \mu$! However the interest of the approach stems from the following properties.

Lemma 10. *Let $\psi : Z \rightarrow Z$ be measurable and integrable, μ and ν be σ -finite measures on (Z, \mathcal{Z}) such that $\nu \gg \mu$ and $\nu \gg \nu^{\psi^{-1}}$. Then*

1. $\nu^{\psi^{-1}} \gg \mu^{\psi^{-1}}$ and therefore $\nu \gg \mu^{\psi^{-1}}$,
2. for ν -almost all $z \in Z$,

$$\frac{d\mu^{\psi^{-1}}}{d\nu}(z) = \frac{d\mu}{d\nu} \circ \psi(z) \frac{d\nu^{\psi^{-1}}}{d\nu}$$

3. we have

$$\mu \gg \mu^{\psi^{-1}} \iff \nu(\{z \in Z : d\mu^{\psi^{-1}}/d\nu(z) > 0, d\mu/d\nu(z) = 0\}) = 0$$

in which case for ν -almost all $z \in Z$

$$\frac{d\mu^{\psi^{-1}}}{d\mu}(z) = \begin{cases} \frac{\mu \circ \psi}{\mu}(z) & \mu(z) > 0 \\ 0 & \text{otherwise} \end{cases}$$

and therefore

$$\int_{Z'} f \circ \psi(z) \mu^{\psi^{-1}}(dz) = \int_Z f \circ \psi(z) \frac{\mu \circ \psi(z)}{\mu(z)} \frac{d\nu^{\psi^{-1}}}{d\nu} \mu(dz).$$

Proof. For the first part of the first statement, let $A \in \mathcal{Z}$ such that $\nu^{\psi^{-1}}(A) = \nu(\psi(A)) > 0$, then since $\psi(A) \in \mathcal{Z}$ and $\nu \gg \mu$ we deduce $\mu(\psi(A)) = \mu^{\psi^{-1}}(A) > 0$ and we conclude; the second parts follows from $\nu \gg \nu^{\psi^{-1}}$. For the

second statement for $f: Z \rightarrow \mathbb{R}$ bounded and measurable,

$$\begin{aligned}
\int f(z) \frac{d\mu^{\psi^{-1}}}{dv}(z) v(dz) &= \int f(z) \mu^{\psi^{-1}}(dz) \\
&= \int f \circ \psi^{-1}(z) \mu(dz) \\
&= \int f \circ \psi^{-1}(z) \frac{d\mu}{dv}(z) v(dz) \\
&= \int f(z) \frac{d\mu}{dv} \circ \psi(z) v^{\psi^{-1}}(dz) \\
&= \int f(z) \frac{d\mu}{dv} \circ \psi(z) \frac{dv^{\psi^{-1}}}{dv}(z) v(dz)
\end{aligned}$$

The third statement is given as [11, Problem 32.6.], which we solve in Lemma 12. □

Corollary 11. *In the scenario when $\psi: Z \rightarrow Z$ and v are such that $v^\psi = v$ then $dv^\psi/dv \equiv 1$.*

Lemma 12 (Billingsley, Problem 32.6.). *Assume μ, ν and v are σ -finite and that $v \gg \nu, \mu$. Then $\mu \gg \nu$ if and only if $v(\{z \in Z: d\nu/dv(z) > 0, d\mu/dv(z) = 0\}) = 0$, in which case*

$$\frac{d\nu}{d\mu}(z) = \mathbf{1}\{z \in Z: d\mu/dv(z) > 0\} \frac{d\nu}{dv} / \frac{d\mu}{dv}(z).$$

Proof. Let $S := \{z \in Z: d\nu/dv(z) > 0, d\mu/dv(z) = 0\}$. For $f: Z \rightarrow \mathbb{R}$ integrable we always have

$$\int f(z) \nu(dz) = \int \mathbf{1}\{z \in S\} f(z) \frac{d\nu}{dv}(z) v(dz) + \int \mathbf{1}\{z \in S^c\} f(z) \frac{d\nu}{dv} / \frac{d\mu}{dv}(z) \mu(dz).$$

Assume $\mu \gg \nu$ then from above for any $f: Z \rightarrow \mathbb{R}$ integrable

$$\begin{aligned}
\int \mathbf{1}\{z \in S\} f(z) \frac{d\nu}{d\mu}(z) \mu(dz) &= \int \mathbf{1}\{z \in S\} f(z) \frac{d\nu}{d\mu}(z) \frac{d\mu}{dv}(z) v(dz) \\
&= 0,
\end{aligned}$$

and therefore $v(S) = 0$ and we conclude from the first identity above. Now assume that $v(S) = 0$, then

$$\begin{aligned}
\int f(z) \nu(dz) &= \int \mathbf{1}\{z \in S\} f(z) \frac{d\nu}{dv}(z) v(dz) + \int \mathbf{1}\{z \in S^c\} f(z) \frac{d\nu}{dv} / \frac{d\mu}{dv}(z) \mu(dz) \\
&= \int \mathbf{1}\{z \in S^c\} f(z) \frac{d\nu}{dv} / \frac{d\mu}{dv}(z) \mu(dz).
\end{aligned}$$

The equivalence is therefore established and when either conditions is satisfied we have

$$\frac{d\nu}{d\mu}(z) = \mathbf{1}\{z \in S^c\} \frac{d\nu}{dv} / \frac{d\mu}{dv}(z)$$

and we conclude. □

C Proofs for Section 2

The results of the following lemma can be deduced from Lemma 17 but we provide more direct arguments for the present scenario.

Lemma 13. *Assume $\mu_{n-1} \gg \bar{\mu}_n$, $\mu_{n-1}R_n = \mu_{n-1}$ and let $\bar{M}_n: \mathbf{Z} \times \mathcal{Z} \rightarrow [0, 1]$ be as in (11). Then for $n \in \llbracket P \rrbracket$,*

1. $\bar{\mu}_{n-1}\bar{M}_n = \mu_{n-1}$,

2. the near optimal kernel $\bar{L}_{n-1}: \mathbf{Z} \times \mathcal{Z} \rightarrow [0, 1]$ is given for any $(z, A) \in \mathbf{Z} \times \mathcal{Z}$ by

$$\bar{L}_{n-1}(z, A) := \frac{d\bar{\mu}_{n-1} \otimes \bar{M}_n(A \times \cdot)}{d\bar{\mu}_{n-1}\bar{M}_n}(z), \quad (29)$$

is well defined $\bar{\mu}_{n-1}\bar{M}_n$ -a.s.

3. \bar{L}_{n-1} in (29) is such that for any $A, B \in \mathcal{Z}$

$$\bar{\mu}_{n-1} \otimes \bar{M}_n(A \times B) = \int_B \bar{\mu}_{n-1}\bar{M}_n(dz)\bar{L}_{n-1}(z, A),$$

4. the importance weight in (12) is well defined and

$$\bar{w}_n(z, z') := \frac{d\bar{\mu}_n}{d\mu_{n-1}}(z').$$

Proof of Lemma 13. The first statement, follows from the definition in (11) of \bar{M}_n and the identity (10). The second statement is a consequence of the following classical arguments, justifying Bayes' rule. For $A \in \mathcal{Z}$ fixed, consider the measure

$$\mathcal{Z} \ni B \mapsto \bar{\mu}_{n-1} \otimes \bar{M}_n(A \times B) \leq \bar{\mu}_{n-1} \otimes \bar{M}_n(\mathbf{Z} \times B) = \bar{\mu}_{n-1}\bar{M}_n(B),$$

implying $\bar{\mu}_{n-1}\bar{M}_n \gg \bar{\mu}_{n-1} \otimes \bar{M}_n(A \times \cdot)$ from which we deduce the existence of a Radon-Nikodym derivative such that

$$\bar{\mu}_{n-1} \otimes \bar{M}_n(A \times B) = \int_B \frac{d\bar{\mu}_{n-1} \otimes \bar{M}_n(A \times \cdot)}{d\bar{\mu}_{n-1}\bar{M}_n}(z') \bar{\mu}_{n-1}\bar{M}_n(dz').$$

For $(z, A) \in \mathbf{Z} \times \mathcal{Z}$, we let

$$\bar{L}_{n-1}(z, A) := \frac{d\bar{\mu}_{n-1} \otimes \bar{M}_n(A \times \cdot)}{d\bar{\mu}_{n-1}\bar{M}_n}(z),$$

and note that almost surely $\bar{L}_{n-1}(z, A) \in [0, 1]$ and $\bar{L}_{n-1}(z, \mathbf{Z}) = 1$. For the third statement note that from the second statement, for $A, B \in \mathcal{Z}$ we have $\bar{\mu}_{n-1} \otimes \bar{M}_n(A \times B) = \bar{\mu}_{n-1}\bar{M}_n \hat{\otimes} \bar{L}_{n-1}(A \times B)$ and from Fubini's and the $\pi - \lambda$ theorem [11, Theorems 3.1 and 3.2] $\bar{\mu}_{n-1} \otimes \bar{M}_n$ and $\bar{\mu}_{n-1}\bar{M}_n \hat{\otimes} \bar{L}_{n-1}$ are probability distributions coinciding on $\mathcal{Z} \otimes \mathcal{Z}$. To conclude proof of the third statement, for $f: \mathbf{Z}^2 \rightarrow [0, 1]$ measurable, we successively apply the definition of the Radon-Nikodym derivative, Fubini's theorem, use that $\mu_{n-1} \gg \bar{\mu}_n$, the first statement of this lemma, Fubini again, the second statement

$$\begin{aligned} \int f(z, z') \frac{d\bar{\mu}_n}{d\mu_{n-1}}(z, z') \bar{\mu}_{n-1} \otimes \bar{M}_n(d(z, z')) &= \int f(z, z') \frac{d\bar{\mu}_n}{d\mu_{n-1}}(z') \bar{\mu}_{n-1}\bar{M}_n \hat{\otimes} \bar{L}_n(d(z, z')) \\ &= \int f(z, z') \frac{d\bar{\mu}_n}{d\mu_{n-1}}(z') \mu_{n-1}(dz') \bar{L}_n(z', dz) \\ &= \int f(z, z') \bar{\mu}_n(dz') \bar{L}_n(z', dz) \end{aligned}$$

therefore establishing that $\bar{\mu}_{n-1} \otimes \bar{M}_n$ -almost surely

$$\frac{d\bar{\mu}_{n-1} \bar{M}_n \bar{\otimes} \bar{L}_{n-1}}{d\bar{\mu}_{n-1} \otimes \bar{M}_n}(z, z') = \frac{d\bar{\mu}_n}{d\mu_{n-1}}(z, z').$$

□

Proof of Proposition 4. In Alg. 3 for any $A \in \mathcal{Z}^{\otimes N}$ we have with (b_1, \dots, b_N) the random vector taking values in $\llbracket N \rrbracket^N$ involved in the resampling step,

$$\begin{aligned} \mathbb{P}_3(z_n^{(1:N)} \in A \mid z_{n-1}^{(1:N)}) &= \mathbb{E}_3 \left\{ \mathbf{1}_A \{(\tilde{x}_{n-1, a_i}^{(i)}, v_n^{(i)}), i \in \llbracket N \rrbracket\} \mathbf{1} \{z_n^{(i)} = z_{n-1}^{(b_i)}, i \in \llbracket N \rrbracket\} \mid z_{n-1}^{(j)}, j \in \llbracket N \rrbracket\} \right\} \\ &= \mathbb{E}_3 \left\{ \mathbf{1}_A \{(x_{n-1, a_i}^{(i)}, v_n^{(i)}), i \in \llbracket N \rrbracket\} \mid z_{n-1}^{(j)}, j \in \llbracket N \rrbracket\} \right\}. \end{aligned}$$

Letting for $(\alpha, \beta) \in \llbracket 0, T \rrbracket^N \times \llbracket N \rrbracket^N$

$$E_A(\alpha, \beta) = E_A(\alpha, \beta, z_{n-1}^{(1:N)}) := \int \mathbf{1}_A \{(x_{n-1, \alpha_i}^{(\beta_i)}, v_n^{(i)}), i \in \llbracket N \rrbracket\} \varpi_n^{\otimes N}(dv_n^{(1:N)})$$

from the tower property we have

$$\mathbb{E}_3 \left\{ \mathbf{1}_A \{(x_{n-1, a_i}^{(i)}, v_n^{(i)}), i \in \llbracket N \rrbracket\} \mid z_{n-1}^{(j)}, b_j = \beta_j, j \in \llbracket N \rrbracket\} \right\} = \sum_{\alpha \in \llbracket 0, T \rrbracket^N} E_A(\alpha, \beta) \prod_{i=1}^N \frac{1}{T+1} \frac{d\mu_{n, \alpha_i}}{d\bar{\mu}_n}(z_{n-1}^{(\beta_i)}).$$

Since

$$\mathbb{P}_3(b_1 = \beta_1, \dots, b_N = \beta_N \mid z_{n-1}^{(i)}, i \in \llbracket N \rrbracket) = \left(\sum_{j=1}^N \frac{d\bar{\mu}_n}{d\mu_{n-1}}(z_{n-1}^{(j)}) \right)^{-N} \prod_{i=1}^N \frac{d\bar{\mu}_n}{d\mu_{n-1}}(z_{n-1}^{(\beta_i)})$$

we deduce

$$\begin{aligned} \mathbb{P}_3(z_n^{(1:N)} \in A \mid z_{n-1}^{(1:N)}) &\propto \sum_{\alpha, \beta} E_A(\alpha, \beta, z_{n-1}^{(1:N)}) \prod_{i=1}^N \frac{d\bar{\mu}_n}{d\mu_{n-1}}(z_{n-1}^{(\beta_i)}) \prod_{i=1}^N \frac{d\mu_{n, \alpha_i}}{d\bar{\mu}_n}(z_{n-1}^{(\beta_i)}) \\ &= \sum_{\alpha, \beta} E_A(\alpha, \beta, z_{n-1}^{(1:N)}) \prod_{i=1}^N \frac{d\bar{\mu}_n}{d\mu_{n-1}}(z_{n-1}^{(\beta_i)}) \frac{d\mu_{n, \alpha_i}}{d\bar{\mu}_n}(z_{n-1}^{(\beta_i)}) \\ &= \sum_{\alpha, \beta} E_A(\alpha, \beta, z_{n-1}^{(1:N)}) \prod_{i=1}^N \frac{d\mu_{n, \alpha_i}}{d\mu_{n-1}}(z_{n-1}^{(\beta_i)}). \end{aligned}$$

Now notice that

$$\begin{aligned} \mathbb{P}_2(z_n^{(j)} = z_{n-1, \alpha_j}^{(\beta_j)} \mid z_{n-1}^{(1:N)}) &= \frac{\frac{d\mu_{n, \alpha_j}}{d\mu_{n-1}}(z_{n-1}^{(\beta_j)})}{\sum_{i, k} \frac{d\mu_{n, k}}{d\mu_{n-1}}(z_{n-1}^{(i)})} \\ &\propto \frac{\frac{d\mu_{n, \alpha_j}}{d\mu_{n-1}}(z_{n-1}^{(\beta_j)})}{\sum_{i=1}^N \frac{d\bar{\mu}_n}{d\mu_{n-1}}(z_{n-1}^{(i)})}, \end{aligned}$$

and the first statement follows from conditional independence of $(b_1, a_1), \dots, (b_N, a_N)$ and the fact that $\mathbb{P}_2(z_n^{(1:N)} \in A \mid \bar{z}_{n-1}^{(1:N)}) = E_A(\alpha, \beta, \bar{z}_{n-1}^{(1:N)})$. Since by construction $\mathbb{P}_3((z_0^{(1)}, \dots, z_0^{(N)}) \in A) = \mathbb{P}_2((z_0^{(1)}, \dots, z_0^{(N)}) \in A)$ for any $A \in \mathcal{Z}$ the second statement follows from a standard Markov chain argument. Now for $g: \mathbf{Z} \rightarrow \mathbb{R}$ and $\iota \in \llbracket N \rrbracket$

$$\begin{aligned} \mathbb{E}_3(g(\bar{z}_n^{(\iota)} \mid z_{n-1}^{(j)}, j \in \llbracket N \rrbracket)) &= \mathbb{E}_3(g(z_{n-1}^{(b_\iota)} \mid z_{n-1}^{(j)}, j \in \llbracket N \rrbracket)) \\ &= \sum_{i=1}^N g(z_{n-1}^{(i)}) \frac{\frac{d\bar{\mu}_n}{d\mu_{n-1}}(z_{n-1}^{(i)})}{\sum_{j=1}^N \frac{d\bar{\mu}_n}{d\mu_{n-1}}(z_{n-1}^{(j)})}. \end{aligned}$$

Therefore for any $k \in \llbracket 0, T \rrbracket$,

$$\begin{aligned} \mathbb{E}_3\left(\frac{d\mu_{n,k}}{d\bar{\mu}_n}(z_n^{(\iota)}) f \circ \psi_{n,k}(z_n^{(\iota)}) \mid z_{n-1}^{(j)}, j \in \llbracket N \rrbracket\right) &= \sum_{i=1}^N \frac{d\mu_{n,k}}{d\bar{\mu}_n}(z_{n-1}^{(i)}) f \circ \psi_{n,k}(z_{n-1}^{(i)}) \frac{\frac{d\bar{\mu}_n}{d\mu_{n-1}}(z_{n-1}^{(i)})}{\sum_{j=1}^N \frac{d\bar{\mu}_n}{d\mu_{n-1}}(z_{n-1}^{(j)})} \\ &= \sum_{i=1}^N \frac{\frac{d\mu_{n,k}}{d\mu_{n-1}}(z_{n-1}^{(i)})}{\sum_{j=1}^N \sum_{l=0}^T \frac{d\mu_{n,l}}{d\mu_{n-1}}(z_{n-1}^{(j)})} f \circ \psi_{n,k}(z_{n-1}^{(i)}). \end{aligned}$$

The third statement follows. \square

D Sampling Markov snippets

In this section we develop the Markov snippet framework, largely inspired by the WF-SMC framework of [26] but provide here a detailed derivation following the standard SMC sampler framework [28] which allows us to consider much more general mutation kernels; integrator snippet SMC is recovered as a particular case. Importantly we provide recipes to compute some of the quantities involved using simple criteria (see Lemma 18 and Corollary 19) which allow us to consider unusual scenarios such as in Appendix D.4.

D.1 Markov snippet SMC sampler or waste free SMC with a difference

Given a sequence $\{\mu_n, n \in \llbracket 0, P \rrbracket\}$ of probability distributions defined on a measurable space $(\mathbf{Z}, \mathcal{Z})$ introduce the sequence of distributions defined on $(\llbracket 0, T \rrbracket \times \mathbf{Z}^{T+1}, \mathcal{P}(\llbracket 0, T \rrbracket) \otimes \mathcal{Z}^{\otimes(T+1)})$ such that for any $(n, k, \mathbf{z}) \in \llbracket 0, P \rrbracket \times \llbracket 0, T \rrbracket \times \mathbf{Z}$

$$\bar{\mu}_n(k, d\mathbf{z}) := \frac{1}{T+1} w_{n,k}(\mathbf{z}) \mu_n \otimes M_n^{\otimes T}(d\mathbf{z})$$

where for $M_n, L_{n-1,k}: \mathbf{Z} \times \mathcal{Z} \rightarrow [0, 1]$, $k \in \llbracket 0, P \rrbracket$ and any $\mathbf{z} = (z_0, z_1, \dots, z_T) \in \mathbf{Z}^{T+1}$,

$$w_{n,k}(\mathbf{z}) := \frac{d\mu_n \hat{\otimes} L_{n-1,k}}{d\mu_n \otimes M_n^k}(z_0, z_k),$$

is assumed to exist for now and $w_{n,0}(\mathbf{z}) := 1$. This yields the marginals

$$\bar{\mu}_n(d\mathbf{z}) := \sum_{k=0}^T \bar{\mu}_n(k, d\mathbf{z}) = \frac{1}{T+1} \sum_{k=1}^n w_{n,k}(\mathbf{z}) \mu_n \otimes M_n^{\otimes T}(d\mathbf{z}). \quad (30)$$

Further, consider $R_n: Z \times \mathcal{Z} \rightarrow [0, 1]$ such that $\mu_{n-1}R_n = \mu_{n-1}$ and define $\bar{M}_n: Z^{T+1} \times \mathcal{Z}^{\otimes(T+1)} \rightarrow [0, 1]$

$$\bar{M}_n(\mathbf{z}, d\mathbf{z}') := \sum_{k=0}^T \bar{\mu}_{n-1}(k | \mathbf{z}) R_n(z_k, dz'_0) M_n^{\otimes T}(z'_0, dz'_{-0}).$$

Note that [26] set $R_n = M_n$, which we do not want in our later application and further assume that M_n is μ_{n-1} -invariant, which is not necessary and too constraining for our application in Appendix D.3 (corresponding to the application in the introductory Subsection 2.2). We only require the condition $\mu_{n-1}R_n = \mu_{n-1}$ is required. As in Subsection 2.2 we consider the optimal backward kernel $\bar{L}_n: Z^{T+1} \times \mathcal{Z}^{\otimes(T+1)} \rightarrow [0, 1]$, given for $(\mathbf{z}, A) \in Z^{T+1} \times \mathcal{Z}^{\otimes(T+1)}$ by

$$\bar{L}_{n-1}(\mathbf{z}, A) = \frac{d\bar{\mu}_{n-1} \otimes \bar{M}_n(A \times \cdot)}{d\bar{\mu}_{n-1} \bar{M}_n}(\mathbf{z}),$$

and as established in Lemma 15 and Lemma 17, one obtains

$$\bar{w}_n(\mathbf{z}') = \frac{d\bar{\mu}_n \widehat{\otimes} \bar{L}_{n-1}}{d\bar{\mu}_{n-1} \otimes \bar{M}_n}(\mathbf{z}, \mathbf{z}') = \frac{d\mu_n}{d\mu_{n-1}}(z'_0) \frac{1}{T+1} \sum_{k=0}^T w_{n,k}(\mathbf{z}'). \quad (31)$$

The corresponding folded version of the algorithm is given in Alg. 6, with $\check{\mathbf{z}}_n := (\check{z}_{n,0}, \check{z}_{n,1}, \dots, \check{z}_{n,T}) \dots$:

- $\{(\check{z}_n^{(i)}, 1), i \in \llbracket N \rrbracket\}$ represents $\bar{\mu}_n(d\mathbf{z})$,
- $\{(z_{n,k}^{(i)}, w_{n+1,k}), (i, k) \in \llbracket N \rrbracket \times \llbracket 0, T \rrbracket\}$ represent $\mu_n(d\mathbf{z})$,
- $\{(z_n^{(i)}, \bar{w}_{n+1}(z_n^{(i)})), i \in \llbracket N \rrbracket\}$ represents $\bar{\mu}_{n+1}(d\mathbf{z})$ and so do $\{(\check{z}_{n+1}^{(i)}, 1), i \in \llbracket N \rrbracket\}$.

Remark 14. Other choices are possible and we detail here an alternative, related to the Waste-free framework of [26]. With notation as above here we take

$$\bar{\mu}_n(k, d\mathbf{z}) := \frac{1}{T+1} w_{n,k}(\mathbf{z}) \mu_{n-1} \otimes M_n^{\otimes T}(d\mathbf{z})$$

with the weights now defined as

$$w_{n,k}(\mathbf{z}) := \frac{d\mu_n \widehat{\otimes} L_{n-1,k}}{d\mu_{n-1} \otimes M_n^k}(z_0, z_k).$$

With these choices we retain the fundamental property that for $f: Z \rightarrow \mathbb{R}$, with $\bar{f}(k, \mathbf{z}) := f(z_k)$ then $\bar{\mu}_n(\bar{f}) = \mu_n(f)$. Now with

$$\bar{M}_n(\mathbf{z}, d\mathbf{z}') := \sum_{k=0}^T \bar{\mu}_{n-1}(k | \mathbf{z}) R_n(z_k, dz'_0) M_n^{\otimes T}(z'_0, dz'_{-0}),$$

assuming $\mu_{n-1}R_n = \mu_{n-1}$, we have the property that for any $A \in \mathcal{Z}^{\otimes(T+1)}$ $\bar{\mu}_{n-1}\bar{M}_n(A) = \mu_{n-1} \otimes M_n^{\otimes T}(A)$, yielding

$$\bar{w}_n(\mathbf{z}') = \frac{1}{T+1} \sum_{k=0}^T w_{n,k}(\mathbf{z}').$$

Finally choosing $L_{n,k}$ to be the optimized backward kernel, the importance weight of the algorithm is,

$$w_{n,k}(\mathbf{z}') = \frac{d\mu_n \widehat{\otimes} L_{n-1,k}}{d\mu_{n-1} \otimes M_n^k}(z_0, z_k) = \frac{d\mu_n}{d\mu_{n-1}}(z_k).$$

```

1 sample  $\check{z}_0^{(i)} \stackrel{\text{iid}}{\sim} \mu_0^{\otimes(T+1)}$ , set  $w_{0,k}(\check{z}_0^{(i)}) = 1$  for  $(i, k) \in \llbracket N \rrbracket \times \llbracket T \rrbracket$ .
2 for  $n = 0, \dots, P - 1$  do
3   for  $i \in \llbracket N \rrbracket$  do
4     sample  $a_i \sim \text{Cat}\left(1, w_{n,1}(\check{z}_n^{(i)}), w_{n,2}(\check{z}_n^{(i)}), \dots, w_{n,T}(\check{z}_n^{(i)})\right)$ 
5     sample  $z_{n,0}^{(i)} = z_n^{(i)} \sim R_{n+1}(\check{z}_n, a_i, \cdot)$ 
6     for  $k \in \llbracket T \rrbracket$  do
7       sample  $z_{n,k}^{(i)} \sim M_{n+1}(z_{n,k-1}^{(i)}, \cdot)$ 
8       compute
          
$$w_{n+1,k}(z_n^{(i)}) = \frac{d\mu_n \widehat{\otimes} L_n^k}{d\mu_n \otimes M_{n+1}^k}(z_{n,0}^{(i)}, z_{n,k}^{(i)})$$

9     end
10    compute
11
          
$$\bar{w}_{n+1}(z_n^{(i)}) = \frac{d\mu_{n+1}(z_{n,0}^{(i)})}{d\mu_n(z_{n,0}^{(i)})} \frac{1}{T+1} \sum_{k \in \llbracket T \rrbracket} w_{n+1,k}(z_n^{(i)}),$$

12  end
13  for  $j \in \mathbb{N}$  do
14    sample  $b_j \sim \text{Cat}\left(\bar{w}_{n+1}(z_n^{(1)}), \bar{w}_{n+1}(z_n^{(2)}), \dots, \bar{w}_{n+1}(z_n^{(N)})\right)$ 
15    set  $\check{z}_{n+1}^{(j)} = z_n^{(b_j)}$ 
16  end
17 end

```

Algorithm 6: (Folded) Markov Snippet SMC algorithm

We note that continuous time Markov process snippets could also be used. For example piecewise deterministic Markov processes such as the Zig-Zag process [10] or the Bouncy Particle Sampler [12] could be used in practice since finite time horizon trajectories can be parametrized in terms of a finite number of parameters. We do not pursue this here.

D.2 Theoretical justification

In this section we provide the theoretical justification for the correctness of Alg. 6 and an alternative proof for Alg. 3, seen as a particular case of Alg. 6.

Throughout this section we use the following notation where μ (resp. ν) plays the rôle of μ_{n+1} (resp. μ_n), for notational simplicity. Let $\mu \in \mathcal{P}(Z, \mathcal{Z})$ and $M, L: Z \times \mathcal{Z} \rightarrow [0, 1]$ be two Markov kernels such that the following condition holds. For $T \in \mathbb{N} \setminus \{0\}$ let $\mathbf{z} := (z_0, z_1, \dots, z_T) \in Z^{T+1}$ and for $k \in \llbracket 0, T \rrbracket$ assume that $\mu \otimes M^k \gg \mu^{\widehat{\otimes}}(L^k)$, implying the existence of the Radon-Nikodym derivatives

$$w_k(\mathbf{z}) := \frac{d\mu^{\widehat{\otimes}}(L^k)}{d\mu \otimes M^k}(z_0, z_k), \quad (32)$$

with the convention $w_0(\mathbf{z}) = 1$. We let $w(\mathbf{z}) := (T+1)^{-1} \sum_{k=0}^T w_k(\mathbf{z})$. For $\mathbf{z} \in Z^{T+1}$, define

$$M^{\otimes T}(z_0, dz_{-0}) := \prod_{i=1}^T M(z_{i-1}, dz_i),$$

and introduce the mixture of distributions, defined on $(Z^{T+1}, \mathcal{Z}^{\otimes(T+1)})$,

$$\bar{\mu}(dz) = \sum_{k=0}^T \bar{\mu}(k, dz), \quad (33)$$

where for $(k, \mathbf{z}) \in \llbracket 0, T \rrbracket \times Z^{T+1}$

$$\bar{\mu}(k, dz) := \frac{1}{T+1} w_k(\mathbf{z}) \mu \otimes M^{\otimes T}(dz),$$

so that one can write $\bar{\mu}(dz) = w(\mathbf{z}) \mu \otimes M^{\otimes T}(dz)$ with $w(\mathbf{z}) := (T+1)^{-1} \sum_{k=0}^T w_k(\mathbf{z})$.

We first establish properties of $\bar{\mu}$, showing how samples from $\bar{\mu}$ can be used to estimate expectations with respect to μ .

Lemma 15. *For any $f: Z \rightarrow \mathbb{R}$ such that $\mu(|f|) < \infty$*

1. we have for $k \in \llbracket 0, T \rrbracket$

$$\int f(z') \frac{d\mu^{\widehat{\otimes}}(L^k)}{d\mu \otimes M^k}(z, z') \mu(dz) M^k(z, dz') = \mu(f),$$

2. with $\bar{f}(k, \mathbf{z}) := f(z_k)$,

(a) then

$$\bar{\mu}(\bar{f}) = \mu(f),$$

(b) in particular,

$$\int \sum_{k=0}^T \bar{f}(k, \mathbf{z}) \bar{\mu}(k | \mathbf{z}) \bar{\mu}(d\mathbf{z}) = \mu(f). \quad (34)$$

Proof. The first statement follows directly from the definition of the Radon-Nikodym derivative

$$\begin{aligned} \int f(z') \frac{d\mu \widehat{\otimes} L^k}{d\mu \otimes M^k}(z, z') \mu \otimes M^k(d(z, z')) &= \int f(z') \mu(dz') L^k(z', dz) \\ &= \int f(z') \mu(dz'). \end{aligned}$$

The second statement follows from the definition of $\bar{\mu}$ and

$$\frac{1}{T+1} \sum_{k=0}^T \int \bar{f}(k, \mathbf{z}) w_k(\mathbf{z}) \mu \otimes M^{\otimes T}(d\mathbf{z}) = \frac{1}{T+1} \sum_{k=0}^T \int f(z_k) \frac{d\mu \widehat{\otimes} (L^k)}{d\mu \otimes M^k}(z_0, z_k) \mu \otimes M^k(d(z_0, z_k)),$$

and the first statement. The last statement follows from the tower property for expectations. \square

Corollary 16. *Assume that $\mathbf{z} \sim \bar{\mu}$, then*

$$\sum_{k=0}^T f(z_k) \frac{w_k(\mathbf{z})}{\sum_{l=0}^T w_l(\mathbf{z})}$$

is an unbiased estimator of $\mu(f)$ since we notice that for $k \in \llbracket 0, T \rrbracket$,

$$\bar{\mu}(k | \mathbf{z}) = \frac{w_k(\mathbf{z})}{\sum_{l=0}^T w_l(\mathbf{z})}.$$

This justifies algorithms which sample from the mixture $\bar{\mu}$ directly in order to estimate expectations with respect to μ .

Let $\nu \in \mathcal{P}(\mathbf{Z}, \mathcal{Z})$ and $\bar{\nu} \in \mathcal{P}(\mathbf{Z}^{T+1}, \mathcal{Z}^{\otimes(T+1)})$ be derived from ν in the same way $\bar{\mu}$ is from μ in (33), but for possibly different Markov kernels $M_\nu, L_\nu: \mathbf{Z} \times \mathcal{Z} \rightarrow [0, 1]$. Define now the kernel $\bar{M}: \mathbf{Z}^{T+1} \times \mathcal{Z}^{\otimes(T+1)} \rightarrow [0, 1]$ be the Markov kernel

$$\bar{M}(\mathbf{z}, d\mathbf{z}') := \sum_{k=0}^T \bar{\nu}(k | \mathbf{z}) R(z_k, dz'_0) M^{\otimes T}(z'_0, dz'_{-0}), \quad (35)$$

with $R: \mathbf{Z} \times \mathcal{Z} \rightarrow [0, 1]$. Remark that M, L, M_ν, L_ν and R can be made dependent on both μ and ν , provided they satisfy all the conditions stated above and below.

The following justifies the existence of \bar{w}_{n+1} in (31) for a particular choice of backward kernel and provides a simplified expression for a particular choices of R .

Lemma 17. *With the notation (32)-(33) and (35),*

1. *there exists $\bar{M}^*: \mathbf{Z}^{T+1} \times \mathcal{Z}^{\otimes(T+1)} \rightarrow [0, 1]$ such that for any $A, B \in \mathcal{Z}^{\otimes(T+1)}$*

$$\bar{\nu} \otimes \bar{M}(A \times B) = (\bar{\nu} \bar{M}) \otimes \bar{M}^*(B \times A)$$

2. *we have*

$$\bar{\nu} \bar{M} = (\nu R) \otimes M^{\otimes T},$$

3. assuming $\nu R \gg \mu$ then with the choice $\bar{L} = \bar{M}^*$ we have $\bar{\nu} \otimes \bar{M} \gg \bar{\mu} \hat{\otimes} \bar{L}$ and for $\mathbf{z}, \mathbf{z}' \in \mathbf{Z}^{T+1}$ almost surely

$$\bar{w}(\mathbf{z}, \mathbf{z}') = \frac{d\bar{\mu} \hat{\otimes} \bar{L}}{d\bar{\nu} \otimes \bar{M}}(\mathbf{z}, \mathbf{z}') = \frac{d\mu}{d\nu R}(z'_0) \frac{1}{T+1} \sum_{k=0}^T w_k(\mathbf{z}') = \frac{d\mu}{d\nu R}(z'_0) w(\mathbf{z}') =: \bar{w}(\mathbf{z}'),$$

that is we introduce notation reflecting this last simplification.

4. Notice the additional simplification when $\nu R = \nu$.

Proof. The first statement is a standard result and \bar{M}^* is a conditional expectation. We however provide the short argument taking advantage of the specific scenario. For a fixed $A \in \mathcal{Z}^{\otimes(T+1)}$ consider the finite measure

$$B \mapsto \bar{\nu} \otimes \bar{M}(A \times B) \leq \bar{\nu} \bar{M}(B),$$

such that $\bar{\nu} \bar{M}(B) = 0 \implies \bar{\nu} \otimes \bar{M}(A \times B) = 0$, that is $\bar{\nu} \bar{M} \gg \bar{\nu} \otimes \bar{M}(A \times \cdot)$. Consequently we have the existence of a Radon-Nikodym derivative such that

$$\bar{\nu} \otimes \bar{M}(A \times B) = \int_B \frac{d\bar{\nu} \otimes \bar{M}(A \times \cdot)}{d(\bar{\nu} \bar{M})}(\mathbf{z}) \bar{\nu} \bar{M}(d\mathbf{z})$$

which indeed has the sought property. This is a kernel since for any fixed $A \in \mathcal{Z}$, for any $B \in \mathcal{Z}$, $\bar{\nu} \otimes \bar{M}(A \times B) \leq 1$ and therefore $\bar{M}^*(\mathbf{z}, A) \leq 1$ $\bar{\nu} \bar{M}$ -a.s., with equality for $A = \mathbf{X}$. For the second statement we have, for any $(\mathbf{z}, A) \in \mathbf{Z}^{T+1} \times \mathcal{Z}^{\otimes(T+1)}$,

$$\bar{M}(\mathbf{z}, A) = \sum_{k=0}^T \bar{\nu}(k | \mathbf{z}) R \otimes M^{\otimes T}(z_k, A),$$

and we can apply (34) in Lemma 15 with the substitutions $\mu \leftarrow \nu$ and $M \leftarrow M_\nu, L \leftarrow L_\nu$ to conclude. For the third statement, since $\nu R \gg \mu$ then $\bar{\nu} \bar{M} = (\nu R) \otimes M^{\otimes T} \gg \mu \otimes M^{\otimes T}$ because for any $A \in \mathcal{Z}^{\otimes(T+1)}$,

$$\int \mathbf{1}\{\mathbf{z} \in A\} \nu R(dz_0) M^{\otimes T}(z_0, dz_{-0}) = 0 \implies \begin{cases} \int \mathbf{1}\{\mathbf{z} \in A\} M^{\otimes T}(z_0, dz_{-0}) = 0 & \nu R - a.s. \\ \text{or} \\ \nu R(\mathfrak{P}(A)) = 0 \end{cases}$$

where $\mathfrak{P}: \mathbf{Z}^{T+1} \rightarrow \mathbf{Z}$ is such that $\mathfrak{P}(\mathbf{z}) = z_0$. In either case, since $\nu R \gg \mu$, this implies that

$$\int \mathbf{1}\{\mathbf{z} \in A\} \mu(dz_0) M^{\otimes T}(z_0, dz_{-0}) = 0,$$

that is $\bar{\nu} \bar{M} \gg \bar{\mu}$ from the definition of $\bar{\mu}$. Consequently

$$\begin{aligned} \bar{\mu} \otimes \bar{M}^*(A \times B) &= \int_A \bar{M}^*(\mathbf{z}, B) \frac{d\bar{\mu}}{d(\bar{\nu} \bar{M})}(\mathbf{z}) \bar{\nu} \bar{M}(d\mathbf{z}) \\ &= \int_A \frac{d\bar{\mu}}{d(\bar{\nu} \bar{M})}(\mathbf{z}) \bar{M}^*(\mathbf{z}, B) \bar{\nu} \bar{M}(d\mathbf{z}) \\ &= \int \mathbf{1}\{\mathbf{z} \in A, \mathbf{z}' \in B\} \frac{d\bar{\mu}}{d(\bar{\nu} \bar{M})}(\mathbf{z}) \bar{\nu}(d\mathbf{z}') \bar{M}(\mathbf{z}', d\mathbf{z}) \end{aligned}$$

and indeed from Fubini's and Dynkin's $\pi - \lambda$ theorems $\bar{\nu} \otimes \bar{M} \gg \bar{\mu} \widehat{\otimes} \bar{L}$ and

$$\frac{d\bar{\mu} \widehat{\otimes} \bar{L}}{d\bar{\nu} \otimes \bar{M}}(z, z') = \frac{d\bar{\mu}}{d(\bar{\nu} \bar{M})}(z').$$

Now for $f: \mathbf{Z}^{T+1} \rightarrow [0, 1]$ and using the second statement and $\nu R \gg \mu$,

$$\begin{aligned} \int f(z) \frac{d\bar{\mu}}{d(\bar{\nu} \bar{M})}(z) (\bar{\nu} \bar{M})(dz) &= \int f(z) w(z) \mu \otimes M^{\otimes T}(dz) \\ &= \int f(z) w(z) \frac{d\mu}{d(\nu R)}(z_0) (\nu R)(dz_0) M^{\otimes T}(z_0, dz_{-0}) \\ &= \int f(z) w(z) \frac{d\mu}{d(\nu R)}(z_0) \bar{\nu} \bar{M}(dz). \end{aligned}$$

We therefore conclude that

$$\frac{d\bar{\mu} \widehat{\otimes} \bar{L}}{d\bar{\nu} \otimes \bar{M}}(z, z') = w(z') \frac{d\mu}{d(\nu R)}(z'_0) = w(z') \frac{d\mu}{d\nu}(z'_0)$$

where the last inequality holds only when $\nu R = \nu$. □

The following result is important in two respects. First it establishes that if M, L satisfy a simple property then w_k always have a simple expression in terms of certain densities of μ and ν – this implies in particular that in Appendix D.1 the kernel M_n is not required to leave μ_{n-1} invariant to make the method implementable [26]. Second it provides a direct justification of the validity of advanced schemes – see Example 23. This therefore establishes that generic and widely applicable sufficient conditions for $\bar{w}(z, z')$ to be tractable are $\nu R = \nu$ and the notion of (ν, M, M^*) -reversibility.

Lemma 18. *Let $\mu, \nu \in \mathcal{P}(\mathbf{Z}, \mathcal{Z}^e)$, ν be a σ -finite measure on $(\mathbf{Z}, \mathcal{Z}^e)$ such that $\nu \gg \mu, \nu$ and assume that we have a pair of Markov kernels $M, M^*: \mathbf{Z} \times \mathcal{Z}^e \rightarrow [0, 1]$ such that*

$$\nu(dz) M(z, dz') = \nu(dz') M^*(z', dz). \quad (36)$$

We call this property (ν, M, M^) -reversibility. Then for $z, z' \in \mathbf{Z}$ such that $\nu(z) := d\nu/d\nu(z) > 0$ we have*

$$\frac{d\mu \widehat{\otimes} M^*}{d\nu \otimes M}(z, z') = \frac{d\mu/d\nu(z')}{d\nu/d\nu(z)}.$$

Proof. For $z, z' \in \mathbf{Z}$ such that $d\nu/d\nu(z) > 0$ we have

$$\begin{aligned} \mu(dz') M^*(z', dz) &= \frac{d\mu}{d\nu}(z') \nu(dz') M^*(z', dz) \\ &= \frac{d\mu}{d\nu}(z') \nu(dz) M(z, dz') \\ &= \frac{d\mu/d\nu(z')}{d\nu/d\nu(z)} \frac{d\nu}{d\nu}(z) \nu(dz) M(z, dz') \\ &= \frac{d\mu/d\nu(z')}{d\nu/d\nu(z)} \nu(dz) M(z, dz'). \end{aligned}$$

□

Corollary 19. Let $\mu_{n-1}, \mu_n \in \mathcal{P}(\mathbf{Z}, \mathcal{Z})$ and ν be a σ -finite measure such that $\nu \gg \mu_{n-1}, \mu_n$, let $M_n, L_{n-1}: (\mathbf{Z}, \mathcal{Z}) \rightarrow [0, 1]$ such that

$$\nu(dz)M_n(z, dz') = \nu(dz')L_{n-1}(z', dz),$$

then for any $z, z' \in \mathbf{Z}$ such that $d\mu_n/d\nu(z) > 0$ and $k \in \mathbb{N}$

$$\frac{\mu_n \widehat{\otimes} L_{n-1}^k}{\mu_n \otimes M_n^k}(z, z') = \frac{d\mu_n/d\nu(z')}{d\mu_n/d\nu(z)}.$$

and provided $\mu_{n-1}R_n = \mu_{n-1}$ we can deduce

$$\begin{aligned} \bar{w}_n(\mathbf{z}) &= \frac{d\mu_n/d\nu(z_0)}{d\mu_{n-1}/d\nu(z_0)} \frac{1}{T+1} \sum_{k=0}^T \frac{d\mu_n/d\nu(z_k)}{d\mu_n/d\nu(z_0)} \\ &= \frac{1}{T+1} \sum_{k=0}^T \frac{d\mu_n/d\nu(z_k)}{d\mu_{n-1}/d\nu(z_0)} \end{aligned}$$

where we have used Lemma 12.

We have shown earlier that standard integrator based mutation kernels used in the context of Monte Carlo method satisfy (36) with ν the Lebesgue measure but other scenarios involved that of the preconditioned Crank–Nicolson (pCN) algorithm where ν is the distribution of a Gaussian process.

D.3 Revisiting sampling with integrator snippets

In this scenario we have $\mu(dz) = \pi(dx)\varpi(dv)$ assumed to have a density w.r.t. a σ -finite measure ν , and ψ is an invertible mapping $\psi: \mathbf{Z} \rightarrow \mathbf{Z}$ such that $\nu^\psi = \nu$ and $\psi^{-1} = \sigma \circ \psi \circ \sigma$ with $\sigma: \mathbf{Z} \rightarrow \mathbf{Z}$ such that $\mu \circ \sigma(z) = \mu(z)$. In his manuscript we focus primarily on the scenario where ψ is a discretization of Hamilton's equations for a potential $U: \mathbf{X} \rightarrow \mathbb{R}$ e.g. a leapfrog integrator. We consider now the scenario where, in the framework developed in Appendix D.1, we let $M(z, dz') := \delta_{\psi(z)}(dz')$ be the deterministic kernel which maps the current state $z \in \mathbf{Z}$ to $\psi(z)$. Define $\Psi(z, dz') := \delta_{\psi(z)}(dz')$ and $\Psi^*(z, dz') := \delta_{\psi^{-1}(z)}(dz')$; we exploit the ideas of [2, Proposition 4] to establish that Ψ^* is the ν -adjoint of Ψ if ν is invariant under ψ .

Lemma 20. Let μ be a probability measure and ν a σ -finite measure, on $(\mathbf{Z}, \mathcal{Z})$ such that $\nu \gg \mu$. Denote $\mu(z) := d\mu/d\nu(z)$ for any $z \in \mathbf{Z}$. Let $\psi: \mathbf{Z} \rightarrow \mathbf{Z}$ be an invertible and volume preserving mapping, i.e. such that $\nu^\psi(A) = \nu(\psi^{-1}(A)) = \nu(A)$ for all $A \in \mathcal{Z}$, then

1. (ν, Ψ, Ψ^*) form a reversible triplet, that is for all $z, z' \in \mathbf{Z}$,

$$\nu(dz)\delta_{\psi(z)}(dz') = \nu(dz')\delta_{\psi^{-1}(z')}(dz),$$

2. for all $z, z' \in \mathbf{Z}$ such that $\mu(z) > 0$

$$\mu(dz')\delta_{\psi^{-1}(z')}(dz) = \frac{\mu \circ \psi(z)}{\mu(z)} \mu(dz)\delta_{\psi(z)}(dz').$$

Proof. For the first statement

$$\begin{aligned}
\int f(z)g \circ \psi(z)v(dz) &= \int f \circ \psi^{-1} \circ \psi(z)g \circ \psi(z)v(dz) \\
&= \int f \circ \psi^{-1}(z)g(z)v^\psi(dz) \\
&= \int f \circ \psi^{-1}(z)g(z)v(dz).
\end{aligned}$$

We have

$$\begin{aligned}
\mu(dz')\delta_{\psi^{-1}(z')}(dz) &= \mu(z')v(dz')\delta_{\psi^{-1}(z')}(dz) \\
&= \mu(z')v(dz)\delta_{\psi(z)}(dz') \\
&= \mu \circ \psi(z)v(dz)\delta_{\psi(z)}(dz') \\
&= \frac{\mu \circ \psi(z)}{\mu(z)}\mu(z)v(dz)\delta_{\psi(z)}(dz') \\
&= \frac{\mu \circ \psi(z)}{\mu(z)}\mu(dz)\delta_{\psi(z)}(dz')
\end{aligned}$$

$$\begin{aligned}
\int f(z')g(z)\mu(dz')\delta_{\psi^{-1}(z')}(dz) &= \int f(z')g(z)\mu(z')v(dz')\delta_{\psi^{-1}(z')}(dz) \\
&= \int f(z')g(z)\mu(z')v(dz)\delta_{\psi(z)}(dz') \\
&= \int f \circ \psi(z)g(z)\mu \circ \psi(z)v(dz) \\
&= \int f \circ \psi(z)g(z)\frac{\mu \circ \psi(z)}{\mu(z)}\mu(z)v(dz) \\
&= \int f(z')g(z)\frac{\mu \circ \psi(z)}{\mu(z)}\mu(dz)\delta_{\psi(z)}(dz')
\end{aligned}$$

As a result

$$\begin{aligned}
\int f(z')\mu(dz') &= \int f(z')\mu(dz')\delta_{\psi^{-1}(z')}(dz) \\
&= \int f(z')\frac{\mu \circ \psi(z)}{\mu(z)}\mu(dz)\delta_{\psi(z)}(dz') \\
&= \int f \circ \psi(z)\frac{\mu \circ \psi(z)}{\mu(z)}\mu(dz)
\end{aligned}$$

□

Corollary 21. *With the assumptions of Lemma 20 above for $k \in \llbracket 0, T \rrbracket$ the weight (32) for $M_\mu = \Psi^k, L_\mu = \Psi^{-k}$ admits the expression*

$$w_k(\mathbf{z}) = \frac{d\mu \widehat{\otimes} \Psi^{-k}}{d\mu \otimes \Psi^k}(z_0, z_k) = \frac{\mu \circ \psi^k(z_0)}{\mu(z_0)},$$

Further, for R a ν -invariant Markov kernel the expression for the weight (31) becomes

$$\bar{w}(z, z') = \frac{\mu(z'_0)}{\nu(z'_0)} \frac{1}{T+1} \sum_{k=0}^T \frac{\mu \circ \psi^k(z'_0)}{\mu(z'_0)},$$

hence recovering the expression used in Section 2. This together with the results of Appendix D.1 provides an alternative justification of correctness of Alg. 3 and hence Alg. 2. Note that this choice for L_μ corresponds to the so-called optimal scenario; this can be deduced from Lemma 20 or by noting that

$$\begin{aligned} \int f(z, z') \mu \Psi(dz') \Psi^{-1}(z', dz) &= \int f(\psi^{-1}(z'), z') \mu \Psi(dz') \\ &= \int f(z, \psi(z)) \mu(dz) \\ &= \int f(z, z') \mu(dz) \Psi(z, dz'). \end{aligned}$$

D.4 More complex integrator snippets

Here we provide examples of more complex integrator snippets to which earlier theory immediately applies thanks to the abstract point of view adopted throughout.

Example 22. Let $\nu \gg \mu$, so that $\mu(z) := d\mu/d\nu(z)$ is well defined. Let, for $i \in \{1, 2\}$, $\psi_i: Z \rightarrow Z$ be invertible and such that $\nu^{\psi_i} = \nu$, $\psi_i^{-1} = \sigma \circ \psi_i \circ \sigma$ for $\sigma: Z \rightarrow Z$ such that $\sigma^2 = \text{Id}$ and $\nu^\sigma = \nu$. Then one can consider the delayed rejection MH transition probability

$$M(z, dz') = \alpha_1(z) \delta_{\psi_1(z)}(dz') + \bar{\alpha}_1(z) [\alpha_2(z) \delta_{\psi_2(z)}(dz') + \bar{\alpha}_2(z) \delta_z(dz')],$$

with $\alpha_i(z) = 1 \wedge r_i(z)$ $\bar{\alpha}_i(z) = 1 - \alpha_i(z)$ and $z \in S_1 \cap S_2$ given below

$$r_1(z) = \frac{d\nu^{\psi_1^{-1}}}{d\nu}(z), \quad r_2(z) = \frac{\bar{\alpha}_1 \circ \sigma \circ \psi_2(z) d\nu^{\psi_2^{-1}}}{\bar{\alpha}_1(z) d\nu}(z).$$

A particular example is when ν is the Lebesgue measure on $X \times V$ and ψ_1 is volume preserving, for instance the leapfrog integrator for Hamilton's equations for some potential U or the bounce update (37). Following [2] notice that ν has density $v(z) = 1/2$ with respect to the measure $\nu + \nu^{\psi_1} = 2\nu$. Now define $S_1 := \{z \in Z: v(z) \wedge \nu \circ \psi_1(z) > 0\}$, we have

$$r_1(z) := \begin{cases} \frac{\nu \circ \psi_1(z)}{v(z)} = 1 & \text{for } z \in S_1 \\ 0 & \text{otherwise} \end{cases},$$

and with $S_2 := \{z \in Z: [\bar{\alpha}_1(z) v(z)] \wedge [\bar{\alpha}_1 \circ \sigma \circ \psi_2(z) \nu \circ \psi_2(z)] > 0\}$

$$r_2(z) := \begin{cases} \frac{\bar{\alpha}_1 \circ \sigma \circ \psi_2(z) \nu \circ \psi_2(z)}{\bar{\alpha}_1(z) v(z)} = 1 & \text{for } z \in S_2 \\ 0 & \text{otherwise} \end{cases}.$$

For instance ψ_1 can be a HMC update, while

$$\psi_2 = \psi_1 \circ b \circ \psi_1 \text{ with } b(x, v) = (x, v - 2\langle v, n(x) \rangle n(x)) \quad (37)$$

for some unit length vector field $n: X \rightarrow X$. This can therefore be used as part of Alg. 6; care must be taken when compute the weights $w_{n,k}$ and \bar{w}_n , see Appendix D-D.3 provide the tools to achieve this. For example, in the situation where ν is the Lebesgue measure on $Z = \mathbb{R}^d$ and $\psi_2 = \text{Id}$ then we recover Alg. 3 or equivalently Alg. 2.

Example 23. An interesting instance of Example 22 is concerned with the scenario where interest is in sampling μ constrained to some set $C \subset \mathbf{Z}$ such that $v(C) < \infty$. Define μ constrained to C , $\mu_C(\cdot) := \mu(C \cap \cdot) / \mu(C)$ and similarly $v_C(\cdot) := v(C \cap \cdot) / v(C)$. We let M be defined as above but targeting v_C . Naturally v_C has a density w.r.t. v , $v_C(z) = \mathbf{1}_C(z) / v(C)$ for $z \in \mathbf{Z}$ and for $i \in \{1, 2\}$ we have $v_C \circ \psi_i(z) = \mathbf{1}_{\psi_i^{-1}(C)}(z)$, $v \circ \psi_1 \circ \psi_2(z) = \mathbf{1}_{\psi_2^{-1} \circ \psi_1^{-1}(C)}(z)$. Consequently $S_1 := \{z \in \mathbf{Z} : \mathbf{1}_{C \cap \psi_1^{-1}(C)}(z) > 0\}$ and $S_2 = \{z \in \mathbf{Z} : \mathbf{1}_{C \cap \psi_1^{-1}(C^c)}(z) \mathbf{1}_{\psi_2^{-1}(C) \cap \psi_2^{-1} \circ \psi_1^{-1}(C^c)}(z) > 0\}$ and as a result

$$\begin{aligned}\alpha_1(z) &:= \mathbf{1}_{A \cap \psi_1^{-1}(C)}(z) \\ \alpha_2(z) &:= \mathbf{1}_{A \cap \psi_1^{-1}(C^c) \cap \psi_2^{-1}(C) \cap \psi_2^{-1} \circ \psi_1^{-1}(C^c)}(z).\end{aligned}$$

The corresponding kernel $M^{\otimes T}$ is described algorithmically in Alg. 7. In the situation where $C := \{x \in \mathbf{X} : c(x) = 0\}$ for a continuously differentiable function $c: \mathbf{X} \rightarrow \mathbb{R}$, the bounces described in (37) can be defined in terms of the field $x \mapsto n(x)$ such that

$$n(x) := \begin{cases} \nabla c(x) / |\nabla c(x)| & \text{for } \nabla c(x) \neq 0 \\ 0 & \text{otherwise.} \end{cases}$$

This justifies the ideas of [8], where a process of the type given in Alg. 7 is used as a proposal within a MH update, although the possibility of a rejection after the second stage seems to have been overlooked in that reference.

```

1 Given  $z_0 = z \in C \subset \mathbf{Z}$ 
2 for  $k = 1, \dots, T$  do
3   if  $\psi_1(z_{k-1}) \in C$  then
4     |  $z_k = \psi_1(z_{k-1})$ 
5   else if  $\psi_2(z_{k-1}) \in C$  and  $\psi_1 \circ \psi_2(z_{k-1}) \notin C$  then
6     |  $z_k = \psi_2(z_{k-1})$ 
7   else
8     |  $z_k = z_{k-1}$ .
9   end
10 end
```

Algorithm 7: $M^{\otimes T}$ for M the delayed rejection algorithm targeting the uniform distribution on C

Naturally a rejection of both transformations ψ_1 and ψ_2 of the current state means that the algorithm gets stuck. We note that it is also possible to replace the third update case with a full refreshment of the velocity, which can be interpreted as a third delayed rejection update, of acceptance probability one.

E Early experimental results: HMC-IS

E.1 Numerical illustration: logistic regression

In this section, we consider sampling from the posterior distribution of a logistic regression model, focusing on the computation of the normalising constant. We follow [26] and consider the sonar dataset, previously used in [24]. With intercept terms, the dataset has responses $y_i \in \{-1, 1\}$ and covariates $z_i \in \mathbb{R}^p$, where $p = 61$. The likelihood of the parameters $x \in \mathbf{X} := \mathbb{R}^p$ is then given by

$$L(x) = \prod_i^n F(z_i^\top x \cdot y_i), \quad (38)$$

where $F(x) := 1/(1 + \exp(-x))$. We ascribe x a product of independent normal distributions of zero mean as a prior, with standard deviation equal to 20 for the intercept and 5 for the other parameters. Denote $p(dx)$ the prior distribution of x , we define a sequence of tempered distributions of densities of the form $\pi_n(x) \propto p(dx)L(x)^{\lambda_n}$ for $\lambda_n: \llbracket 0, P \rrbracket \rightarrow [0, 1]$ non-decreasing and such that $\lambda_0 = 0$ and $\lambda_P = 1$. We apply both Hamiltonian Snippet-SMC and the implementation of waste-free SMC of [26] and compare their performance.

For both algorithms, we set the total number of particles at each SMC step to be $N(T + 1) = 10,000$. For the waste-free SMC, the Markov kernel is chosen to be a random-walk Metropolis-Hastings kernel with covariances adaptively computed as $2.38^2/d \hat{\Sigma}$, where $\hat{\Sigma}$ is the empirical covariance matrix obtained from the particles in the previous SMC step. For the Hamiltonian Snippet-SMC algorithm, we set ψ_n to be the one-step leap-frog integrator with stepsize ϵ , $U_n(x) = -\log(\pi_n(x))$ and ϖ a $\mathcal{N}(0, \text{Id})$. To investigate the stability of our algorithm, we ran Hamiltonian Snippet SMC with $\epsilon = 0.05, 0.1, 0.2$ and 0.3 . For both algorithms, the temperatures λ_n are adaptively chosen so that the effective sample size (ESS) of the current SMC step will be αESS_{max} , where ESS_{max} is the maximum ESS achievable at the current step. In our experiments, we have chosen $\alpha = 0.3, 0.5$ and 0.7 for both algorithms.

Performance comparison

Figure 23 shows the boxplots of estimates of the logarithm of the normalising constant obtained from both algorithms, for different choices of N and ϵ for the Hamiltonian Snippet SMC algorithm. The boxplots are obtained by running both algorithms 100 times for different of the algorithm parameters, with $\alpha = 0.5$ in all setups. Several points are worth observing. For a suitably choice of ϵ , the Hamiltonian Snippet SMC algorithm can produce stable and consistent estimates of the normalising constant with 10,000 particles at each iteration. On the other hand, however, the waste-free SMC algorithm fails to produce accurate results for the same computational budget. It is also clear that with larger values of N (meaning smaller value of T and hence shorter snippets), the waste-free SMC algorithm produces results with larger biases and variability. For Hamiltonian Snippet SMC algorithm, the results are stable both for short and long snippets when ϵ is equal to 0.1 or 0.2. Another point is that when $\epsilon = 0.05$ or 0.3, the Hamiltonian Snippet SMC algorithm becomes unstable with short (i.e. $\epsilon = 0.05$) and long (i.e. $\epsilon = 0.3$). Possible reasons are for too small a stepsize the algorithm is not able to explore the target distribution efficiently, resulting in unstable performances. On the other hand, when the stepsize is too large, the leapfrog integrator becomes unstable, therefore affecting the variability of the weights; this is a common problem of HMC algorithms. Hence, a long trajectory will result in detoriante estimations. Hence, to obtain the best performance, one should find a way of tuning the stepsize and trajectory length along with the SMC steps.

In Figure 24 we display boxplots of the estimates of the posterior expectations of the mean of all coefficients, i.e. $\mathbb{E}_{\pi_P}(d^{-1} \sum_{i=1}^d x_i)$. This quantity is referred to as the *mean of marginals* in [26] and we use this terminology. One can see that the same properties can be seen from the estimations of the mean of marginals, with the instability problems exacerbated with small and large stepsizes.

Computational Cost

In this section, we compare the running time of both algorithms. Since the calculations of the potential energy and its gradient often share common intermediate steps, we can recycle these to save computational cost. As the waste-free SMC also requires density evaluations, the Hamiltonian Snippet SMC algorithm will not require significant additional computations. Figure 25 shows boxplots of the simulation time of both algorithms from 100 runs. The simulations were run on an Apple M1-Pro CPU with 16G of memory. One can see that in comparison to the waste-free SMC the additional computational time is only marginal for the Hamiltonian Snippet SMC algorithm and mostly due to the larger memory needed to store the intermediate values.

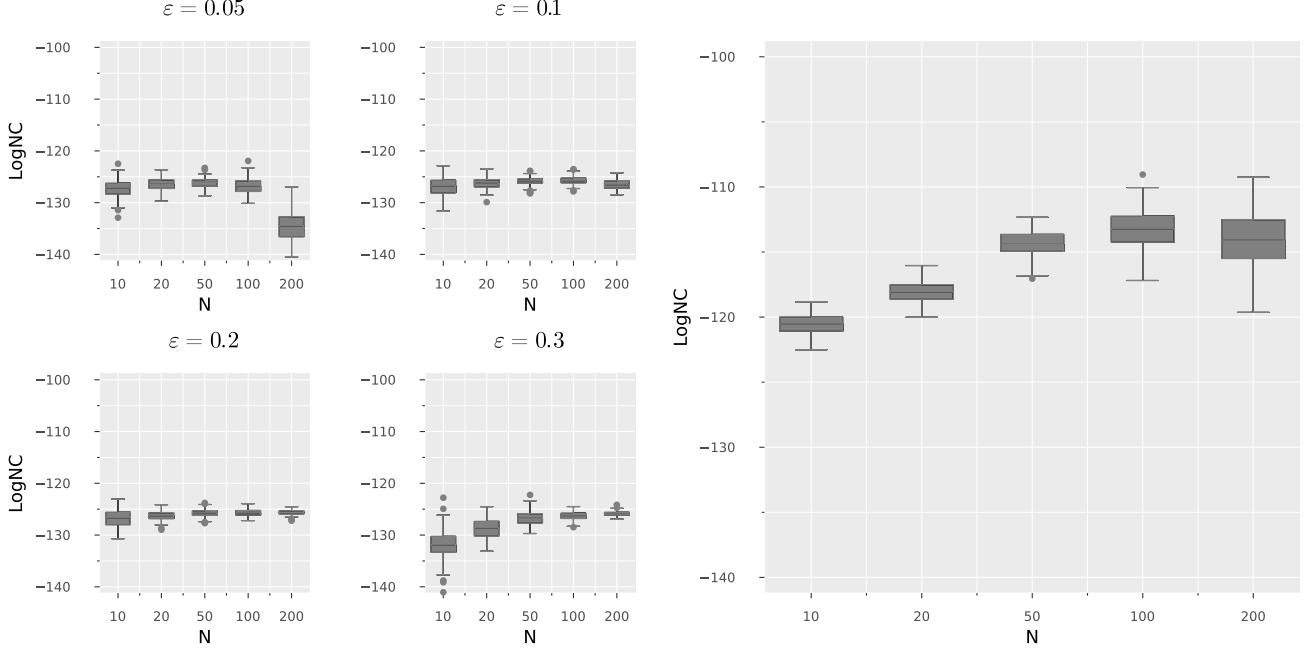


Figure 23: Estimates of the normalising constant (in log scale) obtained from both Hamiltonian Snippet SMC and waste-free SMC algorithm. Left: Estimate obtained from Hamiltonian Snippet SMC algorithm with different values of ϵ . Right: Estimates obtained from waste-free SMC algorithm.

E.2 Numerical illustration: orthant probabilities

In this section, we consider the problem of calculating the Gaussian orthant probabilities, which is given by

$$p(\mathbf{a}, \mathbf{b}, \Sigma) := \mathbb{P}(\mathbf{a} \leq \mathbf{X} \leq \mathbf{b}),$$

where $\mathbf{a}, \mathbf{b} \in \mathbb{R}^d$ are known vectors of dimension d and $\mathbf{X} \sim \mathcal{N}_d(\mathbf{0}, \Sigma)$ with Σ a covariance matrix of size $d \times d$. Consider the Cholesky decomposition of Σ which is given by $\Sigma := LL^\top$, where $L := (l_{ij}, i, j \in \llbracket d \rrbracket)$ is a lower triangular matrix with positive diagonal entries. It is clear that \mathbf{X} can be viewed as $\mathbf{X} := L\eta$, where $\eta \sim \mathcal{N}_d(\mathbf{0}, \text{Id}_d)$. Consequently, one can instead rewrite $p(\mathbf{a}, \mathbf{b}, \Sigma)$ as a product of d probabilities given by

$$p_1 = \mathbb{P}(a_1 \leq l_{11}\eta_1 \leq b_1) = \mathbb{P}(a_1/l_{11} \leq \eta_1 \leq b_1/l_{11}), \quad (39)$$

and

$$p_n = \mathbb{P}\left(a_t \leq \sum_{j=1}^n l_{nj}\eta_j \leq b_t\right) = \mathbb{P}\left((a_t - \sum_{j=1}^{n-1} l_{nj}\eta_j)/l_{nn} \leq \eta_t \leq (b_t - \sum_{j=1}^{n-1} l_{nj}\eta_j)/l_{nn}\right), \quad (40)$$

for $n = 2, \dots, d$. For notational simplicity, we let $\mathcal{B}_n(\eta_{1:n-1})$ denote the interval $[(a_t - \sum_{j=1}^{n-1} l_{nj}\eta_j)/l_{nn}, (b_t - \sum_{j=1}^{n-1} l_{nj}\eta_j)/l_{nn}]$, with the convention $\mathcal{B}_1(\eta_{1:0}) := [a_1/l_{11}, b_1/l_{11}]$. Then, $p(\mathbf{a}, \mathbf{b}, \Sigma)$ can be written as the product of p_n s for $n = 1, 2, \dots, d$. Moreover, one could see that p_n is also the normalising constant of the conditional distribution of η_n given $\eta_{1:n-1}$. To calculate the orthant probability, [54] have proposed an SMC algorithm targetting the

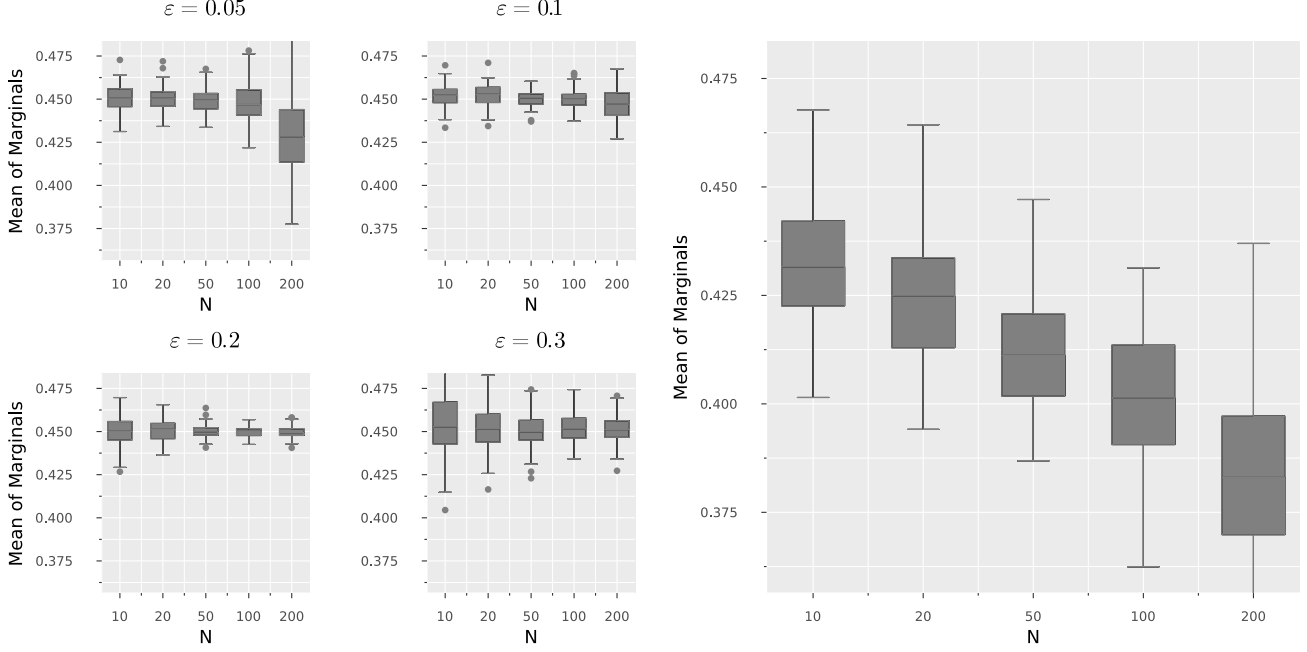


Figure 24: Estimates of the mean of marginals obtained from both Hamiltonian Snippet SMC and the waste-free SMC algorithms. Left: Estimate obtained from the Hamiltonian Snippet SMC algorithm with difference values of ϵ . Right: Estimates obtained from the waste-free SMC algorithm.

sequence of distributions $\pi_n(\eta_{1:n}) := \pi_1(\eta_n) \prod_{k=2}^n \pi_n(\eta_k | \eta_{1:k-1})$ for $n \in \llbracket 1, d \rrbracket$, given by

$$\pi_1(\eta_1) \propto \phi(\eta_1) \mathbf{1}\{\eta_1 \in \mathcal{B}_1\} = \gamma_1(\eta_1) \quad (41)$$

$$\pi_n(\eta_n | \eta_{1:n-1}) \propto \phi(\eta_n) \mathbf{1}\{\eta_n \in \mathcal{B}_n(\eta_{1:n-1})\} = \gamma_n(\eta_n | \eta_{1:n-1}). \quad (42)$$

where ϕ denotes the probability density of a $\mathcal{N}(0, 1)$. One could also note that

$$\pi_n(\eta_n | \eta_{1:n-1}) = 1/\Phi(\mathcal{B}_n(\eta_{1:n-1}))\phi(\eta_n) \mathbf{1}\{\eta_n \in \mathcal{B}_n(\eta_{1:n-1})\}$$

and $\gamma_n(\eta_{1:n}) = \phi(\eta_{1:n}) \prod_{k=1}^n \mathbf{1}\{\eta_k \in \mathcal{B}_k(\eta_{1:k-1})\}$, where $\Phi(\mathcal{B}_n(\eta_{1:n-1}))$ represents the probability of a standard Normal random variable being in the region $\mathcal{B}_n(\eta_{1:n-1})$. Therefore, the SMC algorithm proposed by [54] then proceeds as follows. (1) At time t , particles $\eta_{1:t-1}^{(i)}$ are extended by sampling $\eta_n^n \sim \pi_n(d\eta_t | \eta_{1:t-1}^{(i)})$. (2) Particles $\eta_{1:t}^{(i)}$ are then reweighted by multiplying the incremental weights $\Phi(\mathcal{B}_n(\eta_{1:n-1}^{(i)}))$ to $w_{n-1}^{(i)}$. (3) If the ESS is below a certain threshold, resample the particles and move them through an MCMC kernel that leaves π_t invariant for k iterations. For the MCMC kernel, [54] recommended using Gibbs sampler that leaves π_t invariant to move the particles at step (3). The orthant probability we are interested in can then be viewed as the normalising constant of π_d and this can be estimated as a by-product of the SMC algorithm.

Since we are trying to sample from the constrained Gaussian distributions, the Hamiltonian equation can be solved exactly and $w_{n,k}$ is always 1. As a result, the incremental weights for the trajectories simplify to $\Phi(\mathcal{B}_n(u_{n-1}))$ and each particle on the trajectory starting from z_t will have an incremental weight proportional to $\Phi(\mathcal{B}_n(u_{n-1}))$.

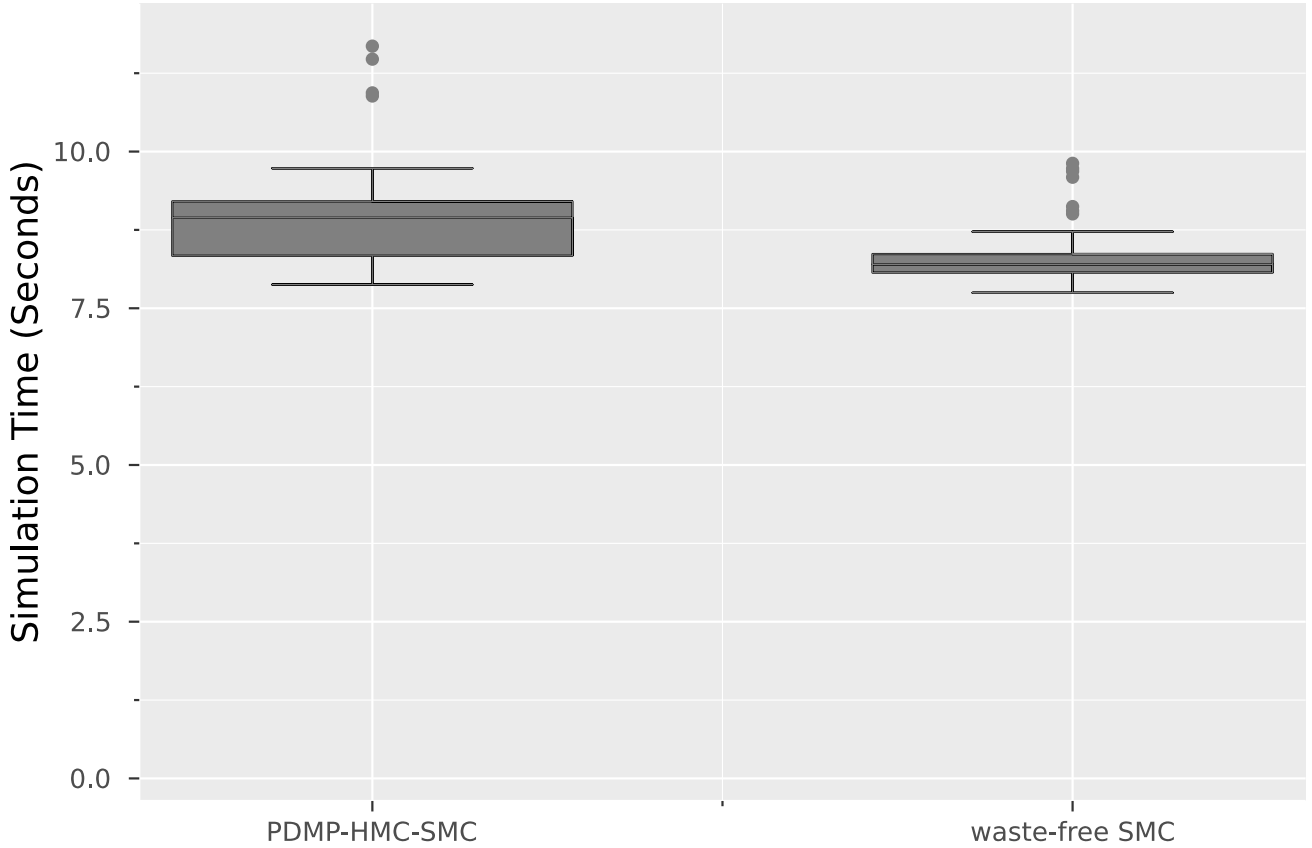


Figure 25: Simulation times for both algorithms. Left: Simulation time for Hamiltonian Snippet SMC algorithm, with $N = 100, \epsilon = 0.2, \alpha = 0.5$. Right: Simulation times for the waste-free SMC with $N = 100$

To obtain a trajectory, we follow [51] who perform HMC with reflections to sample. As the dimension increases, the number of reflections performed under ψ_n will also increase given a fixed integration time. We adaptively tuned the integrating time ϵ to ensure that the average number of reflections at each SMC step does not exceed a given threshold. In our experiment we set this threshold to be 5. To show that the waste-recycling RSMC algorithm scales well in high dimension, we set $d = 150, a = (1.5, 1.5, \dots)$ and $b = (\infty, \infty, \dots)$. Also, we use the same covariance matrix in [26] and perform variable re-ordering as suggested in [54] before the simulation.

Figures 26 and 27 show the results obtained with $N \times (T+1) = 50,000$ and various values for N . With a quarter of the number of particles used in [26], the waste-recycling HSMC algorithm achieves comparable performance when estimating the normalising constant (i.e. the orthant probability). Moreover, the estimates are stable for different choices of N values, although one observes that the algorithm achieves best performance when $N = 500$ (i.e. each trajectory contains 100 particles). This also suggests that the integrating time should be adaptively tuned in a different way to achieve the best performance given a fixed computational budget. Estimates of the function $\varphi(x_{0:d}) = \mathbb{E}(1/d \sum_{i=1}^d x_i)$ with respect to the Gaussian distribution $\mathcal{N}_d(\mathbf{0}, \Sigma)$ truncated between \mathbf{a} and \mathbf{b} are also stable for different choices of N , although they are more variable than those obtained in [26]. This indicates that

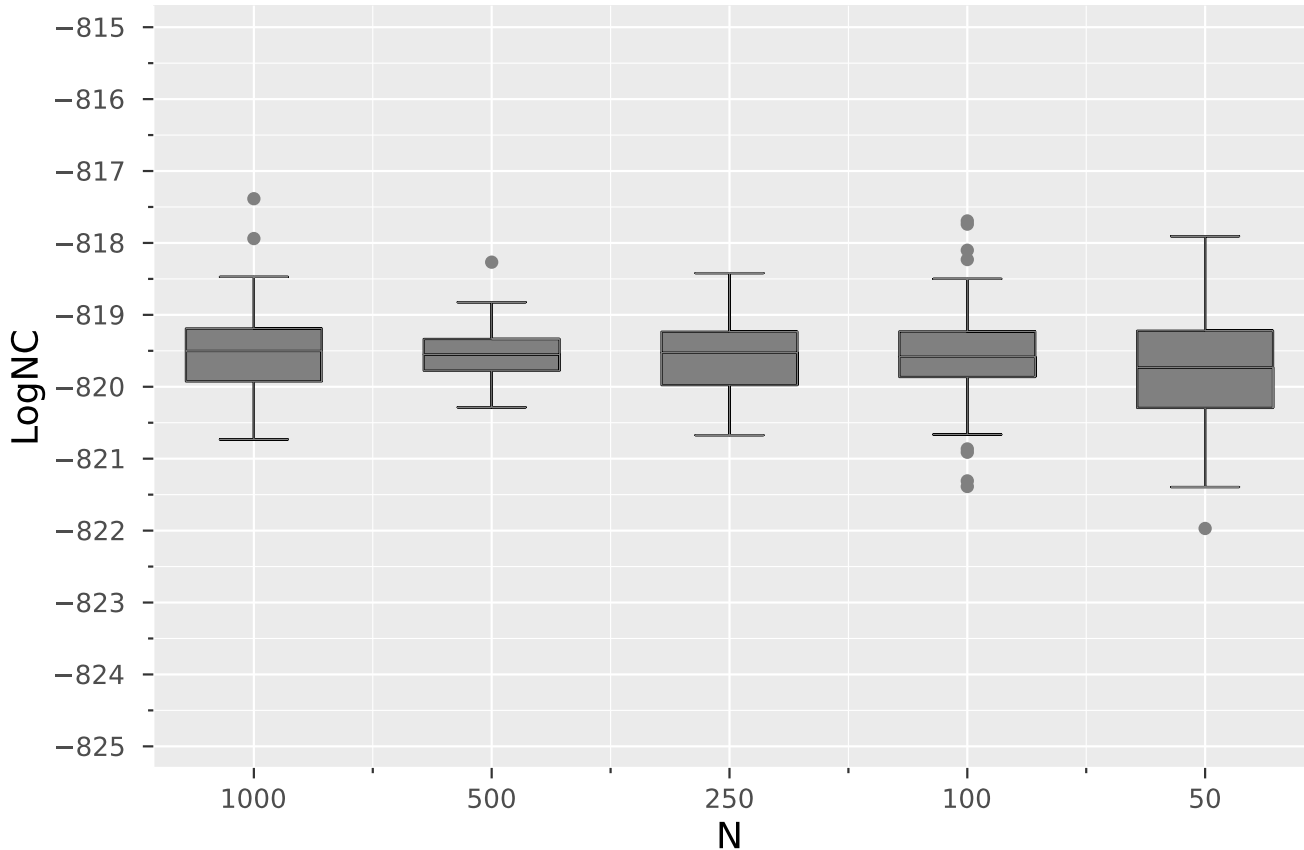


Figure 26: Orthant probability example: estimates of the normalising constant (i.e. the orthant probability) obtained from the waste-recycling HSMC algorithm with $N = 50,000$.

the waste-recycling HSMC algorithm does scale well in high dimension. We note that this higher variance compared to the waste-free SMC of [26], is obtained in a scenario where they are able to exploit the particular structure of the problem and implement an exact Gibbs sampler to move the particles. The integrator snippet SMC we propose is however more general and applicable to scenarios where such a structure is not present.

F Early experimental results: filamentary distributions

F.1 Numerical illustration: simulating from filamentary distributions

We now illustrate the interest of integrator snippets in a scenario where the target distribution possesses specific geometric features. Specifically, we focus here on distributions concentrated around a manifold $\mathcal{M} \subset \mathbb{X} = \mathbb{R}^d$ defined as the zero level set of a smooth function $\ell : \mathbb{R}^d \rightarrow \mathbb{R}^m$

$$\mathcal{M} := \{x \in \mathbb{X} : \ell(x) = 0\},$$

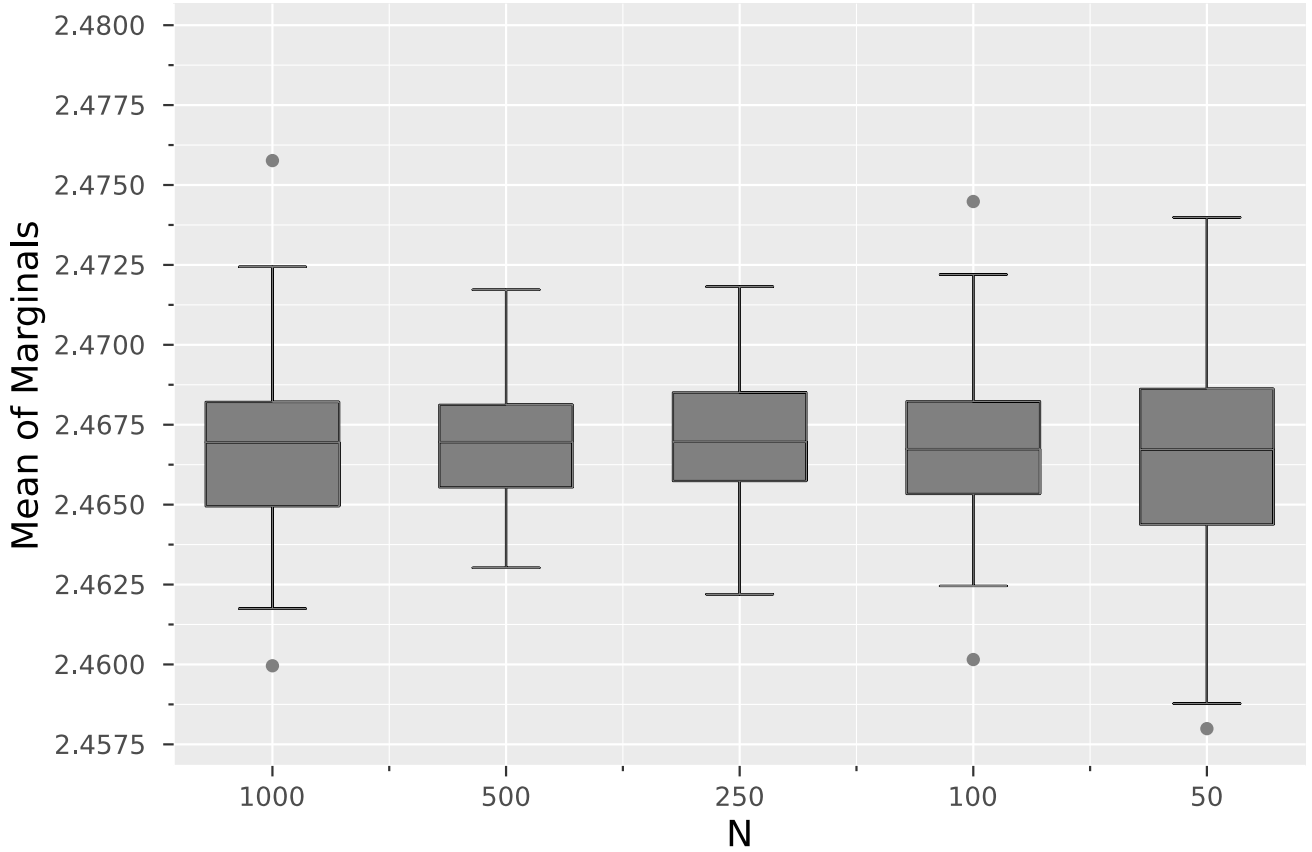


Figure 27: Orthant probability example: estimates of the mean of marginals obtained from the integrator snippet SMC algorithm with $N = 50,000$.

sometimes referred to as filamentary distributions [19, 43, 44]. Such distributions arise naturally in various scenarios, including inverse problems or generalisations of the Gibbs sampler [19, 43, 44] or as a relaxation of problems where the support of the distribution of interest is included in \mathcal{M} or for example generalisation of the Gibbs sampler through disintegration [19]. Such is the case for ABC methods in Bayesian statistics [5]. Assume that π is a probability density with respect to the Lebesgue measure defined on \mathbf{X} and for $\epsilon > 0$ consider a “kernel” function $k_\epsilon(u) := \epsilon^{-m}k(u/\epsilon)$ where $k : \mathbb{R}^m \rightarrow \mathbb{R}_+$ and define the probability density

$$\pi_\epsilon(x) \propto k_\epsilon \circ \ell(x) \pi(x).$$

The corresponding probability distribution can be thought of as an approximation of the probability distribution of density $\pi_0(x) \propto \pi(x)\mathbf{1}\{x \in \mathcal{M}\}$ with respect to the Hausdorff measure on \mathcal{M} . Typical choices for the kernel are $k(u) = \mathbf{1}\{\|u\| \leq 1\}$ or $k(u) = \mathcal{N}(u; 0, \mathbf{I}_m)$. Strong anisotropy may result from such constraints and make exploration of the support of such distributions awkward for standard Monte Carlo algorithms. This is illustrated in Fig. ?? where a standard MH-HMC algorithms is used to sample from π_ϵ defined on \mathbb{R}^2 , for three values $\epsilon = 0.5, 0.1, 0.05$, and performance is observed to deteriorate as ϵ decreases. The samples produced are displayed in blue: for $\epsilon = 0.5$

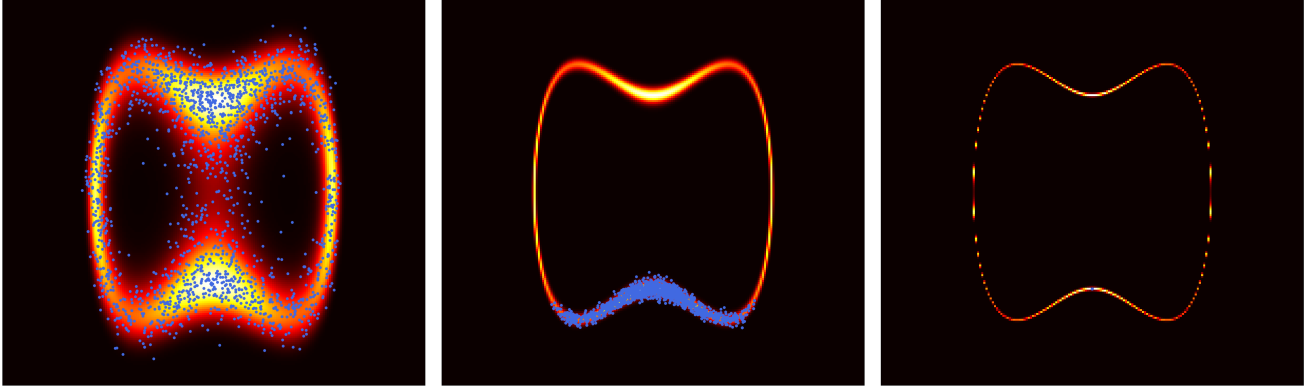


Figure 28: Heat map of $\pi_\epsilon(x) \propto \mathcal{N}(y | F(x), \epsilon^2) \mathcal{N}(x | 0, \mathbf{I}_2)$ with $F(x_1, x_2) := x_2^2 + x_1^2 (x_1^2 - \frac{1}{2})$, defined on \mathbb{R}^2 , for $y \in \mathbb{R}$ and $\epsilon = 0.5, 0.1, 0.05$ (left to right) superimposed with 2000 samples (in blue) obtained from an MH-HMC with step size 0.05 and involving $T = 20$ leapfrog steps.

HMC-MH mixes well and explores the support rapidly, but for $\epsilon = 0.1$ the chain gets stuck in a narrow region of π_ϵ at the bottom, near initialisation, while for $\epsilon = 0.05$, no proposal is ever accepted in the experiment.

To illustrate the properties of integrator snippet techniques we consider the following toy example. For $\epsilon > 0$ and $d \in \mathbb{N}_*$ let

$$\pi_\epsilon(x) \propto \frac{1}{\epsilon^m} \mathbf{1}\{\|\ell(x)\| \leq \epsilon\} \mathcal{N}(x; 0, \mathbf{I}_d) \quad \text{with} \quad \ell(x) = x^\top \Sigma^{-1} x - c,$$

for Σ a $d \times d$ symmetric positive matrix and $c \in \mathbb{R}$, that is we consider the restriction of a standard normal distribution around an ellipsoid defined by $\ell(x) = 0$.

In order to explore the support of the target distribution we use two mechanisms based on reflections either through tangential hyperplanes of equicontours of $\ell(x)$ or through the corresponding orthogonal complements. More specifically for $x \in \mathbf{X}$ such that $\nabla \ell(x) \neq 0$ let $n(x) := \nabla \ell(x) / \|\nabla \ell(x)\|$ and define the tangential HUG (THUG) and symmetrically-normal HUG (SNUG) as $\psi_\parallel := {}_A \psi \circ b \circ {}_A \psi$, and $\psi_\perp := {}_A \psi \circ (-b) \circ {}_A \psi$ respectively, with ${}_A \psi$ and b as in Example 1 and (37). Both updates can be understood as discretisations of ODEs and are volume preserving. Intuitively for $(x, v) \in \mathbf{Z}$ with $v_\parallel = v_\parallel(x + \epsilon v) := n(x + \epsilon v) n(x + \epsilon v)^\top v$ for $\epsilon > 0$ and $v_\perp = v - v_\parallel$ we have $\psi_\parallel(x, v) = (x + 2\epsilon v_\parallel, v_\parallel - v_\perp)$ and $\psi_\perp(x, v) = (x + 2\epsilon v_\perp, v_\perp - v_\parallel)$. This is illustrated in Fig. 29 for $d = 2$. Further, for an initial state $z_0 = (x_0, v_0) \in \mathbf{Z}$, trajectories of the first component of $k \mapsto \psi_\parallel^k(z_0)$ remain close to $\ell^{-1}(\{\ell(x_0)\})$ while $k \mapsto \psi_\perp^k(z_0)$ follows the gradient field $x \mapsto \nabla \ell(x)$ and leads to hops across equicontours.

The sequence of target distributions on $(\mathbf{Z}, \mathcal{Z})$ we consider is of the form

$$\mu_n(dz) \propto \pi_{\epsilon_n}(dx) \mathcal{N}(dv; 0, \mathbf{I}_d), \quad \epsilon_n > 0, n \in \llbracket 0, P \rrbracket,$$

and the Integrator Snippet SMC is defined through the mixture, for $\alpha \in [0, 1]$,

$$\bar{\mu}_n(dz) = \frac{\alpha}{T+1} \sum_{k=0}^T \mu_n^{\psi_\parallel^{-k}}(dz) + \frac{1-\alpha}{T+1} \sum_{k=0}^T \mu_n^{\psi_\perp^{-k}}(dz).$$

We compare performance of integrator snippet with an SMC Sampler relying on a mutation kernel M_n consisting of a mixture of two updates targetting μ_{n-1} each iterating T times a MH kernel applying integrator ψ_\parallel or ψ_\perp once

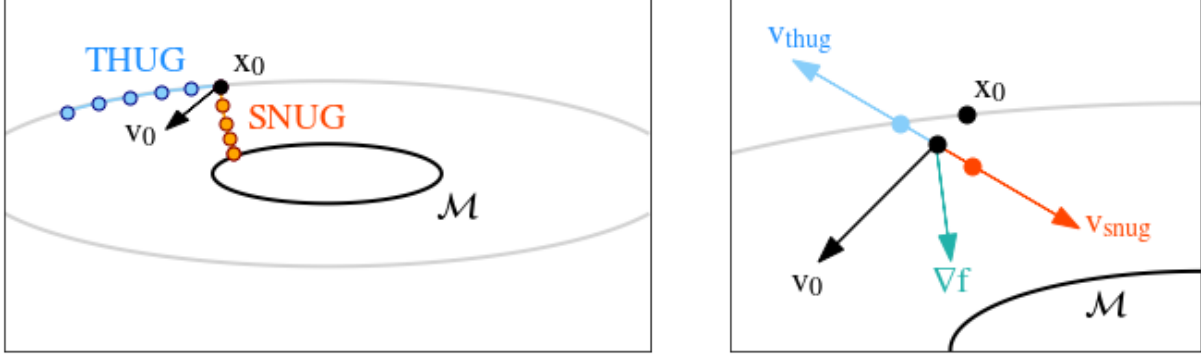


Figure 29: Black line: manifold of interest $\mathcal{M} = \ell^{-1}(0)$, grey line: level set of $\ell^{-1}(\{\ell(x_0)\})$ the ℓ -level set x_0 belongs to. Left: THUG trajectory (blue) remains close to $\ell^{-1}(\{\ell(x_0)\})$, SNUG trajectory (orange) explores different contours of $\ell(x)$. Right: $v_{\text{thug}} = v_y - v_x$ and $v_{\text{snug}} = -(v_y - v_x)$.

after refreshing the velocity; the backward kernels are chosen to correspond to the default choices discussed earlier. In the experiments below we set $d = 50$, $c = 12$, and Σ is the diagonal matrix alternating 1's and 0.1's along the diagonal. We used $N = 5000$ particles, sampled from $\mathcal{N}(0, \mathbf{I}_d)$ at time zero and ϵ_0 is set to the maximum distance of these particles in the ℓ domain from 0 and $\alpha = 0.8$ for both algorithms. We compared the two samplers across three metrics; all results are averaged over 20 runs.

Robustness and Accuracy: we fix the step size for SNUG to $\epsilon_1 = 0.1$ and run both algorithms for a grid of values of T and ϵ_j using a standard adaptive scheme based on ESS to determine $\{\epsilon_n, n \in \llbracket P \rrbracket\}$ until a criterion described below is satisfied and retain the final tolerance achieved, recorded in Fig. 30. As a result the terminal value ϵ_P and computational costs are different for both algorithms: the point of this experiment is only to demonstrate robustness and potential accuracy of Integrator Snippets. Both the SMC sampler and Integrator Snippet are stopped when the average probability of leaving the seed particle drops below 0.01.

Our proposed algorithm consistently achieves a two order magnitude smaller final value of ϵ and is more robust to the choice of stepsize.

Variance: for this experiment we set $T = 50$ steps, $\epsilon_j = 0.01$ and determine and compare the variances of the estimates of the mean of π_{ϵ_P} for the final SMC step, for which $\epsilon_P = 1 \times 10^{-7}$. To improve comparison, and in particular ensure comparable computational costs, both algorithms share the same schedule $\{\epsilon_n, n \in \llbracket P \rrbracket\}$, determined adaptively by the SMC algorithm in a separate pre-run.

The results are reported as componentwise boxplots in Fig. ?? where we observe a significant variance reduction for comparable computational cost.

Efficiency: we report the Expected Squared Jump Distance (ESJD) as a proxy of distance travelled by the two algorithms. For Integrator Snippets, it is possible to estimate this quantity as follows for a function $f : Z \rightarrow \mathbb{R}$

$$\text{ESJD}_n(f) \approx \sum_{i=1}^N \sum_{k=0}^T \sum_{l=k+1}^T \left(f(Z_{n-1,l}^{(i)}) \bar{W}_{n,l}^{(i)} - f(Z_{n-1,k}^{(i)}) \bar{W}_{n,k}^{(i)} \right)^2, \quad \bar{W}_{n,k}^{(i)} = \frac{\bar{w}_{n,k}(Z_{n-1}^{(i)})}{\sum_{l=0}^T \bar{w}_{n,l}(Z_{n-1}^{(i)})}.$$

We report the average of this metric in Table 1 for the functions $f_i(x) = x_i$ $i \in \llbracket d \rrbracket$, normalised by total runtime in seconds for all particles (first row), for the particles using the THUG update (second row) and those using the

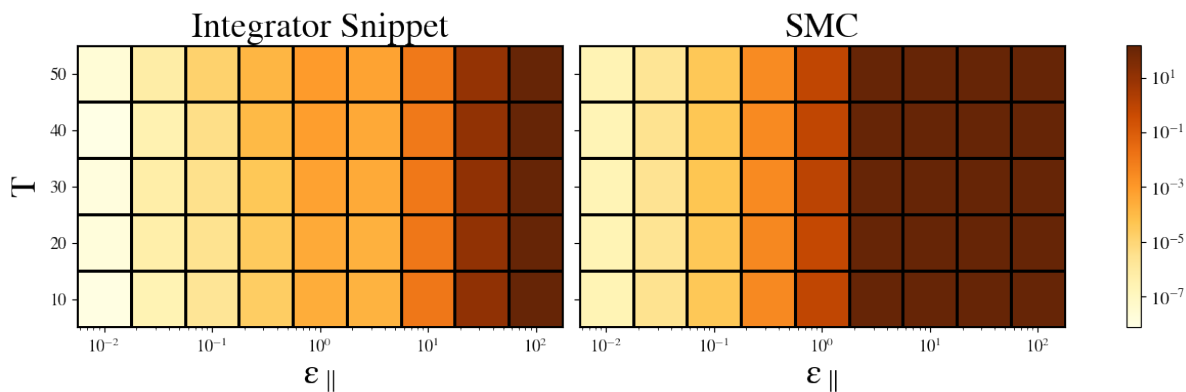


Figure 30: Final tolerances achieved by the two algorithms, averaged over 20 runs.

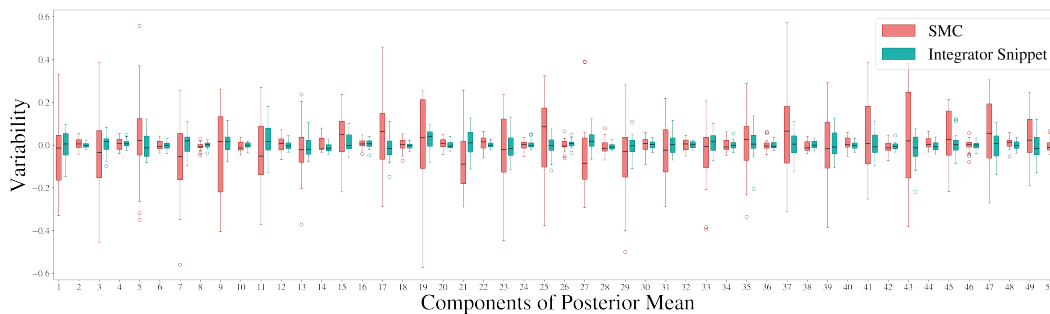


Figure 31: Variability of the estimates of the mean of π_ϵ for the SMC sampler and the Integrator Snippet, using estimator $\hat{\mu}_P(f)$, for the test function $f(x) = x$. Integrator snippet is able uniformly achieve smaller variance, in particular on the odd components corresponding to larger variances in Σ .

	Integrator Snippet	SMC
ESJD/ s	5.3×10^{-5} ($\pm 5.9 \times 10^{-6}$)	1.2×10^{-7} ($\pm 3.7 \times 10^{-9}$)
ESJD-THUG/ s	6.6×10^{-5} ($\pm 7.5 \times 10^{-6}$)	1.7×10^{-7} ($\pm 4.5 \times 10^{-9}$)
ESJD-SNUG/ s	2.7×10^{-4} ($\pm 3.2 \times 10^{-5}$)	1.6×10^{-20} ($\pm 6.0 \times 10^{-21}$)

Table 1: $d^{-1} \sum_{i=1}^d \text{ESJD}_n(f_i)$ normalised by time for Integrator Snippet and an SMC sampler.

SNUG update (third row), with standard deviation shown in parenthesis. Our proposed algorithm is several orders of magnitude more efficient in the exploration of π_ϵ than its SMC counterpart which, thanks to its ability to take full advantage of all the intermediary states of the snippet. This is in contrast with the SMC sampler which creates trajectories of random length.

In Fig. 32 we illustrate robustness of integrator snippet SMC to the choice of ϵ and T through the support covered; note that the computational cost of the three algorithms considered is comparable.

F.2 Going round the bend: bananas and pears

In this section we illustrate how ODEs and associated integrators can be used in order to update states involved in simulation algorithm for probability distributions involving geometrically awkward densities. The banana shaped distribution introduced by [34] in the context of adaptive MCMC algorithm is a prototypical toy example of dependencies encountered in some practical situation e.g. inverse problems. The banana shaped distribution defined on $\mathbf{X} = \mathbb{R}^d$, has density with respect to the Lebesgue measure $\pi(x) \propto \mathcal{N}(\phi(x); 0, \Sigma)$ where $\phi(x) = (x_1, x_2 + 0.03(x_1^2 - 100), x_2, \dots, x_n)$ and $\Sigma = \text{diag}(100, 1, \dots, 1)$ – see its contours for $d = 2$ in Fig. 33. A first suggestion could be to follow the contours of π using the update described in the previous section. Here we suggest the following flow, for $v \in \{-1, 1\}$,

$$t \mapsto \begin{cases} x_1(t) = vt \\ x_2(t) = -0.03(x_1^2(t) - 100) + x_2(0) + 0.03(x_1^2(0) - 100) \\ x_i(t) = x_i(0) \end{cases} \quad \text{for } i > 2$$

Motivation for this is that $t \mapsto x_2(t) + 0.03(x_1^2(t) - 100) = x_2(0) + 0.03(x_1^2(0) - 100)$ is a constant, effectively unbending the banana and effectively applying a standard Gibbs sampler [64] on a Gaussian in a different set of coordinates. This suggests a practical implementation of generalized forms of the Gibbs sampler, which can be traced back to [18] and were recently revived in [52]. Naturally in practice such updates must be completed with other updates to ensure irreducibility.

In more general situations where $\phi(x) = (x_1, u(x_1, x_2), x_3, \dots)$ for some $u: \mathbf{X}^2 \rightarrow \mathbb{R}$ such that π is indeed a probability density, the idea can be generalized with the ideal aim of keeping $t \mapsto u(x_1(t), x_2(t))$ or $t \mapsto x_1(t)^2 + u(x_1(t), x_2(t))^2$ constant, either using THUG or even Hamilton’s equation as suggested by the last constraint. Note however that non-separability may cause additional numerical difficulties in the latter scenario.

Another popular illustrative toy example is Neal’s funnel on which numerous standard algorithms may struggle to converge. The funnel consists of a mixture of normal distributions

$$\pi(x, y) = \mathcal{N}(y; 0, 3)\mathcal{N}(x; 0, \exp(y/2)),$$

defining a probability density on \mathbb{R}^2 of contours shown in Fig. 34—multiple x ’s can be incorporated therefore taking the form of a hierarchical model. It exemplifies some of the difficulties which may be encountered when sampling from hierarchical models.

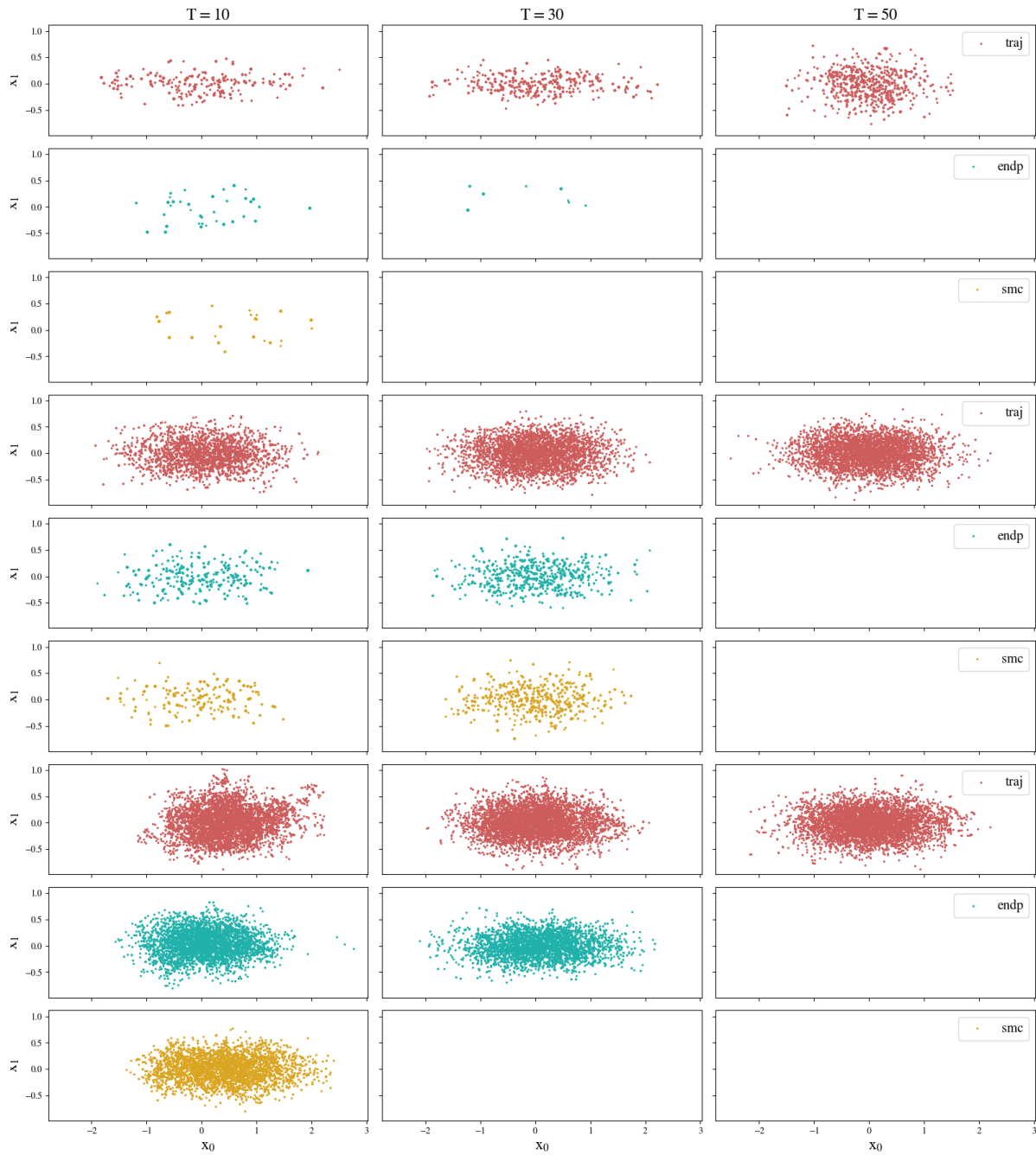


Figure 32: Scatter plot of the first two coordinates of $\{x_{n,k}^{(i)}, i \in \llbracket N \rrbracket, k \in \llbracket 0, T \rrbracket\}$ for three SMC algorithms: Snippet SMC (traj), Snippet SMC using the snippets endpoints only (endp) and the SMC sampler (smc). The stepsize is decreased from a high value for rows 1-3 ($\epsilon = 1.0$), to lower values for rows 4-6 ($\epsilon = 0.1$) and rows 7-9 ($\epsilon = 0.01$). The three columns correspond to different snippet length, $T = 10, 30, 50$.

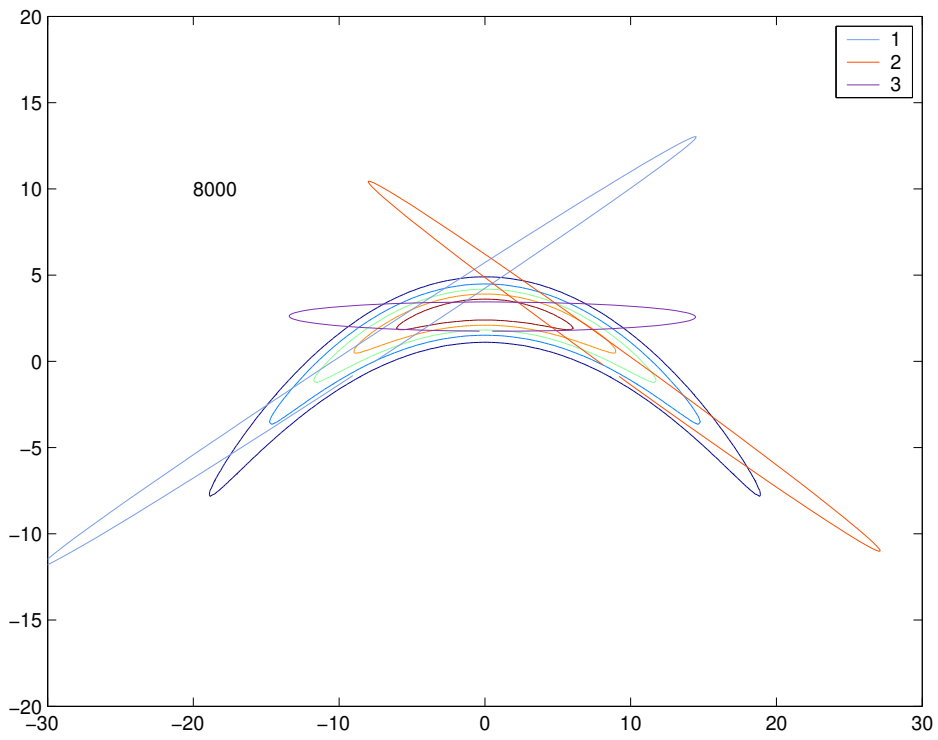


Figure 33: The banana distribution, $d = 2$

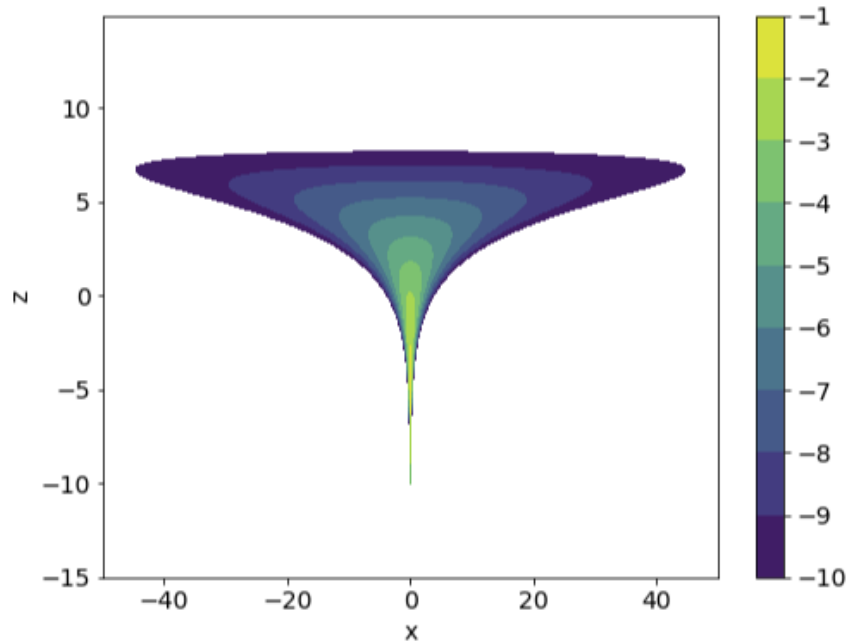


Figure 34: Neal's funnel

The narrow funnel is the cause of failure of traditional algorithms. A simple idea here consists of identifying a flow such that $t \mapsto \mathcal{N}(x_t; 0, \exp(y_t/2)) \equiv \mathcal{N}(x_0; 0, \exp(y_0/2))$ for given (x_0, y_0) . A straightforward choice imposes $\dot{y}_t = v$ with $v \in \{-1, 1\}$ and $x_t/\exp(y_t/4) = x_0/\exp(y_0/4)$ for $t > 0$, therefore ensuring that $x_t \sim \mathcal{N}(0, \exp(y_t/2))$ for $t > 0$. This can be solved analytically

$$\begin{aligned} x_t &= x_0 \exp(y_0/4 + y_t/4) = x_0 \exp((y_0 + vt)/4) \\ y_t &= vt. \end{aligned}$$

This corresponds to a simple reparametrizations, standard in the literature. However our suggested use differs in that both components are updated simultaneously within an MCMC kernel, and illustrate the potential of this type of ideas. Such a dynamic should naturally be mixed with other updates ensuring irreducibility.

G Adaptation: implementational details

G.1 About the structure of the mother distribution

It is useful to provide details about the (hierarchical) structure of the target distributions useful for implementational purposes. The mother distribution in (20) is given by

$$\bar{\mu}(k, d(\epsilon, z); \gamma, \theta) := \frac{1}{T+1} \mu^{\psi_\epsilon^{-k}}(dz; \gamma) \nu_\theta(d\epsilon)$$

from which we notice that

$$\begin{aligned}\bar{\mu}(k, d(\epsilon, z); \theta, \gamma) &= \bar{\mu}(k, dz | \epsilon, \gamma) \nu_\theta(d\epsilon) \\ &= \bar{\mu}(k | \epsilon, z; \gamma) \bar{\mu}(dz | \epsilon; \gamma) \nu_\theta(d\epsilon)\end{aligned}$$

that is the first conditionals do not depend on $\theta \in \Theta$. Indeed, marginalising yields $\bar{\mu}(d\epsilon, z; \theta, \gamma) = \nu_\theta(d\epsilon)$, implying

$$\bar{\mu}(k, dz | \epsilon; \gamma, \theta) = \frac{1}{T+1} \mu^{\psi_\epsilon^{-k}}(dz; \gamma)$$

and justifying the notational simplifications, leading to

$$\begin{aligned}\bar{\mu}(dz | \epsilon; \gamma, \theta) &= \bar{\mu}(dz | \epsilon; \gamma) = \frac{1}{T+1} \sum_{l=0}^T \mu^{\psi_\epsilon^{-l}}(dz; \gamma) \\ \bar{\mu}(k | \epsilon, z; \gamma, \theta) &= \bar{\mu}(k | \epsilon, z; \gamma) = \frac{d\mu^{\psi_\epsilon^{-k}}}{d(\sum_{l=0}^T \mu^{\psi_\epsilon^{-l}})}(z; \gamma).\end{aligned}$$

With $\bar{f} = \bar{f}(\epsilon, K, Z)$ for $\bar{f}(\epsilon, k, z) := f \circ \psi_\epsilon^k(z)$ for $f: Z \rightarrow \mathbb{R}^m$ for $m \in \mathbb{N}$,

$$\bar{\mu}(\bar{f} | \epsilon, z; \gamma) := \sum_{k=0}^T \bar{\mu}(k | \epsilon, z; \gamma) f \circ \psi_\epsilon^k(z).$$

G.2 Kullback-Leibler minimisation

To minimize the KL divergence to determine θ_n we first note that, with C independent of θ and possibly changing on each appearance,

$$\begin{aligned}\theta &\mapsto \text{KL}(\tilde{\mu}(\cdot; \gamma_n, \theta_n), \bar{\mu}(\cdot | \gamma_n, \theta)) \\ &= C + \int \log \left(\frac{v_{\gamma_{n-1}}(\epsilon, z) \nu_{\theta_{n-1}}(d\epsilon) \bar{\mu}(dz | \epsilon; \gamma_{n1})}{\nu_\theta(d\epsilon) \bar{\mu}(dz | \epsilon; \gamma_n)} \right) \tilde{\mu}(d(\epsilon, z); \gamma_n, \theta_n) \\ &= C - \int \log(\nu_\theta(\epsilon)) \tilde{\mu}(d(\epsilon, z); \gamma_n, \theta_n) \\ &= C - \int \log(\nu_\theta(\epsilon)) \tilde{\mu}(d\epsilon; \gamma_n, \theta_n).\end{aligned}$$

We remark that minimization of the above is easily achieved in scenarios where ν_θ is chosen in the exponential family, e.g. ν_θ has density of the form $\nu_\theta(\epsilon) = \exp(\langle \theta, T(\epsilon) \rangle - A(\theta))$, in which case minimisation of (21) amounts to solving

$$\theta \mapsto \mathbb{E}_{\nu_\theta}(T(\epsilon)) = \mathbb{E}_{\tilde{\mu}(\cdot; \gamma_n, \theta_n)}(T(\epsilon)).$$

In practice the expectation with respect to $\tilde{\mu}(\cdot; \gamma_n, \theta_n)$ is obtained using self-normalised importance sampling of the seed particles $\{(\tilde{z}_n^{(i)}, \tilde{\epsilon}_n^{(i)}), i \in \llbracket N \rrbracket\}$ representing $\tilde{\mu}_n$ or weighted samples $\{(z_{n-1}^{(i)}, \epsilon_{n-1}^{(i)}), i \in \llbracket N \rrbracket\}$ (see Alg. (3) and surrounding comments), leading in the exponential family scenario to solving

$$\theta \mapsto \mathbb{E}_{\nu_\theta}(T(\epsilon)) = \frac{\sum_{i=1}^N T(\tilde{\epsilon}_n^{(i)}) v(\tilde{\epsilon}_n^{(i)}, \tilde{z}_n^{(i)})}{\sum_{i=1}^N v(\tilde{\epsilon}_n^{(i)}, \tilde{z}_n^{(i)})}.$$

In the general scenario minimization is equivalent to maximum likelihood estimation with samples $\{(\check{z}_n^{(i)}, \check{\epsilon}_n^{(i)}), i \in \llbracket N \rrbracket\}$ as data.

Now we derive a more expression for $v_\gamma(\epsilon, z) := \text{Tr}[\text{var}(\bar{f} | \epsilon, z; \gamma)]$ useful for implementation.

$$\begin{aligned}
v_\gamma(\epsilon, z) &= \text{Tr}\{\mathbb{E}[(\bar{f} - \mathbb{E}(\bar{f} | \epsilon, z))(\bar{f} - \mathbb{E}(\bar{f} | \epsilon, z))^T | \epsilon, z; \gamma]\} \\
&= \mathbb{E}\{\text{Tr}[(\bar{f} - \mathbb{E}(\bar{f} | \epsilon, z))(\bar{f} - \mathbb{E}(\bar{f} | \epsilon, z))^T | \epsilon, z; \gamma]\} \\
&= \mathbb{E}\{\|\bar{f} - \mathbb{E}(\bar{f} | \epsilon, z)\|^2 | \epsilon, z; \gamma\} \\
&= \frac{1}{T+1} \sum_{k=0}^T \left\| f \circ \psi_\epsilon^k(z) - \bar{\mu}(f | \epsilon, z; \gamma, \theta) \right\|^2 \bar{\mu}(k | \epsilon, z; \gamma, \theta). \tag{43}
\end{aligned}$$

G.3 Calculations in the inverse Gaussian scenario

The Inverse Gaussian with mean $\theta > 0$ and shape parameter $\lambda > 0$ has skewness $s = 3\sqrt{\theta/\lambda}$. Therefore for a fixed skewness $s > 0$ and mean parameter $\theta > 0$ the IG distribution has density

$$\nu_\theta(\epsilon; s) = \sqrt{\frac{9\theta}{2\pi\epsilon^3 s^2}} \exp\left(-\frac{9\theta(\epsilon - \theta)^2}{2\theta^2 \epsilon s^2}\right),$$

w.r.t. the Lebesgue measure. We aim to minimise the Kullback-Leibler divergence $\theta \mapsto \text{KL}(\nu, \nu_\theta)$ for a given probability distribution. The corresponding log-likelihood is

$$\log \nu_\theta(\epsilon; s) = \log(3) + \frac{1}{2} \log(\theta) - \frac{1}{2} \log(2\pi) - \frac{3}{2} \log(\epsilon) - \log(s) - \frac{9(\epsilon^2 + \theta^2 - 2\epsilon\theta)}{2\theta\epsilon s^2},$$

and its derivative w.r.t. $\theta > 0$ is

$$\begin{aligned}
\frac{d}{d\theta} \log \nu_\theta(\epsilon; s) &= \frac{1}{2\theta} - \frac{9}{2\epsilon s^2} \left[\frac{d}{d\theta} \left(\frac{\epsilon^2}{\theta} + \theta - 2\epsilon \right) \right] \\
&= \frac{1}{2\theta} - \frac{9}{2\epsilon s^2} \left[-\frac{\epsilon^2}{\theta^2} + 1 \right] \\
&= \frac{1}{2\theta} - \frac{9(\theta^2 - \epsilon^2)}{2\epsilon s^2 \theta^2}.
\end{aligned}$$

Therefore

$$\frac{d}{d\theta} \text{KL}(\nu, \nu_\theta) = \frac{1}{2\theta^2} \frac{9}{s^2} \left\{ \frac{s^2}{9} \theta - \theta^2 \mathbb{E}_\nu[\epsilon^{-1}] + \mathbb{E}_\nu[\epsilon] \right\} = 0,$$

which has unique positive solution

$$\hat{\theta} = \frac{\frac{s^2}{9} + \sqrt{\frac{s^4}{81} + 4\mathbb{E}_\nu[\epsilon^{-1}]\mathbb{E}_\nu[\epsilon]}}{2\mathbb{E}_\nu[\epsilon^{-1}]}$$

Using that $\mathbb{E}_\nu[\epsilon^{-1}] = \mathbb{E}_\nu[\epsilon]^{-1} + \lambda^{-1}$, $\lambda = 9\mathbb{E}_\nu[\epsilon]/s^2$ we deduce $\mathbb{E}[\epsilon^{-1}]\mathbb{E}[\epsilon] = (9+s^2)/9$ yielding the simpler expression

$$\begin{aligned}\hat{\theta} &= 9\mathbb{E}_\nu[\epsilon] \left[\frac{\frac{s^2}{9} + \sqrt{\frac{s^4}{81} + 4\frac{(9+s^2)}{9}}}{2(9+s^2)} \right] \\ &= \mathbb{E}_\nu[\epsilon] \frac{s^2 + \sqrt{(s^2+18)^2}}{2(9+s^2)}.\end{aligned}$$

The constrained minimisation problem is therefore akin to a moment matching problem.

H Additional theoretical properties

In this section we omit the index $n \in \llbracket 0, P \rrbracket$ and provide precise elements to understand the properties of the algorithms and estimators considered in this manuscript.

H.1 Variance using folded mixture samples

The following provides us with a notion of effective sample size for estimators of the form $\check{\mu}(f)$ as defined in Proposition 5.

Theorem 24. *Assume that $v \gg \mu^{\psi^{-k}}$ for $k \in \llbracket T \rrbracket$, then with $\check{Z} \sim \bar{\mu}$,*

1. for $f: Z \rightarrow \mathbb{R}$,

$$\text{var}(\check{\mu}(f)) \leq \frac{2}{N} \frac{\text{var}(\sum_{k=0}^T \mu \circ \psi^k(\check{Z}) f \circ \psi^k(\check{Z})) + \|f\|_\infty^2 \text{var}(\sum_{k=0}^T \mu \circ \psi^k(\check{Z}))}{\mathbb{E}_{\bar{\mu}}(\sum_{k=0}^T \mu \circ \psi^k(\check{Z}))^2},$$

2. further

$$\text{var}(\check{\mu}(f)) \leq \frac{2\|f\|_\infty^2}{N} \left\{ \frac{2\mathbb{E}_{\bar{\mu}}((\sum_{k=0}^T \mu \circ \psi^k(\check{Z}))^2)}{\mathbb{E}_{\bar{\mu}}(\sum_{k=0}^T \mu \circ \psi^k(\check{Z}))^2} - 1 \right\}.$$

Remark 25. Multiplying μ by any constant $C_\mu > 0$ does not alter the values of the upper bounds, making the results relevant to the scenario where μ is known up to a constant only. From the second statement we can define a notion of effective sample size (ESS)

$$\frac{N}{2} \frac{\mathbb{E}_{\bar{\mu}}(\sum_{k=0}^T \mu \circ \psi^k(\check{Z}))^2}{2\mathbb{E}_{\bar{\mu}}((\sum_{k=0}^T \mu \circ \psi^k(z))^2) - \mathbb{E}_{\bar{\mu}}(\sum_{k=0}^T \mu \circ \psi^k(\check{Z}))^2},$$

which could be compared to $N(T+1)$ or N .

Proof. We have

$$\text{var}(\check{\mu}(f)) = \frac{1}{N} \text{var}_{\bar{\mu}} \left(\frac{\sum_{k=0}^T \mu \circ \psi^k(\check{Z}) f \circ \psi^k(\check{Z})}{\sum_{l=0}^T \mu \circ \psi^l(\check{Z})} \right)$$

and we apply Lemma 29

$$\begin{aligned} \text{var}_{\bar{\mu}} \left(\frac{\sum_{k=0}^T \mu \circ \psi^k(\check{Z}) f \circ \psi^k(\check{Z})}{\sum_{l=0}^T \mu \circ \psi^l(\check{Z})} \right) &\leq 2 \frac{\text{var}(\sum_{k=0}^T \mu \circ \psi^k(\check{Z}) f \circ \psi^k(\check{Z})) + \|f\|_\infty^2 \text{var}(\sum_{k=0}^T \mu \circ \psi^k(\check{Z}))}{\mathbb{E}_{\bar{\mu}}(\sum_{k=0}^T \mu \circ \psi^k(z))^2} \\ &\leq 2 \|f\|_\infty^2 \left\{ \frac{2\mathbb{E}_{\bar{\mu}}((\sum_{k=0}^T \mu \circ \psi^k(\check{Z}))^2)}{\mathbb{E}_{\bar{\mu}}(\sum_{k=0}^T \mu \circ \psi^k(\check{Z}))^2} - 1 \right\}. \end{aligned}$$

□

H.2 Variance using unfolded mixture samples

For $\psi: Z \rightarrow \mathbb{R}$ invertible, ν a probability distribution such that $\nu \gg \mu^{\psi^{-1}}$ and $f: Z \rightarrow \mathbb{R}$ such that $\mu(f)$ exists we have the identity

$$\mu(f) = \int f \circ \psi(z) \mu^{\psi^{-1}}(dz) = \int f \circ \psi(z) \frac{d\mu^{\psi^{-1}}}{d\nu}(z) \nu(dz).$$

As a result for $\{\psi_k: Z \rightarrow \mathbb{R}, k \in \llbracket K \rrbracket\}$, all invertible and such that $\nu \gg \mu^{\psi_k^{-1}}$ for $k \in \llbracket K \rrbracket$, we have

$$\mu(f) = \int \left\{ \frac{1}{K} \sum_{k \in \llbracket K \rrbracket} f \circ \psi_k(z) \frac{d\mu^{\psi_k^{-1}}}{d\nu}(z) \right\} \nu(dz), \quad (44)$$

which suggests the Pushforward Importance Sampling (PISA) estimator, for $Z^i \stackrel{\text{iid}}{\sim} \nu$, $i \in \llbracket N \rrbracket$ and with $\bar{\mu}_{/\nu}(f | z) := K^{-1} \sum_{k \in \llbracket K \rrbracket} f \circ \psi_k(z) \frac{d\mu^{\psi_k^{-1}}}{d\nu}(z)$

$$\hat{\mu}(f) = \sum_{i=1}^N \frac{\bar{\mu}_{/\nu}(f | Z^i)}{\sum_{j=1}^N \bar{\mu}_{/\nu}(1 | Z^j)} = \frac{\frac{1}{N} \sum_{i=1}^N \bar{\mu}_{/\nu}(f | Z^i)}{\frac{1}{N} \sum_{j=1}^N \bar{\mu}_{/\nu}(1 | Z^j)}, \quad (45)$$

This is the estimator in (7) when $\nu = \mu_{n-1}$ and $\mu = \mu_n$.

H.2.1 Relative efficiency for unfolded estimators

In order to define the notion of relative efficiency for the estimator $\hat{\mu}(f)$ in (45) we first establish the following bounds.

Theorem 26. *With the notation above and $Z \sim \nu$ throughout. For any $f: Z \rightarrow \mathbb{R}$,*

1.

$$\text{var}(\hat{\mu}(f)) \leq \mathbb{E}(|\hat{\mu}(f) - \mu(f)|^2) \leq \frac{2}{N} \left\{ \text{var}(\bar{\mu}_{/\nu}(f | Z)) + \|f\|_\infty^2 \text{var}(\bar{\mu}_{/\nu}(1 | Z)) \right\},$$

2. more simply

$$\mathbb{E}(|\hat{\mu}(f) - \mu(f)|^2) \leq \frac{2\|f\|_\infty^2}{KN} \left\{ \frac{2\mathbb{E}[(\sum_{k \in \llbracket K \rrbracket} d\mu^{\psi_k^{-1}}/d\nu(Z))^2]}{K} - K \right\}, \quad (46)$$

3. and

$$|\mathbb{E}[\hat{\mu}(f)] - \mu(f)| \leq \frac{2\|f\|_\infty^2}{KN} \frac{\mathbb{E}\left[\left(\sum_{k \in \llbracket K \rrbracket} d\mu^{\psi_k^{-1}} / d\nu(Z)\right)^2\right]}{K}.$$

Remark 27. The upper bound in the first statement confirms the control variate nature of integrator snippets, even when using the unfolded perspective, a property missed by the rougher bounds of the last two statements.

Remark 28 (ESS for PISA). The notion of efficiency is usually defined relative to the “perfect” Monte Carlo scenario that is the standard estimator $\hat{\mu}_0$ of $\mu(f)$ relying on KN iid samples from μ for which we have

$$\text{var}\left(\hat{\mu}_0(f)\right) = \frac{\text{var}_\mu(f)}{KN} \leq \frac{\|f\|_\infty^2}{KN}. \quad (47)$$

The RE_0 , is determined by the ratio of the upper bound in (46) by (47). Our point below is that the notion of efficiency can be defined relative to any competing algorithm, virtual or not, in order to characterize particular properties. For example we can compute the efficiency relative to that of the “ideal” PISA estimator i.e. for which $\bar{\mu}_{/\nu}(\bar{f} \mid Z^i)$ is replaced with $K^{-1} \sum_{k \in \llbracket K \rrbracket} f \circ \psi_k(Z^{i,k}) \frac{d\mu^{\psi_k^{-1}}}{d\nu}(Z^{i,k})$, $Z^{i,k} \stackrel{\text{iid}}{\sim} \nu$ and

$$\text{var}\left(\hat{\mu}_1(f)\right) \leq \frac{2\|f\|_\infty^2}{KN} \left\{ \frac{2 \sum_{k \in \llbracket K \rrbracket} \mathbb{E}\left[\left(d\mu^{\psi_k^{-1}} / d\nu(Z)\right)^2\right]}{K} - K \right\}. \quad (48)$$

The corresponding RE_1 captures the loss incurred because of dependence along a snippet. However, given our initial motivation of recycling the computation of a standard HMC based SMC algorithm we opt to define the RE_2 relative to the estimator relying on both ends of the snippet only, i.e.

$$\hat{\mu}_2(f) = \frac{1}{N} \sum_{i=1}^N \frac{\frac{1}{2} \frac{d\mu}{d\nu}(z^i) f(Z^i) + \frac{1}{2} \frac{d\mu^{\psi_K^{-1}}}{d\nu}(Z^i) f \circ \psi_K(Z^i)}{\sum_{j=1}^N \frac{1}{2} \frac{d\mu}{d\nu}(Z^j) + \frac{1}{2} \frac{d\mu^{\psi_K^{-1}}}{d\nu}(Z^j)}.$$

In the SMC scenario considered in this manuscript (see Section 1) the above can be thought of as a proxy for estimators obtained by a “Rao-Blackwellized” SMC algorithm using $P_{n-1,T}$ in (6), where N particles $\{z_{n-1}^{(i)}, i \in \llbracket N \rrbracket\}$ in Alg. 1 give rise to $2N$ weighted particles

$$\left\{ (z^i, \bar{\alpha}_{n-1}(z_i; T) \frac{\mu_n}{\mu_{n-1}}(z_i)); (z^i, \alpha_{n-1}(z_i; T) \frac{\mu_n}{\mu_{n-1}} \circ \psi_n^T(z_i)), i \in \llbracket N \rrbracket \right\},$$

with $\alpha_{n-1}(\cdot; T)$ defined in (5). Resampling with these weights is then applied to obtain N particles and followed by an update of velocities to yield $\{z_n^{(i)}, i \in \llbracket N \rrbracket\}$. Now, we observe the similarity between

$$\alpha_{n-1}(z; T) \frac{\mu_n}{\mu_{n-1}} \circ \psi_n^T(z) = \min \left\{ 1, \frac{\mu_{n-1} \circ \psi_{n-1}^T(z)}{\mu_{n-1}} \right\} \times \frac{\mu_n \circ \psi_n^T(z)}{\mu_{n-1} \circ \psi_n^T(z)}, \quad (49)$$

and the corresponding weight in Alg. 2, in particular when μ_{n-1} and μ_n are similar, and hence ψ_{n-1} and ψ_n . This motivates our choice of reference to define ESS_2 which has a clear computational advantage since it involves ignoring $T-1$ terms only. In the present scenario, following Lemma 29, we have

$$\text{var}\left(\hat{\mu}_2(f)\right) \leq \frac{\|f\|_\infty^2}{N} \left\{ \mathbb{E} \left[\left(\frac{d\mu}{d\nu}(Z) + \frac{d\mu^{\psi_K^{-1}}}{d\nu}(Z) \right)^2 \right] - \frac{1}{2} \right\},$$

which leads to the relative efficiency for PISA,

$$\text{RE}_2 = \frac{4\mathbb{E}\left[\left(\sum_{k \in \llbracket K \rrbracket} d\mu^{\psi_k^{-1}}/d\nu(Z)\right)^2\right] - 2}{\mathbb{E}\left[\left(\frac{d\mu}{d\nu}(Z) + \frac{d\mu^{\psi_{K^{-1}}}}{d\nu}(Z)\right)^2\right] - 2},$$

which can be estimated using empirical averages.

Proof of Theorem 26. We apply Lemma 29 with

$$A(Z^1, \dots, Z^N) = \frac{1}{N} \sum_{i=1}^N \bar{\mu}_{/\nu}(f | Z^i) \quad B(Z^1, \dots, Z^N) = \frac{1}{N} \sum_{j=1}^N \bar{\mu}_{/\nu}(1 | Z^j).$$

With $Z^i \stackrel{\text{iid}}{\sim} \nu$, we have directly

$$a = \mathbb{E}(A) = \mathbb{E}(\bar{\mu}_{/\nu}(f | Z)) = \mu(f) \quad b = \mathbb{E}(B) = 1,$$

and

$$\begin{aligned} \text{var}(B) &= \frac{1}{N} \text{var}(\bar{\mu}_{/\nu}(1 | Z^j)) \\ &= \frac{1}{K^2 N} \left\{ \mathbb{E}\left[\left(\sum_{k \in \llbracket K \rrbracket} d\mu^{\psi_k^{-1}}/d\nu(Z)\right)^2\right] - K^2 \right\}. \end{aligned}$$

Now with $\|f\|_\infty < \infty$

$$\begin{aligned} \text{var}(A) &= \frac{1}{N} \text{var}(\bar{\mu}_{/\nu}(f | Z)) \\ &= \frac{1}{K^2 N} \left\{ \|f\|_\infty^2 \mathbb{E}\left[\left(\sum_{k \in \llbracket K \rrbracket} d\mu^{\psi_k^{-1}}/d\nu(Z)\right)^2\right] - K^2 \mu(f)^2 \right\} \\ &\leq \frac{\|f\|_\infty^2}{K^2 N} \mathbb{E}\left[\left(\sum_{k \in \llbracket K \rrbracket} d\mu^{\psi_k^{-1}}/d\nu(Z)\right)^2\right]. \end{aligned}$$

We conclude noting that we have $|A/B| \leq \|f\|_\infty$. □

For clarity we reproduce the very useful lemma [61, Lemma 6], correcting a couple of minor typos along the way.

Lemma 29. *Let A, B be two integrable random variables satisfying $|A/B| \leq M$ almost surely for some $M > 0$ and let $a = \mathbb{E}(A)$ and $b = \mathbb{E}(B) \neq 0$. Then*

$$\begin{aligned} \text{var}(A/B) &\leq \mathbb{E}[|A/B - a/b|^2] \leq \frac{2}{b^2} \left\{ \text{var}(A) + M^2 \text{var}(B) \right\}, \\ |\mathbb{E}[A/B] - a/b| &\leq \frac{\sqrt{\text{var}(A/B)\text{var}(B)}}{b}. \end{aligned}$$

H.2.2 Optimal weights

As mentioned in Subsection 2.4 it is possible to consider the more general scenario where unequal probability weights $\omega = \{\omega_k \in \mathbb{R}, k \in \llbracket 0, T \rrbracket : \sum_{k=0}^T \omega_k = 1\}$ are ascribed to the elements of the snippets, yielding the estimator

$$\hat{\mu}_\omega(f) := \frac{\sum_{i=1}^N \sum_{k=0}^T \omega_k \frac{d\mu^{\psi_k^{-1}}}{d\nu}(Z^i) f \circ \psi_k(Z^i)}{\sum_{j=1}^N \sum_{l=0}^T \omega_l \frac{d\mu^{\psi_l^{-1}}}{d\nu}(Z^j)},$$

and a natural question is that of the optimal choice of ω . Note that in the context of PISA the condition $\omega_k \geq 0$ is not required, as suggested by the justification of the identity (44). However it should be clear that this condition should be enforced in the context of integrator snippet SMC, since the probabilistic interpretation is otherwise lost, or if the expectation is known to be non-negative. Here we discuss optimization of the variance upperbound provided by Lemma 29,

$$\begin{aligned} \frac{2\|f\|_\infty^2}{N} \left\{ \text{var} \left(\sum_{k \in \llbracket K \rrbracket} \omega_k \frac{d\mu^{\psi_k^{-1}}}{d\nu}(Z) \frac{f \circ \psi_k}{\|f\|_\infty}(Z) \right) + \text{var} \left(\sum_{k \in \llbracket K \rrbracket} \omega_k \frac{d\mu^{\psi_k^{-1}}}{d\nu}(Z) \right) \right\} \\ \leq \frac{2\|f\|_\infty^2}{N} \omega^\top (\Sigma(f; \psi) + \Sigma_\psi(1; \psi)) \omega \end{aligned}$$

where for $k, l \in \llbracket K \rrbracket$,

$$\Sigma_{kl}(f; \psi) = \mathbb{E} \left[\frac{d\mu^{\psi_k^{-1}}}{d\nu}(Z) \frac{f \circ \psi_k}{\|f\|_\infty}(Z) \frac{d\mu^{\psi_l^{-1}}}{d\nu}(Z) \frac{f \circ \psi_l}{\|f\|_\infty}(Z) \right] - \mu(f/\|f\|_\infty)^2.$$

It is a classical result that $\omega^\top (\Sigma(f; \psi) + \Sigma_\psi(1; \psi)) \omega \geq \lambda_{\min}(\Sigma(f; \psi) + \Sigma_\psi(1; \psi)) \omega^\top \omega$ and that minimum is reached for the eigenvector(s) ω_{\min} corresponding to the smallest eigenvalue $\lambda_{\min}(\Sigma(f; \psi) + \Sigma_\psi(1; \psi))$ of $\Sigma(f; \psi) + \Sigma_\psi(1; \psi)$. If the constraint of non-negative entries is to be enforced then a standard quadratic programming procedure should be used. The same ideas can be applied to the function independent upperbounds used in our definitions of efficiency.

H.3 More on variance reduction and optimal flow

We now focus on some properties of the estimator $\hat{\mu}(f)$ of $\mu(f)$ in (14). To facilitate the analysis and later developments we consider the scenario where, with $t \mapsto \psi_t(z)$ the flow solution of an ODE, assume the dominating measure $\nu \gg \mu$ and ν is invariant by the flow. We consider

$$\bar{\mu}(dt, dz) = \frac{1}{T} \mu^{\psi^{-t}}(dz) \mathbf{1}\{0 \leq t \leq T\} dt,$$

and notice that similarly to the integrator scenario, for any $f: Z \rightarrow \mathbb{R}$, $\bar{f}(t, z) := f \circ \psi_t(z)$ we have $\mathbb{E}_{\bar{\mu}}(\bar{\mu}(\bar{f} | \check{Z})) = \bar{\mu}(\bar{f}) = \mu(f)$. where for any $z \in Z$, where

$$\bar{\mu}(\bar{f} | z) = \frac{1}{T} \int_0^T f \circ \psi_t(z) \frac{\mu \circ \psi_t(z)}{\int \mu \circ \psi_u(z) du} dt$$

the following estimator of $\mu(f)$ is considered, with $\check{Z}_i \stackrel{\text{iid}}{\sim} \bar{\mu}$

$$\hat{\mu}(f) = \frac{1}{N} \sum_{i=1}^N \bar{\mu}(\bar{f}(T, \check{Z}_i) | \check{Z}_i).$$

We now show that in the examples considered in this paper our approach can be understood as implementing unbiased Riemann sum approximations of line integrals along contours. Adopting a continuous time approach can be justified as follows. For numerous integrators, the conditions of the following proposition are satisfied; this is the case for the leapfrog integrator of Hamilton's equation e.g. [35, 61, Theorem 3.4] and [61, Appendix 3.1, Theorem 9] for detailed results.

Proposition 30. *Let $\tau > 0$, for any $z \in \mathbf{Z}$ let $[0, \tau] \ni t \mapsto \psi_t(z)$ be a flow and for $\epsilon > 0$ let $\{\psi^k(z; \epsilon), 0 \leq k\epsilon \leq \tau\}$ be a discretization of $t \mapsto \psi_t$ such that that for any $z \in \mathbf{Z}$ there exists $C > 0$ such that for any $(k, \epsilon) \in \mathbb{N} \times \mathbb{R}_+$*

$$|\psi^k(z; \epsilon) - \psi_{k\epsilon}(z)| \leq C\epsilon^2.$$

Then for any continuous $g: \mathbf{Z} \rightarrow \mathbb{R}$ such that the Riemann integral

$$I(g) := \int_0^\tau g \circ \psi_t(z) dt,$$

exists we have

$$\lim_{T \rightarrow \infty} \frac{1}{n} \sum_{k=0}^{n-1} g \circ \psi_{k\tau/n}(z; \tau/n) = I(g).$$

Proof. We have

$$\begin{aligned} \lim_{n \rightarrow \infty} \frac{1}{n} \sum_{k=0}^{n-1} g \circ \psi_{k\tau/n}(z) &= \int_0^\tau g \circ \psi_t(z) dt \\ \lim_{n \rightarrow \infty} \frac{1}{n} \left| \sum_{k=0}^{n-1} g \circ \psi_{k\tau/n}(z) - g \circ \psi^k(z; \tau/n) \right| &= 0, \end{aligned}$$

and we can conclude. □

Remark 31. Naturally convergence is uniform in $z \in \mathbf{Z}$ with additional assumptions and we note that in some scenarios dependence on τ can be characterized, allowing in principle τ to grow with n .

H.3.1 Hamiltonian contour decomposition

Assume μ has a probability density with respect to the Lebesgue measure and let $\zeta: \mathbf{Z} \subset \mathbb{R}^d \rightarrow \mathbb{R}$ be Lipschitz continuous such that $\nabla \zeta(z) \neq 0$ for all $z \in \mathbf{Z}$, then the co-area formula states that

$$\int_{\mathbf{Z}} f(z) \mu(z) dz = \int \left[\int_{\zeta^{-1}(s)} f(z) |\nabla \zeta(z)|^{-1} \mu(z) \mathcal{H}_{d-1}(dz) \right] ds,$$

where \mathcal{H}_{d-1} is the $(d-1)$ -dimensional Hausdorff measure, used here to measure length along the contours $\zeta^{-1}(s)$. For example in the HMC setup where $\mu(z) \propto \exp(-H(z))$ and $z = (x, v)$ one may choose $\zeta(z) = H(z) = -\log(\mu(z))$, leading to a decomposition of the expectation $\mu(f)$ according to equi-energy contours of $H(z)$

$$\mu(f) = \int \exp(-s) \left[\int_{\zeta^{-1}(s)} f(z) |\nabla H(z)|^{-1} \mathcal{H}_{d-1}(dz) \right] ds.$$

We now show how the solution of Hamilton's equation could be used as the basis for estimators of $\mu(f)$ mixing Riemannian sum-like and Monte Carlo estimation techniques.

Favourable scenario where $d = 2$. Let $s \in \mathbb{R}$ such that $H^{-1}(s) \neq \emptyset$ and assume that for some $(x_0, v_0) \in H^{-1}(s)$ Hamilton's equations $\dot{x} = -\nabla_v H(x, v)$ and $\dot{v} = \nabla_x H(x, v)$ have solutions $t \mapsto (x_t, v_t) = \psi_t(z_0) \in H^{-1}(s)$ with $(x_{\tau(s)}, v_{\tau(s)}) = (x_0, v_0) = z_0$ for some $\tau(s) > 0$, that is the contours $H^{-1}(s)$ can be parametrised with the solutions of Hamilton's equation at corresponding level.

Proposition 32. *We have*

$$\int_{\mathbb{Z}} f(z) \mu(dz) = \int_{\mathbb{Z}} \left[[\tau \circ H(z_0)]^{-1} \int_0^{\tau \circ H(z_0)} f(z_t) dt \right] \mu(dz_0),$$

implying that, assuming the integral along the path $t \mapsto z_t$ is tractable,

$$[\tau \circ H(z_0)]^{-1} \int_0^{\tau \circ H(z_0)} f(z_t) dt \text{ for } z_0 \sim \mu, \quad (50)$$

is an unbiased estimator of $\mu(f)$.

Proof. Since $H^{-1}(s)$ is rectifiable we have that [14, Theorem 2.6.2] for $g: \mathbb{Z} \rightarrow \mathbb{R}$,

$$\int_{H^{-1}(s)} g(z) \mathcal{H}_{d-1}(dz) = \int_0^{\tau(s)} g(z_t) |\nabla H(z_t)| dt.$$

Consequently

$$\int_{\mathbb{Z}} f(z) \mu(dz) = \int \tau(s) \exp(-s) \left[\tau(s)^{-1} \int_0^{\tau(s)} f(z_{s,t}) dt \right] ds, \quad (51)$$

where the notation now reflects dependence on s of the flow and notice that since

$$H^{-1}(s) \ni z_0 \mapsto [\tau \circ H(z_0)]^{-1} \int_0^{\tau \circ H(z_0)} f(z_t)$$

is constant, $z_{0,s} \in H^{-1}(s)$ can be arbitrary. since indeed from (51)

$$\begin{aligned} \int_{\mathbb{Z}} \mathbf{1}\{H(z) \in A\} \mu(dz) &= \int \tau(s) \exp(-s) \left[\tau(s)^{-1} \int_0^{\tau(s)} \mathbf{1}\{s \in A\} dt \right] ds \\ &= \int \tau(s) \exp(-s) \mathbf{1}\{s \in A\} ds. \end{aligned}$$

Note that we can write, since for $s \in \mathbb{R}$, $H^{-1}(s) \ni z_0 \mapsto [\tau \circ H(z_0)]^{-1} \int_0^{\tau \circ H(z_0)} f(z_t)$ is constant,

$$\begin{aligned} &\int_{\mathbb{Z}} \left[[\tau \circ H(z_0)]^{-1} \int_0^{\tau \circ H(z_0)} f(z_t) dt \right] \mu(dz_0) \\ &= \int \tau(s) \exp(-s) \left\{ \tau(s)^{-1} \int_0^{\tau(s)} \left[(\tau \circ H(z_{s,0}))^{-1} \int_0^{\tau \circ H(z_0)} f(z_{s,t}) dt \right] \right\} dt ds \\ &= \int \tau(s) \exp(-s) \left[\tau(s)^{-1} \int_0^{\tau(s)} f(z_{s,t}) dt \right] dt ds. \end{aligned}$$

□

A remarkable point is that the strategy developed in this manuscript provides a general methodology to implement numerically the ideas underpinning the decomposition of Proposition 32 by using the estimator $\check{\mu}(f)$ in (13) and invoking Proposition 30, assuming $s \mapsto \tau(s)$ to be known. This point is valid outside of the SMC framework and it is worth pointing out that $\check{\mu}(f)$ in (13) is unbiased if the samples used are marginally from $\bar{\mu}$.

Remark the promise of dimension free estimators if the one dimensional line integrals in (50) were easily computed and sampling from the one-dimensional energy distribution was routine – however the scenario $d \geq 3$ is more subtle.

General scenario In the scenario where $d \geq 3$ the co-area decomposition still holds, but the solution to Hamilton’s equation can in general not be used to compute integrals over the hypersurface $H^{-1}(s)$. This would require a form of ergodicity [58, 63] of the form, for $z_0 \in H^{-1}(s)$,

$$\lim_{\tau \rightarrow \infty} \frac{1}{\tau} \int_0^\tau f \circ \psi_t(z_0) dt = \bar{f}(z_0) = \frac{\int_{\zeta^{-1}(s)} f(z) |\nabla H(z)|^{-1} \mathcal{H}_{d-1}(dz)}{\int_{\zeta^{-1}(s)} |\nabla H(z)|^{-1} \mathcal{H}_{d-1}(dz)},$$

where the limit always exists in the $L^2(\mu)$ sense and constitutes Von Neumann’s mean ergodic theorem [65, 58], and the rightmost equality forms Boltzmann’s conjecture. An interesting property in the present context is that $\mathbb{E}_{\bar{\mu}}(\bar{f}(Z)) = \mathbb{E}_{\mu}(f(Z))$ for $f \in L^2(\mu)$ and one could replicate the variance reduction properties developed earlier. Boltzmann’s conjecture has long been disproved, as numerous Hamiltonians can be shown not to lead to ergodic systems, although some sub-classes do. However a weaker, or local, form of ergodicity can hold on sets of a partition of Z

Example 33 (Double well potential). Consider the scenario where $X = V = \mathbb{R}$, $U(x) = (x^2 - 1)^2$ and kinetic energy v^2 [56]. Elementary manipulations show that satisfying Hamilton’s equations (2) imposes $t \mapsto H(x_t, \dot{x}_t) = (x_t^2 - 1)^2 + \dot{x}_t^2 = s > 0$ and therefore requires $t \mapsto x_t \in [-\sqrt{1 + \sqrt{s}}, -\sqrt{1 - \sqrt{s}}] \cup [\sqrt{1 - \sqrt{s}}, \sqrt{1 + \sqrt{s}}]$ – importantly the intervals are not connected for $s < 1$. Rearranging terms any solution of (2) must satisfy

$$\dot{x}_t = \pm \sqrt{s - (x_t^2 - 1)^2},$$

that is the velocity is a function of the position in the double well, maximal for $x_t^2 = 1$, vanishing as $x_t^2 \rightarrow 1 \pm \sqrt{s}$ and a sign flip at the endpoints of the intervals. Therefore the system is not ergodic, but ergodicity trivially occurs in each well.

In general this partitioning of Z can be intricate but it should be clear that in principle this could reduce variability of an estimator. In the toy Example 33, a purely mathematical algorithm inspired by the discussions above would choose the right or left well with probability 1/2 and then integrate deterministically, producing samples taking at most two values which could be averaged to compute $\mu(f)$. We further note that in our context a relevant result would be concerned with the limit, for any $x_0 \in X$,

$$\lim_{\tau \rightarrow \infty} \int \left[\frac{1}{\tau} \int_0^\tau f \circ \psi_t(x_0, \rho \mathbf{e}) dt \right] \varpi_{\mathbf{e}}(d\mathbf{e}),$$

where we have used a polar reparametrization $v = \rho \mathbf{e}$ ($\rho, \mathbf{e} \in \mathbb{R}_+ \times \mathcal{S}_{d-1}$), and whether a marginal version of Boltzmann’s conjecture holds for this limit. Example 33 indicates that this is not true in general but the cardinality of the partition of X may be reduced.

H.3.2 Advantage of averaging and control variate interpretation

Consider the scenario where $(\mathbb{T}, \check{Z}) \sim \bar{\mu}(t, dz) = \frac{1}{\tau} \mu^{\psi_{-t}}(dz) \mathbf{1}\{0 \leq t \leq \tau\}$, $[0, \tau] \ni t \mapsto \psi_t$ for some $\tau > 0$ is the flow solution of an ODE of the form $\dot{z}_t = F \circ z_t$ for some field $F: \mathbb{Z} \rightarrow \mathbb{Z}$. For $f: \mathbb{Z} \rightarrow \mathbb{R}$ we have

$$\text{var}_{\mu}(f(Z)) = \text{var}_{\bar{\mu}}(\mathbb{E}_{\bar{\mu}}(\bar{f}(\mathbb{T}, \check{Z}) \mid \check{Z})) + \mathbb{E}_{\bar{\mu}}(\text{var}_{\bar{\mu}}(\bar{f}(\mathbb{T}, \check{Z}) \mid \check{Z})).$$

and we are interested in determining $t \mapsto \psi_t$ (or F) in order to minimize $\text{var}_{\bar{\mu}}(\mathbb{E}_{\bar{\mu}}(\bar{f}(\mathbb{T}, \check{Z}) \mid \check{Z}))$ and maximize improvement over simple Monte Carlo. We recall that the Jacobian determinant of the flow $t \mapsto \psi_t(z)$ is given by [31, p. 174108-5]

$$J_t(z) = |\det(\nabla \otimes \psi_t(z))| = \mathcal{J} \circ \psi_t(z) \text{ with } \mathcal{J}(z) := \exp\left(\int_0^t (\nabla \cdot F)(z) du\right).$$

Lemma 34. *Let $t \mapsto \psi_t$ be a flow solution of $\dot{z}_t = F \circ z_t$ and assume that with ν the Lebesgue measure, $\nu \gg \mu$. Then*

$$\begin{aligned} \mathbb{E}_{\bar{\mu}}\left(\mathbb{E}_{\bar{\mu}}(\bar{f}(\mathbb{T}, \check{Z}) \mid \check{Z})^2\right) &= 2 \int_0^{\tau} \left\{ \int_0^{\tau-t} [\bar{\mu} \circ \psi_{-t}(z)]^{-1} dt \right\} \left\{ \int \mu(dz) f(z) f \circ \psi_u(z) \mu \circ \psi_u(z) \mathcal{J} \circ \psi_u(z) \right\} du \\ &\leq 2 \left\{ \int_0^{\tau} [\bar{\mu} \circ \psi_{-t}(z)]^{-1} dt \right\} \int_0^{\tau} \left\{ \int \mu(dz) f(z) f \circ \psi_u(z) \mu \circ \psi_u(z) \mathcal{J} \circ \psi_u(z) \right\} du, \end{aligned}$$

with

$$\bar{\mu} \circ \psi_{-t}(z) = \int_{-t}^{\tau-t} \mu \circ \psi_u(z) \mathcal{J} \circ \psi_u(z) du.$$

In particular for $t \mapsto \psi_t$ the flow solution of Hamilton's equations associated with μ we have

$$\mathbb{E}_{\bar{\mu}}\left(\mathbb{E}_{\bar{\mu}}(\bar{f}(\mathbb{T}, \check{Z}) \mid \check{Z})^2\right) = 2 \int (1 - t/\tau) \int \mu(dz) f(z) f \circ \psi_t(z) dt.$$

Proof. Using Fubini's theorem we have

$$\begin{aligned} &\left\{ \int_0^{\tau} f \circ \psi_t(z) \frac{d\mu^{\psi_{-t}}}{d\bar{\mu}}(z) dt \right\}^2 \bar{\mu}(dz) = \\ &= 2 \int_0^{\tau} \int_0^{\tau} \mathbf{1}\{t' \geq t\} \int \bar{\mu}(dz) f \circ \psi_t(z) \frac{d\mu^{\psi_{-t}}}{d\bar{\mu}}(z) f \circ \psi_{t'-t+t}(z) \frac{d\mu^{\psi_{-t'}}}{d\bar{\mu}} \circ \psi_{-t} \circ \psi_t(z) dt' dt \\ &= 2 \int_0^{\tau} \int_0^{\tau} \mathbf{1}\{t' \geq t\} \int \mu(dz) f(z) f \circ \psi_{t'-t}(z) \frac{d\mu^{\psi_{-t'}}}{d\bar{\mu}} \circ \psi_{-t}(z) dt' dt. \end{aligned}$$

Further, we have

$$\frac{d\mu^{\psi_{-t'}}}{d\bar{\mu}}(z) = \frac{\mu \circ \psi_{t'}(z) \mathcal{J} \circ \psi_{t'}(z)}{\bar{\mu}(z)},$$

with $\bar{\mu}(z) = \int_0^{\tau} \mu \circ \psi_u(z) \mathcal{J} \circ \psi_u(z) du$. It is straightforward that

$$\begin{aligned} \bar{\mu} \circ \psi_{-t}(z) &= \int_0^{\tau} \mu \circ \psi_{u-t}(z) \mathcal{J} \circ \psi_{u-t}(z) du \\ &= \int_{-t}^{\tau-t} \mu \circ \psi_{u'}(z) \mathcal{J} \circ \psi_{u'}(z) du'. \end{aligned}$$

Consequently

$$\begin{aligned}
\int \left\{ \int_0^\tau f \circ \psi_t(z) \frac{d\mu^{\psi_{-t}}}{d\bar{\mu}}(z) dt \right\}^2 \bar{\mu}(dz) &= \\
&= 2 \int_0^\tau \int_0^{\tau-t} \frac{\mathbf{1}\{\tau-t \geq u \geq 0\}}{\bar{\mu} \circ \psi_{-t}(z)} \int \mu(dz) f(z) f \circ \psi_u(z) \mu \circ \psi_u(z) \mathcal{J} \circ \psi_u(z) du dt \\
&= 2 \int_0^\tau \left\{ \int_0^{\tau-u} [\bar{\mu} \circ \psi_{-t}(z)]^{-1} dt \right\} \int \mu(dz) f(z) f \circ \psi_u(z) \mu \circ \psi_u(z) \mathcal{J} \circ \psi_u(z) du
\end{aligned}$$

For the second statement we have $\bar{\mu} \circ \psi_{-t}(z) = \tau \mu(z)$ and

$$\begin{aligned}
\int \left\{ \int_0^\tau f \circ \psi_t(z) \frac{d\mu^{\psi_{-t}}}{d\bar{\mu}}(z) dt \right\}^2 \bar{\mu}(dz) &= \\
&= 2 \int_0^\tau (1-u/\tau) \int \mu(dz) f(z) f \circ \psi_u(z) dt''
\end{aligned}$$

which is akin to the integration correlation time encountered in MCMC. \square

This is somewhat reminiscent of what is advocated in the literature in the context of HMC or randomized HMC where the integration time t (or T when using an integrator) is randomized [48, 37].

Example 35. Consider the Gaussian scenario where $\mathbf{X} = \mathbf{V} = \mathbb{R}^d$, $\pi(x) = \mathcal{N}(x; 0, \Sigma)$ with diagonal covariance matrix such that for $i \in \llbracket d \rrbracket$, $\Sigma_{ii} = \sigma_i^2$ and $\varpi(v) = \mathcal{N}(v; 0, \text{Id})$. Using the reparametrization $(x_0(i), v_0(i)) = (a_i \sigma_i \sin(\phi_i), a_i \cos \phi_i)$ the solution of Hamilton's equations is given for $i \in \llbracket d \rrbracket$ by

$$\begin{aligned}
x_t(i) &= a_i \sigma \sin(t/\sigma_i + \phi_i) \\
v_t(i) &= a_i \cos(t/\sigma_i + \phi_i).
\end{aligned}$$

We have for each component $\mathbb{E}_\mu[X_0(i)X_t(i)] = \sigma_i^2 \cos(t/\sigma_i)$, which clearly does not vanish as t , or τ , increase: this is a particularly negative result for standard HMC where the final state of the computed integrator is used. Worse, as noted early on in [48] this implies that for heterogeneous values $\{\sigma_i^2, i \in \llbracket d \rrbracket\}$ no integration time may be suitable simultaneously for all coordinates. This motivated the introduction of random integration times [48] which leads to the average correlation

$$\mathbb{E}_\mu \left\{ \frac{1}{\tau} \int_0^\tau X_0(i)X_t(i) dt \right\} = \frac{\sin(\tau/\sigma_i)}{\tau/\sigma_i},$$

where it is assumed that τ is independent of the initial state. This should be contrasted with the fixed integration time scenario since as τ increases this vanishes and is even negative for some values of τ (the minimum is here reached for about $\tau_i = 4.5\sigma_i$ for a given component).

The example therefore illustrates that our approach implements this averaging feature, and therefore shares its benefits, within the context of an iterative algorithm. The example also highlights a control variate technique interpretation. More specifically in the discrete time scenarios $\{f \circ \psi^k(z), k \in \llbracket P \rrbracket\}$ can be interpreted as control variates, but can induce both positive and negative correlations.

H.3.3 Towards an optimal flow?

In this section we are looking to determine a flow for some $\tau > 0$ $[0, \tau] \ni t \mapsto \psi_t$ of an ODE of the form $\dot{z}_t = F \circ z_t$ for some field $F: Z \rightarrow Z$ which defines as above the probability model

$$\bar{\mu}(dt, dz) = \frac{1}{\tau} \mu^{\psi_{-t}}(dz) \mathbf{1}\{0 \leq t \leq \tau\} dt,$$

which has the property that for any $f: Z \rightarrow \mathbb{R}$, defining $\bar{f}(t, z) := f \circ \psi_t(z)$, then $\bar{\mu}(\bar{f}) = \mu(f)$. This suggests the use of a Rao-Blackwellized estimator inspired by $\mathbb{E}_{\bar{\mu}}(\bar{f} | Z)$. Assuming $Z = \mathbb{R}^d \times \mathbb{R}^d$ and that μ has a density with respect to the Lebesgue measure, then for $z \in Z$

$$\bar{\mu}(\bar{f} | z) = \frac{1}{\tau} \int_0^\tau f \circ \psi_t(z) \frac{\mu \circ \psi_t(z) \mathcal{J} \circ \psi_t(z)}{\int \mu \circ \psi_u(z) \mathcal{J} \circ \psi_u du} dt \quad (52)$$

In the light of Lemma 34 we aim to find for any $z \in Z$ the flow solutions $t \mapsto \psi_t(z)$ of ODEs $\dot{z}_t = F_z(z_t)$ such that the function $t \mapsto \int \mu(dz) f(z) f \circ \psi_t(z) \mu \circ \psi_t(z) \mathcal{J} \circ \psi_t(z)$ decreases as fast as possible. This is motivated by the fact that the integral on $[0, \tau]$ of this mapping appears in the variance upper bound for (52) in Lemma 34, which we want to minimize. Note that we also expect this mapping to be smooth under general conditions not detailed in this preliminary work. For smooth enough flow and f we have, with $g := f \times \mu \times \mathcal{J}$,

$$\frac{d}{dt} \mathbb{E}_\mu \left[f(Z) \frac{g \circ \psi_t(Z)}{\bar{\mu}(Z)} \right] = \mathbb{E}_\mu \left[\frac{f(Z)}{\bar{\mu}(Z)} \langle \nabla g \circ \psi_t(Z), \dot{\psi}_t(Z) \rangle \right]$$

Pointwise, the steepest descent direction is given by

$$\dot{\psi}_t(z) = -C_t(z) \frac{f(z) \nabla g \circ \psi_t(z)}{|f(z) \nabla g \circ \psi_t(z)|}$$

for a positive function $C_t(z)$ to be determined optimally. In this scenario we therefore have

$$\frac{d}{dt} \mathbb{E}_\mu \left[f(Z) \frac{g \circ \psi_t(Z)}{\bar{\mu}(Z)} \right] = -\mathbb{E}_\mu \left[\frac{C_t(z)}{\bar{\mu}(Z)} |f(Z) \nabla g \circ \psi_t(Z)| \right]$$

and by Cauchy-Schwartz the (positive) expectation is maximized for

$$C_t(z) = C_t \frac{|f(z) \nabla g \circ \psi_t(z)|}{\bar{\mu}(z)}.$$

and the trajectories we are interested in must be such that, for some $C > 0$,

$$\dot{\psi}_t(z) = -\frac{C}{\bar{\mu}(z)} f(z) \nabla g \circ \psi_t(z) = -\frac{C}{\bar{\mu}(z)} f(z) F \circ \psi_t(z).$$

Note that for any z the term $|f(z)/\bar{\mu}(z)|$ is only a change of speed and that the trajectory of $\mathbb{R}_+ \ni t \mapsto \psi_t(z)$ is independent of this factor, despite the remarkable fact that $\bar{\mu}(z)$ depends on this flow. The result seems fairly natural.

I MCMC with integrator snippets

We restrict this discussion to integrator snippet based algorithms, but more general Markov snippet algorithms could be considered. Consider again the target distribution

$$\bar{\mu}(\mathrm{d}z) = \sum_{k=0}^T \bar{\mu}(k, \mathrm{d}z),$$

with

$$\bar{\mu}(k, \mathrm{d}z) = \frac{1}{T+1} \mu_k(\mathrm{d}z),$$

where $\mu_k(\mathrm{d}z) := \mu^{\psi^{-k}}(\mathrm{d}z)$ for $k \in \llbracket 0, T \rrbracket$.

I.1 Windows of states

Assume that we are in the context of Example 1, dropping n for simplicity, the HMC algorithm using the integrator ψ^s is as follows

$$\bar{P}(z, \mathrm{d}z') = \alpha(z) \delta_{\psi^s(z)}(\mathrm{d}z) + \bar{\alpha}(z) \delta_{\sigma(z)}(\mathrm{d}z') \quad (53)$$

with here

$$\alpha(z) = \min \left\{ 1, \frac{\mathrm{d}\bar{\mu}^{\sigma \circ \psi^s}}{\mathrm{d}\bar{\mu}}(z) \right\} = \min \left\{ 1, \frac{\bar{\mu} \circ \psi^w(z)}{\bar{\mu}(z)} \right\}$$

where the last equality holds when $v \gg \bar{\mu}$, $v^{\psi^s} = v$ and we let $\bar{\mu}(z) = \mathrm{d}\bar{\mu}/\mathrm{d}v(z)$. In other words the snippet $\mathbf{z} = (z, \psi(z), \psi^2(z), \dots, \psi^T(z))$ is shifted along the orbit $\{\psi^k(z), k \in \mathbb{Z}\}$ by ψ^s . Naturally this needs to be combined with updates of the velocity to lead to a viable ergodic MCMC algorithm. This can be achieved with the following kernel, with $\psi^k(z) = (\psi_x^k(z), \psi_v^k(z))$ and $A \in \mathcal{Z}$,

$$\bar{Q}(z, A) := \sum_{k,l=0}^T \bar{\mu}(k | z) \frac{1}{T+1} \int \mathbf{1}\{\psi^{-l}(\psi_x^k(z), v') \in A\} \varpi(\mathrm{d}v'),$$

described algorithmically in Alg. 8. Indeed for any $(l, v') \in \llbracket 0, T \rrbracket \times \mathbb{V}$, using identity (10),

$$\int \sum_{k=0}^T \bar{\mu}(k | z) \int \mathbf{1}\{\psi^{-l}(\psi_x^k(z), v') \in A\} \bar{\mu}(\mathrm{d}z) = \int \sum_{k=0}^T \int \mathbf{1}\{\psi^{-l}(x, v') \in A\} \mu(\mathrm{d}z),$$

and hence

$$\begin{aligned} \bar{\mu} \bar{Q}(A) &= \frac{1}{T+1} \sum_{l=0}^T \int \mathbf{1}\{\psi^{-l}(x, v') \in A\} \varpi(\mathrm{d}v') \mu(\mathrm{d}z) \\ &= \frac{1}{T+1} \sum_{l=0}^T \int \mathbf{1}\{\psi^{-l}(x, v) \in A\} \mu(\mathrm{d}z) \\ &= \int \mathbf{1}\{z \in A\} \frac{1}{T+1} \sum_{l=0}^T \mu^{\psi^{-l}}(\mathrm{d}z) \\ &= \bar{\mu}(A). \end{aligned}$$

Again samples from this MCMC targetting $\bar{\mu}$ can be used to estimate expectations with respect to μ using the identity (10). This is closely related to the “windows of states” approach of [47, 48, 53], where a window of states is what we call a Hamiltonian snippet in the present manuscript. Indeed the windows of states approach corresponds to the Markov update

$$P(z, A) = \sum_{k,l=0}^T \frac{1}{T} \int \bar{P}(\psi^{-k}(z), dz') \bar{\mu}(l | z') \mathbf{1}\{\psi^l(z') \in A\}, \quad (54)$$

which, we show below, leaves μ invariant. Indeed, note that for $k, l \in \llbracket 0, T \rrbracket$ and $A \in \mathcal{Z}$,

$$\int \mu(dz) \int \bar{P}(\psi^{-k}(z), dz') \bar{\mu}(l | z') \mathbf{1}\{\psi^l(z') \in A\} = \int_A \mu^{\psi^{-k}}(dz) \int \bar{P}(z, dz') \bar{\mu}(l | z') \mathbf{1}\{\psi^l(z') \in A\},$$

and therefore

$$\begin{aligned} \int \mu(dz) \int P(z, dz') \mathbf{1}\{z' \in A\} &= \int \bar{\mu}(dz) \bar{P}(z, dz') \sum_{l=0}^T \bar{\mu}(l | z') \mathbf{1}\{\psi^l(z') \in A\} \\ &= \int \bar{\mu}(dz') \sum_{l=0}^T \bar{\mu}(l | z') \mathbf{1}\{\psi^l(z') \in A\} \\ &= \int \mu(dz) \mathbf{1}\{z \in A\}, \end{aligned}$$

where we obtain the last line from (10). P is not μ -reversible in general, making theoretical comparisons challenging.

- 1 Given z
- 2 Sample $k \sim \bar{\mu}(\cdot | z)$ and $l \sim \mathcal{U}(\llbracket 0, T \rrbracket)$.
- 3 Compute $\psi^k(z) = (\psi_x^k(z), \psi_v^k(z))$.
- 4 Sample $v' \sim \varpi(\cdot)$
- 5 Return $\psi^{-l}(\psi_x^k(z), v')$

Algorithm 8: Kernel \bar{Q}

I.2 Multinomial HMC

Multinomial HMC is another related MCMC update suggested in [9] which can be rephrased in terms of our framework as follows. For $(z, A) \in \mathbf{Z} \times \mathcal{Z}$ define the kernel

$$P(z, A) = \frac{1}{T+1} \sum_{k,l \in \llbracket 0, T \rrbracket} \bar{\mu}(k | \psi^{-l}(z)) \mathbf{1}\{\psi^{k-l}(z) \in A\}.$$

Introducing velocity refreshment before returning $\psi^{k-l}(z)$, can be reframed in terms $\bar{M}: \mathbf{Z} \times \mathcal{Z}$ as defined in (10) leading the the Markov kernel

$$P'(z, A) = \frac{1}{T+1} \sum_{l \in \llbracket 0, T \rrbracket} \bar{M}(\psi^{-l}(z), A).$$

We focus below on the version with no refreshment, P . Establishing μ -invariance is direct since with $z \sim \mu$ and $l \sim \mathcal{U}(\llbracket 0, T \rrbracket)$ then $\psi^{-l}(z) \sim \bar{\mu}$ and with $k \sim \bar{\mu}(\cdot | \psi^{-l}(z))$ we know that $\psi^{k-l}(z) \sim \mu$ from (10). More formally

$$\begin{aligned} \mu P(A) &= \frac{1}{T+1} \sum_{k \in \llbracket 0, T \rrbracket} \int \mu(dz) \sum_{l \in \llbracket 0, T \rrbracket} \bar{\mu}(k | \psi^{-l}(z)) \mathbf{1}\{\psi^k \circ \psi^{-l}(z) \in A\} \\ &= \sum_{k \in \llbracket 0, T \rrbracket} \int \bar{\mu}(dz) \bar{\mu}(k | z) \mathbf{1}\{\psi^k(z) \in A\} \\ &= \mu(A). \end{aligned}$$

This Markov kernel is in fact reversibility, that is for $f, g: Z \rightarrow \mathbb{R}$

$$\begin{aligned} \sum_{k, l \in \llbracket 0, T \rrbracket} \int f(z) \mu(dz) \bar{\mu}(k | \psi^{-l}(z)) g \circ \psi^{k-l}(z) \\ &= \frac{1}{T+1} \sum_{k, l \in \llbracket 0, T \rrbracket} \int f \circ \psi^l(z) \mu^{\psi^{-l}}(dz) \frac{d\mu^{\psi^{-k}}}{d\bar{\mu}}(z) g \circ \psi^k(z) \\ &= \frac{1}{T+1} \sum_{k, l \in \llbracket 0, T \rrbracket} \int f \circ \psi^l(z) \frac{d\mu^{\psi^{-l}}}{d\bar{\mu}}(z) \mu^{\psi^{-k}}(dz) g \circ \psi^k(z) \\ &= \frac{1}{T+1} \sum_{k, l \in \llbracket 0, T \rrbracket} \int f \circ \psi^{l-k}(z) \frac{d\mu^{\psi^{-l}}}{d\bar{\mu}} \circ \psi^{-k}(z) \mu(dz) g(z) \\ &= \sum_{k, l \in \llbracket 0, T \rrbracket} \int f \circ \psi^{l-k}(z) \mu(dz) \bar{\mu}(l | \psi^{-k}(z)) g(z) \end{aligned}$$

A standard SMC implementation relying on this kernel and corresponding near optimal backward kernel would lead to an algorithm different from ours. Indeed in this scenario, for $n \in \llbracket P \rrbracket$, for particles $\{\dot{z}_n^{(i)}, i \in \llbracket N \rrbracket\}$ the weights are of the standard form $\{d\mu_{n+1}/d\mu_n(\dot{z}_{n+1}^{(i)}), i \in \llbracket N \rrbracket\}$, which should be contrasted with the weights in Alg. (6) $\{d\bar{\mu}_{n+1}/d\mu_n(z_n^{(i)}), i \in \llbracket N \rrbracket\}$ where resampling “looks ahead” and uses the information provided by the snippets stemming from $\{z_n^{(i)}, i \in \llbracket N \rrbracket\}$. Note that there is no indexing mistake here and that the additional dots have been added for coherence: in Alg. (6) the output of iteration $n+1$ are $\{\dot{z}_{n+1}^{(i)}, i \in \llbracket N \rrbracket\}$ and $\{z_n^{(i)}, i \in \llbracket N \rrbracket\}$ intermediate states to which resampling is applied. One expects robustness to arise from this difference.

References

- [1] Christophe Andrieu, Nicolas Chopin, Ettore Fincato, and Mathieu Gerber. Gradient-free optimization via integration, 2024.
- [2] Christophe Andrieu, Anthony Lee, and Sam Livingstone. A general perspective on the Metropolis-Hastings kernel. *arXiv preprint arXiv:2012.14881*, 2020.
- [3] Christophe Andrieu, Anthony Lee, Sam Power, and Andi Q. Wang. Explicit convergence bounds for Metropolis Markov chains: Isoperimetry, spectral gaps and profiles. *The Annals of Applied Probability*, 34(4):4022 – 4071, 2024.

- [4] Christophe Andrieu, James Ridgway, and Nick Whiteley. Sampling normalizing constants in high dimensions using inhomogeneous diffusions, 2018.
- [5] Mark A Beaumont. Approximate bayesian computation in evolution and ecology. *Annual review of ecology, evolution, and systematics*, 41:379–406, 2010.
- [6] Albert Benveniste, Michel Métivier, and Pierre Priouret. *Adaptive algorithms and stochastic approximations*, volume 22. Springer Science & Business Media, 2012.
- [7] Alexandros Beskos, Natesh Pillai, Gareth Roberts, Jesus-Maria Sanz-Serna, and Andrew Stuart. Optimal tuning of the hybrid Monte Carlo algorithm. *Bernoulli*, 19(5A):1501–1534, 2013.
- [8] Michael Betancourt. Nested sampling with constrained Hamiltonian Monte Carlo. In *AIP Conference Proceedings*, volume 1305, pages 165–172. American Institute of Physics, 2011.
- [9] Michael Betancourt. A conceptual introduction to hamiltonian monte carlo. *arXiv preprint arXiv:1701.02434*, 2017.
- [10] Joris Bierkens and Gareth Roberts. A piecewise deterministic scaling limit of lifted Metropolis–Hastings in the Curie–Weiss model. *The Annals of Applied Probability*, 27(2):846–882, 2017.
- [11] P Billingsley. Probability and measure. 3rd wiley. *New York*, 1995.
- [12] Alexandre Bouchard-Côté, Sebastian J Vollmer, and Arnaud Doucet. The bouncy particle sampler: A non-reversible rejection-free Markov chain monte carlo method. *Journal of the American Statistical Association*, 113(522):855–867, 2018.
- [13] Alexander Buchholz, Nicolas Chopin, and Pierre E. Jacob. Adaptive tuning of Hamiltonian Monte Carlo within sequential Monte Carlo, 2020.
- [14] Dmitri Burago, Yuri Burago, and Sergei Ivanov. *A course in metric geometry*, volume 33. American Mathematical Society, 2022.
- [15] Mari Paz Calvo, Daniel Sanz-Alonso, and Jesús María Sanz-Serna. HMC: reducing the number of rejections by not using leapfrog and some results on the acceptance rate. *Journal of Computational Physics*, 437:110333, 2021.
- [16] Cédric M Campos and Jesús María Sanz-Serna. Extra chance generalized hybrid Monte Carlo. *Journal of Computational Physics*, 281:365–374, 2015.
- [17] Bob Carpenter, Andrew Gelman, Matthew D Hoffman, Daniel Lee, Ben Goodrich, Michael Betancourt, Marcus A Brubaker, Jiqiang Guo, Peter Li, and Allen Riddell. Stan: A probabilistic programming language. *Journal of statistical software*, 76, 2017.
- [18] J. T. Chang and D. Pollard. Conditioning as disintegration. *Statistica Neerlandica*, 51(3):287–317, 1997.
- [19] Joseph T Chang and David Pollard. Conditioning as disintegration. *Statistica Neerlandica*, 51(3):287–317, 1997.
- [20] Zongchen Chen and Santosh S Vempala. Optimal convergence rate of Hamiltonian Monte Carlo for strongly logconcave distributions. *Theory of Computing*, 18(1):1–18, 2022.

- [21] N. Chopin and O. Papaspiliopoulos. *An Introduction to Sequential Monte Carlo*. Springer Series in Statistics. Springer International Publishing, 2020.
- [22] Nicolas Chopin. Particles package. <https://github.com/nchopin/particles>, 2023-24.
- [23] Nicolas Chopin and James Ridgway. Leave Pima Indians alone: binary regression as a benchmark for Bayesian computation, 2015.
- [24] Nicolas Chopin and James Ridgway. Leave pima indians alone: binary regression as a benchmark for Bayesian computation. *Statistical Science*, 32(1):64–87, 2017.
- [25] Ole F. Christensen, Gareth O. Roberts, and Jeffrey S. Rosenthal. Scaling Limits for the Transient Phase of Local Metropolis–Hastings Algorithms. *Journal of the Royal Statistical Society Series B: Statistical Methodology*, 67(2):253–268, 03 2005.
- [26] Hai-Dang Dau and Nicolas Chopin. Waste-free sequential Monte Carlo. *arXiv preprint arXiv:2011.02328*, 2020.
- [27] Pierre Del Moral and Pierre Del Moral. *Feynman-kac formulae*. Springer, 2004.
- [28] Pierre Del Moral, Arnaud Doucet, and Ajay Jasra. Sequential Monte Carlo samplers. *Journal of the Royal Statistical Society: Series B (Statistical Methodology)*, 68(3):411–436, 2006.
- [29] Simon Duane, Anthony D Kennedy, Brian J Pendleton, and Duncan Roweth. Hybrid Monte Carlo. *Physics letters B*, 195(2):216–222, 1987.
- [30] Mauro Camara Escudero. *Approximate Manifold Sampling: Robust Bayesian Inference for Machine Learning*. PhD thesis, School of Mathematics, January 2024.
- [31] Youhan Fang, J. M. Sanz-Serna, and Robert D. Skeel. Compressible generalized hybrid Monte Carlo. *The Journal of Chemical Physics*, 140(17):174108, 05 2014.
- [32] Paul Fearnhead and Benjamin M. Taylor. An Adaptive Sequential Monte Carlo Sampler. *Bayesian Analysis*, 8(2):411 – 438, 2013.
- [33] Mark Girolami and Ben Calderhead. Riemann manifold Langevin and Hamiltonian Monte Carlo methods. *Journal of the Royal Statistical Society: Series B (Statistical Methodology)*, 73(2):123–214, 2011.
- [34] Heikki Haario, Eero Saksman, and Johanna Tamminen. Adaptive proposal distribution for random walk metropolis algorithm. *Computational statistics*, 14:375–395, 1999.
- [35] Ernst Hairer, SP Nørsett, and G. Wanner. *Solving ordinary differential equations I, Nonstiff problems*. Springer-Verlag, 1993.
- [36] J Heng and P E Jacob. Unbiased Hamiltonian Monte Carlo with couplings. *Biometrika*, 106(2):287–302, 02 2019.
- [37] Matthew Hoffman, Alexey Radul, and Pavel Sountsov. An adaptive-MCMC scheme for setting trajectory lengths in Hamiltonian Monte Carlo. In *International Conference on Artificial Intelligence and Statistics*, pages 3907–3915. PMLR, 2021.
- [38] Matthew D Hoffman, Andrew Gelman, et al. The No-U-Turn sampler: adaptively setting path lengths in Hamiltonian Monte Carlo. *J. Mach. Learn. Res.*, 15(1):1593–1623, 2014.

- [39] Matthew D Hoffman and Pavel Sountsov. Tuning-Free Generalized Hamiltonian Monte Carlo. In *International Conference on Artificial Intelligence and Statistics*, pages 7799–7813. PMLR, 2022.
- [40] Pierre E. Jacob. Debiased HMC. <https://github.com/pierrejacob/debiasedhmc/blob/master/inst/coxprocess/hmc.repeats.R>, 2017.
- [41] Samuel Livingstone and Giacomo Zanella. The Barker proposal: combining robustness and efficiency in gradient-based MCMC. *Journal of the Royal Statistical Society Series B: Statistical Methodology*, 84(2):496–523, 2022.
- [42] Paul B Mackenze. An improved hybrid Monte Carlo method. *Physics Letters B*, 226(3-4):369–371, 1989.
- [43] Florian Maire and Pierre Vandekerkhove. On markov chain monte carlo for sparse and filamentary distributions. *ArXiv e-prints*, 2018.
- [44] Florian Maire and Pierre Vandekerkhove. Markov kernels local aggregation for noise vanishing distribution sampling. *SIAM Journal on Mathematics of Data Science*, 4(4):1293–1319, 2022.
- [45] Youssef Marzouk, Tarek Moselhy, Matthew Parno, and Alessio Spantini. *Sampling via Measure Transport: An Introduction*, pages 1–41. Springer International Publishing, Cham, 2016.
- [46] Xiao-Li Meng and Stephen Schilling. Warp bridge sampling. *Journal of Computational and Graphical Statistics*, 11(3):552–586, 2002.
- [47] Radford M Neal. An improved acceptance procedure for the hybrid Monte Carlo algorithm. *Journal of Computational Physics*, 111(1):194–203, 1994.
- [48] Radford M. Neal. *MCMC Using Hamiltonian Dynamics*, chapter 5. CRC Press, 2011.
- [49] Yann Ollivier. Ricci curvature of Markov chains on metric spaces. *Journal of Functional Analysis*, 256(3):810–864, 2009.
- [50] Yann Ollivier. A survey of Ricci curvature for metric spaces and Markov chains. In *Probabilistic approach to geometry*, volume 57, pages 343–382. Mathematical Society of Japan, 2010.
- [51] Ari Pakman and Liam Paninski. Exact Hamiltonian Monte Carlo for truncated multivariate Gaussians. *Journal of Computational and Graphical Statistics*, 23(2):518–542, 2014.
- [52] Qian Qin, Nianqiao Ju, and Guanyang Wang. Spectral gap bounds for reversible hybrid gibbs chains, 2023.
- [53] Zhaohui S. Qin and Jun S. Liu. Multipoint Metropolis method with application to Hybrid Monte Carlo. *Journal of Computational Physics*, 172(2):827–840, 2001.
- [54] James Ridgway. Computation of gaussian orthant probabilities in high dimension. *Statistics and computing*, 26(4):899–916, 2016.
- [55] Grant M Rotskoff and Eric Vanden-Eijnden. Dynamical computation of the density of states and Bayes factors using nonequilibrium importance sampling. *Physical review letters*, 122(15):150602, 2019.
- [56] Gabriel Stoltz, Mathias Rousset, et al. *Free energy computations: A mathematical perspective*. World Scientific, 2010.

- [57] C. Sunyach. Une classe de chaînes de Markov récurrentes sur un espace métrique complet. *Annales de l'I.H.P. Probabilités et statistiques*, 11(4):325–343, 1975.
- [58] D Szasz. *Boltzmann's ergodic hypothesis, a conjecture for centuries?*, chapter Hard ball systems and the Lorentz gas, pages 421–446. Springer, 2000.
- [59] Esteban G Tabak and Eric Vanden-Eijnden. Density estimation by dual ascent of the log-likelihood. *Communications in Mathematical Sciences*, 8(1):217–233, 2010.
- [60] Erik H Thiede, Brian Van Koten, Jonathan Weare, and Aaron R Dinner. Eigenvector method for umbrella sampling enables error analysis. *The Journal of chemical physics*, 145(8), 2016.
- [61] Achille Thin, Yazid Janati El Idrissi, Sylvain Le Corff, Charles Ollion, Eric Moulines, Arnaud Doucet, Alain Durmus, and Christian X Robert. Neo: Non equilibrium sampling on the orbits of a deterministic transform. *Advances in Neural Information Processing Systems*, 34:17060–17071, 2021.
- [62] G.M. Torrie and J.P. Valleau. Nonphysical sampling distributions in Monte Carlo free-energy estimation: Umbrella sampling. *Journal of Computational Physics*, 23(2):187–199, 1977.
- [63] Paul F Tupper. Ergodicity and the numerical simulation of Hamiltonian systems. *SIAM Journal on Applied Dynamical Systems*, 4(3):563–587, 2005.
- [64] V. F. Turchin. On the computation of multidimensional integrals by the monte-carlo method. *Theory of Probability & Its Applications*, 16(4):720–724, 1971.
- [65] J. von Neumann. Proof of the quasi-ergodic hypothesis. *Proc. Natl. Acad. Sci. USA*, 18:70–82, 1932.
- [66] Chang Zhang. *On the Improvements and Innovations of Monte Carlo Methods*. PhD thesis, School of Mathematics, <https://research-information.bris.ac.uk/en/studentTheses/on-the-improvements-and-innovations-of-monte-carlo-methods>, June 2022.